Perturbation theory of LSS in the ΛCDM Universe:
exact time evolution and the two-loop power spectrum

Matteo Fasiello,[1, 2, ∗] Tomohiro Fujita,[3, 4, †] and Zvonimir Vlah[5, 6, 7, ‡]

[1]*Instituto de Física Teórica UAM/CSIC, calle Nicolás Cabrera 13-15, Cantoblanco, 28049, Madrid, Spain*
[2]*Institute of Cosmology and Gravitation, University of Portsmouth, PO1 3FX, UK*
[3]*Waseda Institute for Advanced Study, Waseda University, 1-6-1 Nishi-Waseda, Shinjuku, Tokyo 169-8050, Japan*
[4]*Research Center for the Early Universe, The University of Tokyo, Bunkyo, Tokyo 113-0033, Japan*
[5]*Ruđer Bošković Institute, Bijenička cesta 54, 10000 Zagreb, Croatia*
[6]*Kavli Institute for Cosmology, University of Cambridge, Cambridge CB3 0HA, UK*
[7]*Department of Applied Mathematics and Theoretical Physics, University of Cambridge, Cambridge CB3 0WA, UK*

We derive exact analytic solutions for density and velocity fields to all orders in Eulerian standard perturbation theory for ΛCDM cosmology. In particular, we show that density and velocity field kernels can be written in a separable form in time and momenta at each perturbative order. The kernel solutions are built from an analytic basis of momentum operators and their time-dependent coefficients, which solve a set of recursive differential equations. We also provide an exact closed perturbative solution for such coefficients, expanding around the (quasi-)EdS approximation. We find that the perturbative solution rapidly converges towards the numerically obtained solutions and its leading order result suffices for any practical requirements. To illustrate our findings, we compute the exact two-loop dark matter density and velocity power spectra in ΛCDM cosmology. We show that the difference between the exact ΛCDM and the (quasi-)EdS approximated result can reach the level of several percent (at redshift zero, for wavenumbers $k < 1h/\text{Mpc}$). This deviation can be partially mitigated by exploiting the degeneracy with the EFT counterterms. As an additional benefit of our algorithm for the solutions of time-dependent coefficients, the computational complexity of power spectra loops in ΛCDM is comparable to the EdS case. In performing the two-loop computation, we devise an explicit method to implement the so-called IR cancellations, as well as the cancellations arising as a consequence of mass and momentum conservation.

PACS numbers:

I. INTRODUCTION

The large scale structure (LSS) is a repository of key information on our universe's origin and evolution, all the way to the current dark energy dominated era. Data on inflationary interactions is encoded in the initial conditions for structure formation while LSS dynamical evolution also depends on the presence of additional components that may drive late-time acceleration. Astronomical surveys of the galaxy distribution (e.g. Euclid, LSST, SKA) promise to soon cross the qualitative threshold on cosmological parameter, such as a percent level accuracy on the dark energy equation of state parameters [1–3]. Crucially, it is by going beyond the background cosmology that we will, for example, extract information on non-Gaussianities and identify different dark energy models that otherwise support the same expansion history.

LSS dynamics is amenable to a perturbative description for a limited range of wavenumbers: those for which the separation of scales underlying a consistent effective treatment can be advocated. The large hierarchy separating the size of the observable Universe $1/H_0$ and the onset of non-linearities $1/k_{\text{NL}}$ in structure formation explains the success of linear perturbation theory in describing the essential features observed in galaxy surveys. At scales as large as 10 Mpc, non-linearities become relevant: different Fourier modes stop evolving independently showing hints of a UV/IR mixing typical of non-linear regimes.

∗Electronic address: matteo.fasiello@csic.es
†Electronic address: tomofuji@aoni.waseda.jp
‡Electronic address: zvlah@irb.hr

At the interface between the linear and highly non-linear regime are so-called quasi-(or mildly-non-) linear scales. Gaining perturbative control over the quasi-linear range significantly increases the number of modes at our disposal ($N \propto k^3$). A plethora of distinct perturbative approaches have been put forward in this direction [4–25], a programme that has been altogether quite successful. The exact k-reach of the perturbative treatment in particular has been the subject of intense research activity, especially within the context of the EFT framework [12, 13] (see also [26, 27] for recent reviews). Even though several aspects need further development on the "model building" front, there are already definite predictions on given observables, consisting mainly of the one-loop power spectrum and the tree-level bispectrum, that have already been employed in obtaining cosmological information from the LSS galaxy surveys [28–35].

Our work tackles the perturbative treatment of LSS in ΛCDM cosmology. In this context, striving for *exact analytical* solutions serves multiple purposes. Besides being necessary for a view of the projected accuracy of soon-to-be operational probes, such solutions are also important to ensure that approximations do not get in the way (i.e. create degeneracies out) of otherwise distinct signatures. In this work, we present all order exact recursive solutions for perturbation theory kernels of the density and velocity fields (i.e. F_n, G_n) in ΛCDM cosmology. The need to go beyond the so-called extended (quasi-)EdS approximation[1] has long been recognised as a timely step (see, e.g. [13, 36–44]), with our own previous work [45] providing for the first time exact all order solutions for ΛCDM and beyond. In this manuscript we shall take [45] as the starting point and report on the significant progress in manifold directions.

We are after separable solutions accounting for the time and momenta dependence of density and velocity kernels. We identify, for each order in perturbation theory (PT), a complete "basis" of operators in a separable form that make up the solution for the F, G kernels. We derive such basis recursively, i.e. by employing the results at lower perturbative orders as building blocks. By construction, the derivation of time-dependent coefficients needs no input from the momenta operators and vice-versa, greatly simplifying and speeding up the calculation. We provide an algorithm that unambiguously couples time and momenta operators to give each basis element. Our algorithm completely eliminates the need (still present in [45]) for an ansatz to be put forward at every perturbative step to identify the solution. This is a striking improvement, especially relevant as the community has been increasingly recognising the importance of tackling higher orders in PT [46–55]. Moreover, we derive explicit perturbative solutions for time-dependent coefficients. By a suitable choice of time variable our perturbative solutions are valid for generic cosmological parameters within the ΛCDM cosmology.

We also develop a systematic way to deal with IR (and UV) divergences in loop integrals. As is well-known (see e.g. [6, 47, 56, 57]) the equivalence principle guarantees the cancellation of leading and sub-leading IR divergencies. The presence of several large IR contributions in the expression for higher order observables ahead of their overall cancellation hinder calculational efficiency. In addition to the cancellation of these IR divergences, mass and momentum conservation also plays a role in determining the scale dependence of loop contributions by imposing cancellations of large contributions sensitive to UV scales [4, 8, 58, 59]. By introducing suitable window functions, we are able to renormalize correlation functions and make contact with so-called perturbation theory counterterms in the context of the EFT framework.

This paper is organised as follows: in *Section* II we set the stage with the equations of motion for the ΛCDM system, we also briefly report on previous works on the subject. In *Section* III we lay out our algorithm and derive recursive separable solutions for the kernels that may be used up to any order in perturbation theory. We further show how, starting from the Einstein-de Sitter approximation, one may derive solutions arbitrarily close to the exact result. In *Section* IV we focus on one- and two-loop results for the density and velocity cross and auto power spectra. We draw our conclusions in *Section* V and comment on future work. A significant fraction of our derivations has been delegated to the appendices. Thus, in *Appendix* A we review the linear growth equations and derive a new expansion of the specific form of the linear growth rate combination. In *Appendix* B we review the integral solutions for perturbation theory kernels. Based on these results in *Appendix* C we derive separable kernel form, for which we give the perturbative solution of the time-dependence in the *Appendix* D. In *Appendix* E we explore the various IR and UV limits of the newly obtained kernels, which we use in *Appendix* F to explore the IR and UV properties of the two-loop power spectra.

Throughout the paper, we assume a Euclidean cosmology with $\Omega_m = 0.3$, $\sigma_8 = 0.8$ and $h = 0.7$ with the BBKS linear power spectrum. We work under the assumptions of adiabatic Gaussian perturbations and General Relativity. As mentioned in footnote [1], in the rest of the paper when we refer to the EdS solutions, we have in mind the usual

---

[1]This method consists in handling the time dependence of kernels as in an Einstein-de Sitter universe (only matter content), where e.g. $\delta^{(n)}(a) \propto D^n(a)$ but with the added prescription to employ the linear growth rate D of a ΛCDM universe. Henceforth, in order to adhere to common parlance, we refer to this approximation as EdS, rather than (quasi-)EdS.

(quasi-EdS) approximation of setting the n-th order growth factor D_+^n, instead of the a^n which would be the solution in the actual EdS Universe. Our results for time coefficients and momentum kernels are provided in the *Mathematica* notebook, in the *arXiv* source file of this paper.

II.   DYNAMICS IN THE ΛCDM UNIVERSE

As is well known, we may describe the large-scale structure as a fluid in the non-relativistic limit obeying the following equations of motion for the fluctuations of the density contrast δ and the peculiar velocity $\theta \equiv \partial_i v^i$:

$$\frac{\partial \delta_{\boldsymbol{k}}}{\partial \tau} + \theta_{\boldsymbol{k}} = -\int_{\boldsymbol{q}_1,\boldsymbol{q}_2} \delta^D_{\boldsymbol{k}-\boldsymbol{q}_{12}} \alpha(\boldsymbol{q}_1,\boldsymbol{q}_2) \theta_{\boldsymbol{q}_1} \delta_{\boldsymbol{q}_2} , \tag{1}$$

$$\frac{\partial \theta_{\boldsymbol{k}}}{\partial \tau} + \mathcal{H}\theta_{\boldsymbol{k}} + \frac{3}{2}\Omega_m \mathcal{H}^2 \delta_{\boldsymbol{k}} = -\int_{\boldsymbol{q}_1,\boldsymbol{q}_2} \delta^D_{\boldsymbol{k}-\boldsymbol{q}_{12}} \beta(\boldsymbol{q}_1,\boldsymbol{q}_2) \theta_{\boldsymbol{q}_1} \theta_{\boldsymbol{q}_2} ,$$

where $\delta^D_{\boldsymbol{q}}$ is the Dirac's delta function, $\boldsymbol{q}_{12} \equiv \boldsymbol{q}_1 + \boldsymbol{q}_2$, $\int_{\boldsymbol{q}} \equiv \int \mathrm{d}^3 q/(2\pi)^3$, and $\mathcal{H} = d\ln a/d\tau$. Here a is the scale factor, and τ is conformal time. The kernels α, β are defined as $\alpha(\boldsymbol{q}_1,\boldsymbol{q}_2) \equiv 1 + (\boldsymbol{q}_1 \cdot \boldsymbol{q}_2)/q_1^2$, $\beta(\boldsymbol{q}_1,\boldsymbol{q}_2) \equiv (\boldsymbol{q}_{12})^2(\boldsymbol{q}_1 \cdot \boldsymbol{q}_2)/2q_1^2 q_2^2$. At linear order, assuming the growing mode initial conditions, the time and momentum dependent parts are clearly separable

$$\delta^{(1)}_{\boldsymbol{k}}(\tau) \equiv D_+(\tau)\delta^{\mathrm{in}}_{\boldsymbol{k}} , \qquad \theta^{(1)}_{\boldsymbol{k}}(\tau) \equiv -\mathcal{H}(\tau) f_+(\tau) D_+(\tau)\delta^{\mathrm{in}}_{\boldsymbol{k}} , \tag{2}$$

where D_+ is the linear growth factor, $f_+ \equiv d\ln D_\pm/d\ln a$ is the linear growth rate (see Appendix A for a brief review of results in the linear regime). In addition to the growth mode, we also have the decaying mode with linear decay factor D_-, and equivalently defined decay rate f_-. $\delta^{\mathrm{in}}_{\boldsymbol{k}}$ represents the initial value of the density contrast. The growing and decaying factors D_+ and D_- satisfy the differential equation,

$$\frac{d^2 D(\tau)}{d\tau^2} + \mathcal{H}(\tau)\frac{dD(\tau)}{d\tau} - \frac{3}{2}\Omega_m(\tau)\mathcal{H}^2(\tau)\, D(\tau) = 0 . \tag{3}$$

In ΛCDM cosmology, the solutions for $D_\pm(\tau)$ can be expressed in a closed form (see Eq. (A1)). In order to identify the solutions for density contrast and velocity beyond the linear order, we employ the following perturbative ansatz:

$$\delta_{\boldsymbol{k}}(\tau) = \sum_{n=1}^{\infty} \delta^D_{\boldsymbol{k}-\boldsymbol{q}_{1n}} F_n^s(\boldsymbol{q}_1,..,\boldsymbol{q}_n,\tau) D_+^n(\tau)\delta^{\mathrm{in}}_{\boldsymbol{q}_1}..\delta^{\mathrm{in}}_{\boldsymbol{q}_n}, \tag{4}$$

$$\theta_{\boldsymbol{k}}(\tau) = \sum_{n=1}^{\infty} \delta^D_{\boldsymbol{k}-\boldsymbol{q}_{1n}} G_n^s(\boldsymbol{q}_1,..,\boldsymbol{q}_n,\tau) D_+^n(\tau)\delta^{\mathrm{in}}_{\boldsymbol{q}_1}..\delta^{\mathrm{in}}_{\boldsymbol{q}_n},$$

where $\boldsymbol{q}_{1n} \equiv \boldsymbol{q}_1 + \boldsymbol{q}_2 + \cdots \boldsymbol{q}_n$. Henceforth we shall not display the integration over $\boldsymbol{q}_1 \ldots \boldsymbol{q}_n$ on the right-hand side, which is taken as granted. The kernel functions F_n^s, and G_n^s are fully symmetrized with respect to the momenta in their argument. Hereafter all the kernels are to be understood as symmetrized and we omit the superscript "s". Although the non-linear kernels F_n, G_n are constant in time and more easily obtained in the EdS universe [4, 8], they become time-dependent functions in ΛCDM. The standard approximation in the field is to keep the ΛCDM growth rate D_+^n and keep the EdS, time-independent, solution for the F_n, G_n kernels.

Recently the full time-dependent solution for the kernels in ΛCDM has been found in [45]. This solution has been derived in an integral recursive form which is somewhat impractical for direct use when computing correlators in perturbation theory. Here we will start from the results of [45], casting them in a slightly modified but equivalent form, with the goal of expressing such solutions in an explicitly separable form, disentangling the time dependence of the kernels from their momentum dependence.

We thus start from the full implicit ΛCDM solution of the kernels at n-th order

$$F_n(\boldsymbol{q}_1,..,\boldsymbol{q}_n,a) = \int_0^a \frac{\mathrm{d}\tilde{a}}{\tilde{a}}\left(w_\alpha^{(n)}(a,\tilde{a})h_\alpha^{(n)}(\boldsymbol{q}_1,..,\boldsymbol{q}_n,\tilde{a}) + w_\beta^{(n)}(a,\tilde{a})h_\beta^{(n)}(\boldsymbol{q}_1,..,\boldsymbol{q}_n,\tilde{a})\right), \tag{5}$$

$$G_n(\boldsymbol{q}_1,..,\boldsymbol{q}_n,a) = \int_0^a \frac{\mathrm{d}\tilde{a}}{\tilde{a}}\left(u_\alpha^{(n)}(a,\tilde{a})h_\alpha^{(n)}(\boldsymbol{q}_1,..,\boldsymbol{q}_n,\tilde{a}) + u_\beta^{(n)}(a,\tilde{a})h_\beta^{(n)}(\boldsymbol{q}_1,..,\boldsymbol{q}_n,\tilde{a})\right),$$

where we use the scale factor a as the time variable, and $w_{\alpha,\beta}^{(n)}, u_{\alpha,\beta}^{(n)}$ are the "Green's functions", given in the explicit form (B7). As clear by inspection, these are completely determined by the $D_\pm$ and $f_\pm$ functions. In addition to

the purely time-dependent Green's functions, we have source terms $h_{\alpha,\beta}^{(n)}$, which also depend on time as well as the momenta. These source terms are recursively constructed from the lower order kernels $F_{n'}$ and $G_{n'}$, such that $n' < n$. The explicit form of these source terms is given in (B2). For the full derivation of this result see Appendix B.

As mentioned, in the integral solution in Eq. (5), the source functions $h_{\alpha,\beta}^{(n)}$ depend both on time and momenta, and a considerable calculational advantage would be achieved if one could provide solutions whose time and momenta dependent parts are separable. Furthermore, given the importance of higher order corrections, one should aim at recursive solutions, which would enable us to do without, for example, the order-specific ansatz used in [45] to arrive at the exact analytical solution for the $n = 3$ case. Here we present a systematic derivation of recursive separable functions that make up the kernels solution at any given order.

We start by suggesting the separable ansatze for the ΛCDM solutions in Eq. (5),

$$F_n(\boldsymbol{q}_1,..,\boldsymbol{q}_n,a) = \sum_{\ell=1}^{N(n)} \lambda_n^{(\ell)}(a) H_n^{(\ell)}(\boldsymbol{q}_1,..,\boldsymbol{q}_n) = \boldsymbol{\lambda}_n(a) \cdot \boldsymbol{H}_n(\boldsymbol{q}_1,..,\boldsymbol{q}_n)\,, \tag{6}$$

$$G_n(\boldsymbol{q}_1,..,\boldsymbol{q}_n,a) = \sum_{\ell=1}^{N(n)} \kappa_n^{(\ell)}(a) H_n^{(\ell)}(\boldsymbol{q}_1,..,\boldsymbol{q}_n) = \boldsymbol{\kappa}_n(a) \cdot \boldsymbol{H}_n(\boldsymbol{q}_1,..,\boldsymbol{q}_n)\,,$$

where the time dependent coefficients $\lambda_n^{(\ell)}, \kappa_n^{(\ell)}$ and the momentum operators part $H_n^{(\ell)}$ are explicitly separated. The last equalities in Eqs. (6) are written with a more compact notation that we shall be using later in the text. For now, we keep the index "ℓ" explicit to make each manipulation of the operators as clear as possible. We stress that the same momentum operators $H_n^{(\ell)}$ are used for both F_n and G_n, while the time-dependent coefficients $\lambda_n^{(\ell)}$ and $\kappa_n^{(\ell)}$ are different. The number of terms in the sum $N(n)$ gives us the number of the basis elements at n-th perturbative order which are, for the first few orders,

$$N(1) = 1, \quad N(2) = 2, \quad N(3) = 6, \quad N(4) = 25, \quad N(5) = 111. \tag{7}$$

In general, counting the number of terms generated by the recursive form of Eq. (5), gives us the expression

$$N(n) = \delta_{\frac{n}{2},\lfloor \frac{n}{2} \rfloor}^K \frac{1}{2} N\left(\tfrac{n}{2}\right)\left(3N\left(\tfrac{n}{2}\right)+1\right) + 3 \sum_{m=1}^{\lfloor (n-1)/2 \rfloor} N(m)N(n-m)\,. \tag{8}$$

Note that $N(n)$ provides a useful upper bound on the dimension of the basis operators at each given order so that our basis may contain redundant elements. In order to obtain the minimal number of independent terms, one would need to employ relations such as the one in Eq. (B9) as well as other physical constraints that arise from requirements such as the equivalence principle as well as mass and momentum conservation [59, 60]. We shall not linger on extracting all such relations at this stage but just point out that the solutions for the time coefficient we obtain should manifest all such properties, as we will show later on. Our task is thus split in two parts: determining the explicit form of the momentum operator basis $H_n^{(\ell)}$, as well as computing the time coefficients $\lambda_n^{(\ell)}$ and $\kappa_n^{(\ell)}$ at each perturbative order. For the detailed derivation of how the split of the momentum operators and the time coefficients is performed, we refer the reader to Appendix C. Here we focus on presenting the main results.

The momentum operator basis $H_n^{(\ell)}$ is given by the recursive relation involving only the lower order basis operators. This is similar to the EdS solutions for the F_n and G_n kernels, although the expression for the $H_n^{(\ell)}$ contains more terms, and we have

$$H_n^{(\ell)}(\boldsymbol{q}_1,..,\boldsymbol{q}_n) = \delta_{\frac{n}{2},\lfloor \frac{n}{2} \rfloor}^K \sum_{i=1}^{N(n/2)} \left[\sum_{j=1}^{N(n/2)} [h_\alpha]_{\frac{n}{2},\frac{n}{2}}^{(ij)} \delta_{\ell,\phi_1}^K + \sum_{j=i}^{N(n/2)} \left[2 - \delta_{ij}^K\right] [h_\beta]_{\frac{n}{2},\frac{n}{2}}^{(ij)} \delta_{\ell,\phi_2}^K \right] \tag{9}$$

$$+ \sum_{m=1}^{\lfloor (n-1)/2 \rfloor} \sum_{i=1}^{N(m)} \sum_{j=1}^{N(n-m)} \left([h_\alpha]_{m,n-m}^{(ij)} \delta_{\ell,\phi_3}^K + [h_\alpha]_{n-m,m}^{(ji)} \delta_{\ell,\phi_4}^K + 2[h_\beta]_{m,n-m}^{(ij)} \delta_{\ell,\phi_5}^K \right),$$

where the sourcing term $[h_\alpha]$ above is given by

$$[h_\alpha]_{m,n-m}^{(ij)}(\boldsymbol{q}_1,..,\boldsymbol{q}_n) = \frac{m!(n-m)!}{n!} \sum_{\pi-\text{cross}} \alpha(\boldsymbol{q}_m,\boldsymbol{q}_{n-m}) H_m^{(i)}(\boldsymbol{q}_1,..,\boldsymbol{q}_m) H_{n-m}^{(j)}(\boldsymbol{q}_{m+1},..,\boldsymbol{q}_n)\,, \tag{10}$$

and the expression for $[h_\beta]^{(ij)}_{m,n-m}$ is obtained by simply replacing α with β in Eq.(10). The Kronecker delta δ^K_{ℓ,ϕ_i} selects only one of the specific $[h_{\alpha,\beta}]^{(ij)}_{m,n-m}(\boldsymbol{q}_1,..,\boldsymbol{q}_n)$ operators and identifies it with $H_n^{(\ell)}$. The key to this counting are the bijective maps ϕ_i, which depend on the indices $\{n,m,i,j\}$ and relate them to the set of numbers that go from 1 to $N(n)$. The explicit expressions for ϕ_i are provided in (C4). At second order, one immediately recovers $H_2^{(1)} = \alpha_s$, $H_2^{(2)} = \beta$, as expected. Having obtained the expressions for the momentum operator basis, we now move on to determining the time dependent coefficients.

The expressions for the coefficients $\lambda_n^{(\ell)}$ (and similarly for $\kappa_n^{(\ell)}$) introduced in Eq. (6) give

$$\lambda_n^{(\ell)}(a) = \delta^K_{\frac{n}{2},\lfloor \frac{n}{2} \rfloor} \sum_{i=1}^{N(n/2)} \left[\sum_{j=1}^{N(n/2)} W^{(ij)}_{\alpha;n/2,n/2} \delta^K_{\ell,\phi_1} + \sum_{j=i}^{N(n/2)} W^{(ij)}_{\beta;\frac{n}{2},\frac{n}{2}} \delta^K_{\ell,\phi_2} \right] \tag{11}$$
$$+ \sum_{m=1}^{\lfloor (n-1)/2 \rfloor} \sum_{i=1}^{N(m)} \sum_{j=1}^{N(n-m)} \left(W^{(ij)}_{\alpha;m,n-m} \delta^K_{\ell,\phi_3} + W^{(ji)}_{\alpha;n-m,m} \delta^K_{\ell,\phi_4} + W^{(ij)}_{\beta;m,n-m} \delta^K_{\ell,\phi_5} \right),$$

where the explicit time-integral representation for functions W is given in Eq. (C3). Analogously to what happens for the momentum basis "vector" $H_n^{(\ell)}$, one of the $W^{(ij)}_{\alpha;m,n-m}(a)$ or $W^{(ij)}_{\beta;m,n-m}(a)$ functions with fixed indices is identified as $\lambda_n^{(\ell)}$. Equivalent expression holds for κ_n as shown in Eq. (C6), which identifies one of functions U as $\kappa_n^{(\ell)}$. Note that, the momenta operators $[h]^{(ij)}_{m,n-m}$ and the time coefficients $W^{(ij)}_{m,n-m}$ and $U^{(ij)}_{m,n-m}$ share the same index structure. For $n=1$ one has $\lambda_1^{(1)} = \kappa_1^{(1)} = 1$ and at $n=2$ one finds

$$\lambda_2^{(1)}(a) = W^{2\,(1,1)}_{\alpha;1,1}, \qquad \lambda_2^{(2)}(a) = W^{2\,(1,1)}_{\beta;1,1}, \qquad \kappa_2^{(1)}(a) = U^{2\,(1,1)}_{\alpha;1,1}, \qquad \kappa_2^{(2)}(a) = U^{2\,(1,1)}_{\beta;1,1}, \tag{12}$$

which, as expected, agrees with the previous findings [45, 61]. Combined with those in Appendix C, the formulas in Eqs. (9) and (11) for $H_n^{(\ell)}, \lambda_n^{(\ell)}, \kappa_n^{(\ell)}$ have a close (recursive) structure allowing us to systematically compute kernels up to an arbitrary order n. The operators $H_n^{(\ell)}$ are made up by a combination of the basic building blocks α and β, making it straightforward to automatize the calculation with a computer program.

Although the time-dependent coefficients, $\lambda_n^{(\ell)}, \kappa_n^{(\ell)}$, can also be systematically written down, their expressions given in (C3) involve recursive time integrals. This in itself is not a problem and these expressions can easily be used to obtain the numerical values for the time coefficients. However, instead of these integral representations, we can recast these expressions in the form of coupled differential equations

$$\dot{W}^{n\,(ij)}_{\alpha;m_1,m_2} + nW^{n\,(ij)}_{\alpha;m_1,m_2} - U^{n\,(ij)}_{\alpha;m_1,m_2} = \kappa^{(i)}_{m_1} \lambda^{(j)}_{m_2}, \tag{13}$$
$$\dot{W}^{n\,(ij)}_{\beta;m_1,m_2} + nW^{n\,(ij)}_{\beta;m_1,m_2} - U^{n\,(ij)}_{\beta;m_1,m_2} = 0,$$
$$\dot{U}^{n\,(ij)}_{\alpha;m_1,m_2} + (n-1)U^{n\,(ij)}_{\alpha;m_1,m_2} - \frac{f_-}{f_+^2} \left[U^{n\,(ij)}_{\alpha;m_1,m_2} - W^{n\,(ij)}_{\alpha;m_1,m_2} \right] = 0,$$
$$\dot{U}^{n\,(ij)}_{\beta;m_1,m_2} + (n-1)U^{n\,(ij)}_{\beta;m_1,m_2} - \frac{f_-}{f_+^2} \left[U^{n\,(ij)}_{\beta;m_1,m_2} - W^{n\,(ij)}_{\beta;m_1,m_2} \right] = \kappa^{(i)}_{m_1} \kappa^{(j)}_{m_2},$$

where one may identify $m_1 = m$, $m_2 = n - m$. The time variable is $\eta \equiv \ln D_+$, and a dot denotes a derivative w.r.t. to η, that is $\dot{} \equiv \mathrm{d}/\mathrm{d}\eta$. According to Eq. (11), one selects time coefficients $\lambda_n^{(\ell)}$ and $\kappa_n^{(\ell)}$ from the functions W and U, respectively. One can recursively solve Eq. (13) with the initial conditions $\lambda_1^{(1)} = \kappa_1^{(1)} = 1$ and obtain the time-dependent coefficients up to the desired order.

The differential equation for the time coefficients of the kernels is amenable to the direct numerical treatment, and indeed we will use this approach to obtain our main reference results further on. In addition, the differential equation representation is particularly useful in formulating the analytical, perturbative solution which we discuss in the next section.

Before we continue towards the solution of these equations, we stress here an interesting and practical point about the dependence of Eqs. (13) on cosmological parameters. The only dependence on the cosmological parameters Ω_{m0} and $\Omega_{\Lambda0}$ ($z = 0$ values) comes from the f_-/f_+^2 factor in the equations for U_α and U_β. Moreover, in Appendix A we show that the functional dependence of f_-/f_+^2 can be written in the form of the single variable $\Omega_{\Lambda0}/\Omega_{m0}e^{3\eta}$, which captures the full dependence on the cosmological parameters. In other words, in Eq. (A7) we show that we can write

$$\frac{f_-}{f_+^2} = -\frac{3}{2} + c_1 \left(\frac{\Omega_{\Lambda0}}{\Omega_{m0}} e^{3\eta} \right) + c_2 \left(\frac{\Omega_{\Lambda0}}{\Omega_{m0}} e^{3\eta} \right)^2 + c_3 \left(\frac{\Omega_{\Lambda0}}{\Omega_{m0}} e^{3\eta} \right)^3 + \dots, \tag{14}$$
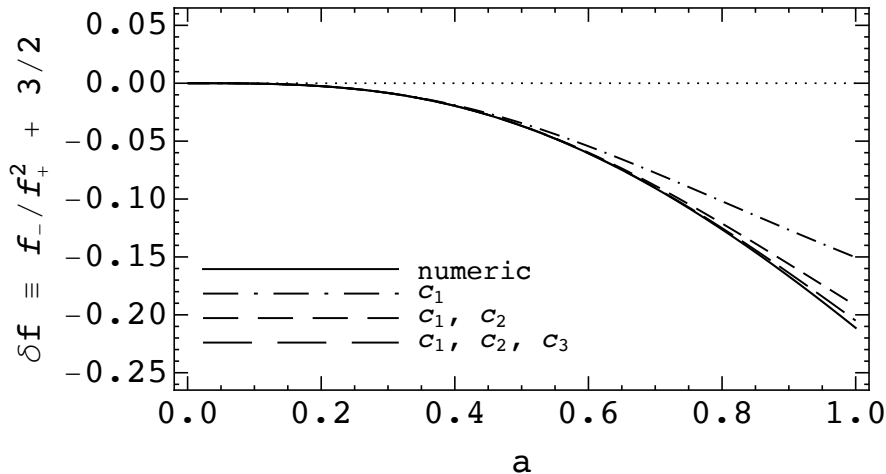
Figure 1: $\delta f \equiv f_-/f_+^2 + 3/2$ is shown as a function of the scale factor. Numerical results (solid black line) are compared to the perturbative expansion in powers of $\zeta = \Omega_{\Lambda 0}/\Omega_{m0}e^{3\eta}$. The expansion up to the first (dot-dashed lines), second (dashed) and third (long-dashed) order is shown using the c_1, c_2 and c_3 coefficients given in Eq. (18). In EdS approximation this quantity vanishes identically, while beyond EdS the deviations from zero source the time dependence of all the $\lambda_n^{(\ell)}$ and $\kappa_n^{(\ell)}$ coefficients.

with some numerical coefficients c_i, fixed within the ΛCDM paradigm. Figure 1 shows the convergence of this expansion. This implies that in Eqs. (13) we can change the variable to $\zeta \equiv \Omega_{\Lambda 0}/\Omega_{m0}e^{3\eta}$, which would alter only the first derivative terms with $\partial_\eta = 3\zeta\partial_\zeta$. Then a change of the cosmological parameters merely results in a shift of time ζ.[2]

Thus, our equations are independent from cosmological parameters Ω_{m0} and $\Omega_{\Lambda 0}$ and once solved, the solutions are valid for all choices of cosmological parameters.

III.   NUMERICAL AND PERTURBATIVE SOLUTIONS OF THE KERNEL TIME DEPENDENCE

As we have anticipated in the previous section, the $\lambda_n^{(\ell)}$ and $\kappa_n^{(\ell)}$ solutions can be obtained either by using the explicit integral solutions given in Eqs. (C3), or alternatively by numerically solving the differential Eqs. (13) and using the correspondence in Eq. (11). Either one is a viable option, although given the plethora of existing tools for solving coupled differential equations, the path via differential equations seems the most practical and efficient. We have used this method to obtain the results in Figure 2. Solid lines denote the relative deviations of $\lambda_n^{(\ell)}$ and $\kappa_n^{(\ell)}$ obtained in the EdS limit from the exact numerical results. Since the ΛCDM universe matches the EdS universe at early times, the deviations vanish at $a = 0$. As expected, the deviations grow with time in all the panels of Figure 2, and can reach values barely shy of ten percent. Note in particular that the typical deviation at redshift $z = 1$ is a factor of a few smaller than its $z = 0$ counterpart. One expects this difference to propagate all the way to correlators.

Given that the number of coefficients at higher orders is large (see Eq. (7)), in Figure 2 we show the average value of all of the deviations and the typical spread (in terms of the one standard deviation). From this, we can observe the trend that, at later times, the deviation of the coefficients from the EdS approximation tends to grow with n, (i.e. when considering higher perturbative orders) and the spread of the coefficient values may also grow (i.e. some tend to be close to the EdS values while for others the deviations can be larger). One might wonder how much of a role outliers play in such analysis. To address this, in Figure 3 we show the relative deviations of the ΛCDM and the EdS results for all the time-dependent coefficients at $a = 1$, up to $n = 5$. Although the $\Delta\lambda_n^{(\ell)}$ are typically $\mathcal{O}(1\%)$ in size, $\Delta\kappa_n^{(\ell)}$ can be as large as $\mathcal{O}(10\%)$, which is not at all negligible when compared to the precision of upcoming observations.

Motivated by the discussion in the last section, we now embark on a journey to find the analytic perturbative solution for the time dependence of the $\lambda_n^{(\ell)}$ and $\kappa_n^{(\ell)}$ coefficients. As shown in Figure 2, EdS approximation for these coefficients is a good starting point, and the deviation are relatively small. It will thus serve us well to use the EdS solution as the result around which to organise the perturbative expansion. These deviations from the EdS approximation are

---

[2]This fact has subsequently been also observed, at the level of one-loop results, in the reference [62].
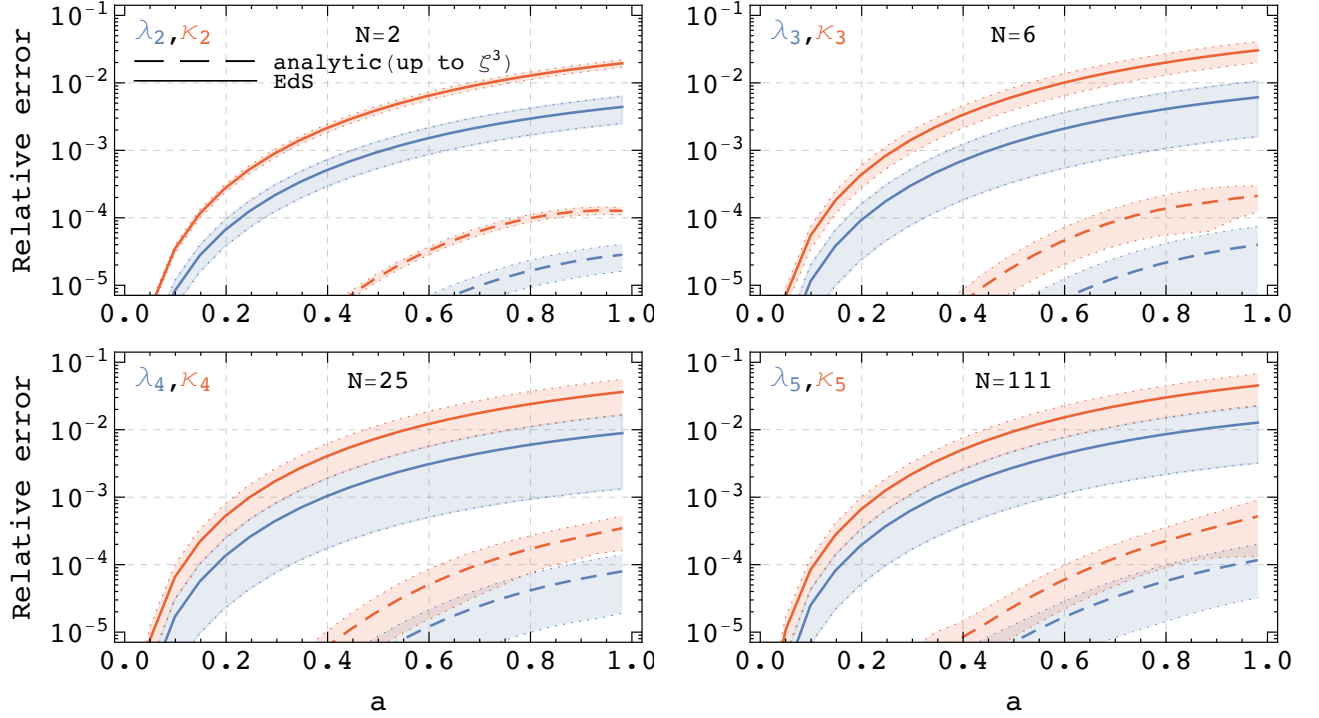
Figure 2: Relative error showing the deviation of the analytic (dashed) and EdS (solid) λ_n and κ_n coefficients from the numerical calculations. The error is defined as $X/X_{\text{num}} - 1$ for $X = \lambda_n^{(\ell)}$ (blue) and $\kappa_n^{(\ell)}$ (red). The above four panels illustrate the typical time evolution of the relative deviations for $n =$ 2 (top left), 3 (top right), 4 (bottom left) and 5 (bottom right). Analytic results correspond to the perturbative calculations up to the third order in ζ, see Eqs. (19) and (D12). The central lines are the average of $N(n)$ lines for each order, while the coloured bands indicate the spread of all of the coefficients in ℓ (i.e. one standard deviation around the mean of all coefficients in ℓ is used). As can be seen in the figure, the analytic results generally agree with the full numerical solution to 0.1% accuracy while the deviation associated to the EdS results can reach up 10% at late times.

encoded in the factor f_-/f_+^2 in the differential Eqs. (13), as well as in the higher order source terms. Since this ratio is exactly $-3/2$ in the EdS limit, we introduce the deviation from the EdS value as a small perturbative parameter,

$$\delta f(\tau) \equiv \frac{f_-(\tau)}{f_+^2(\tau)} + \frac{3}{2}. \tag{15}$$

Figure 1, shows that this dimensionless parameter is $\lesssim 0.2$ in absolute terms throughout the evolution of the Universe. This is a good indication that a convergent perturbative expansion can be obtained by treating δf as a small parameter. In addition to the expansion in δf we are interested in representing δf as a power series in $\zeta \equiv \Omega_{\Lambda 0}/\Omega_{m0}e^{3\eta}$ which would allow us to express the final $\lambda_n^{(\ell)}$ and $\kappa_n^{(\ell)}$ results as a power series in the same variable. We thus expand $W_{m1,m2}^{n\,(ij)}$ and $U_{m1,m2}^{n\,(ij)}$ appearing in Eqs. (13) as

$$W^n = W^{n[0]} + W^{n[1]} + W^{n[2]} + \cdots, \qquad U^n = U^{n[0]} + U^{n[1]} + U^{n[2]} + \cdots, \tag{16}$$

where the superscript $[n]$ denotes the perturbative order with respect to δf, namely $\mathcal{O}(\delta f^n)$, and the suppressed indices are the same in both sides of the equations. Note that order $[0]$ means the solution in the EdS limit. This also corresponds to the static limit of the Eqs. (13), where we drop the time derivative terms turning these equations into recursive algebraic equations. In this limit, once the coefficients are combined with the momentum basis $H_n^{(\ell)}$, one just recovers the usual EdS solutions for the F_n and G_n kernels.

For a detailed derivation of the perturbative results, we refer the reader to Appendix D. Here we just note that the solutions of Eq. (13) at the order of $\mathcal{O}(\delta f^l)$ can be expressed in the integral form of lower order terms

$$W_\alpha^{n[l]} = \mathcal{I}_n \left[\left(\partial_\eta + n + \tfrac{1}{2} \right) (\kappa\lambda)^{[l]} + \delta f \left(\dot{W}_\alpha^{n[l-1]} + (n-1)W_\alpha^{n[l-1]} - (\kappa\lambda)^{[l-1]} \right) \right], \tag{17}$$

$$W_\beta^{n[l]} = \mathcal{I}_n \left[(\kappa\kappa)^{[l]} + \delta f \left(\dot{W}_\beta^{n[l-1]} + (n-1)W_\beta^{n[l-1]} \right) \right],$$
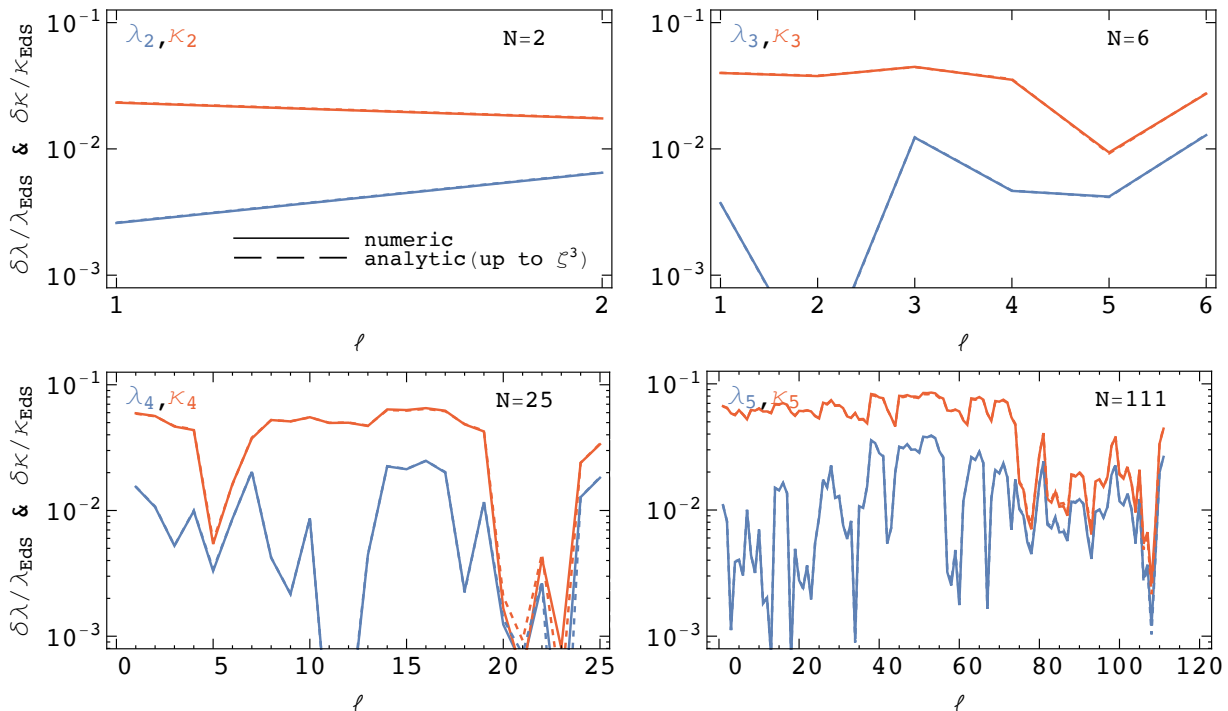
Figure 3: Relative deviation of the $\lambda_n^{(\ell)}$ (blue) $\kappa_n^{(\ell)}$ (red) coefficients in ΛCDM cosmology to the EdS values at the present time, $a = 1$. Shown are both numerical (solid lines) and analytic (dashed lines) results, calculated up to the third power in ζ. Different values of n are given in each panel, coefficients range is $(n, \ell) = (2, 2), (3, 6), (4, 25)$ and $(5, 111)$. $\kappa_n^{(\ell)}$'s tend to have larger errors ranging from 0.1% to almost ten percent, while $\lambda_n^{(\ell)}$'s errors are somewhat smaller reaching up to a few percent. This figure also shows that differences between the ΛCDM and EdS coefficients tend to grow with perturbative order n.

where $\mathcal{I}_n[X]$ is the time functional defined in (D3). Using the above recursive relations repeatedly, one can obtain the expression for the perturbative solutions (D9) for W_α^n and W_β^n. Moreover, to analytically evaluate the integral expressions so obtained, we rely on the expansion of δf in power law form. In Appendix A we show how one may obtain the expansion of δf in powers of $\zeta = \Omega_{\Lambda 0}/\Omega_{m0} e^{3\eta}$. Up to the third order, it reads

$$\delta f(\eta) \simeq c_1 \zeta + c_2 \zeta^2 + c_3 \zeta^3 , \qquad c_1 = -\frac{3}{22}, \; c_2 = -\frac{141}{4114}, \; c_3 = -\frac{9993}{1040842}. \tag{18}$$

Upon performing these steps, we derive the analytic expressions for $\lambda_n^{(\ell)}$ and $\kappa_n^{(\ell)}$ for a generic choice of cosmological parameters $\Omega_{\Lambda 0}$, Ω_{m0}. For instance, at $n = 2$, we obtain

$$\lambda_2^{(1)} = \frac{5}{7} - \frac{c_1}{91}\zeta - \frac{4c_2}{931}\zeta^2 - \frac{2c_3}{875}\zeta^3 , \qquad \lambda_2^{(2)} = \frac{2}{7} + \frac{c_1}{91}\zeta + \frac{4c_2}{931}\zeta^2 + \frac{2c_3}{875}\zeta^3 , \tag{19}$$
$$\kappa_2^{(1)} = \frac{3}{7} - \frac{5c_1}{91}\zeta - \frac{32c_2}{931}\zeta^2 - \frac{22c_3}{875}\zeta^3 , \qquad \kappa_2^{(2)} = \frac{4}{7} + \frac{5c_1}{91}\zeta + \frac{32c_2}{931}\zeta^2 + \frac{22c_3}{875}\zeta^3 ,$$

where we write explicitly only the leading order results in δf, suppressing the $\mathcal{O}(\delta f^2)$ terms. The results for $n = 3$ and 4, namely $\lambda_3^{(\ell)}, \kappa_3^{(\ell)}, \lambda_4^{(\ell)}, \kappa_4^{(\ell)}$, are reported in Eqs. (D12) and (D13). Using this perturbative approach, it is straightforward to generate all terms at higher orders.[3] It suffices here to derive the ones that will be needed for the two-loop calculation (up to the $\lambda_5^{(\ell)}$ and $\kappa_5^{(\ell)}$ coefficients). Given the number of components (recall that for $n = 5$ we have 111 terms), we do not report the explicit expression. Nonetheless, in Figs. 2 and 3 we compare the analytical results at leading order in δf to the numerical ones. One observes that our analytic expressions typically achieve $\mathcal{O}(10^{-3})$ accuracy at the present time and better accuracy at earlier times. Compared to the EdS results, our analytic expressions are about 100 times more accurate.

---

[3] *Mathematica* notebook for these coefficients and H_n kernels, up to the fifth order, can be found in the *arXiv* source file of this paper.

IV. ONE- AND TWO-LOOP POWER SPECTRA

Equipped with the results of the last section, we are now ready to tackle observables such as the matter density and velocity power spectra, as well as the cross power spectrum. In the process, we shall develop and illustrate the utility of a systematic method to handle infrared and ultraviolet divergences in loop integrals. The equivalence principle, fully at work in ΛCDM, guarantees that specific cancellations will take place in the IR configurations of the kernels. Similar cancellations take place due to the mass and momentum conservation, in the absence of which there would be large UV contributions. Such cancellations between large contributions typically require very high precision, thus making numerical integration more difficult and less stable. As we show in the rest of this section, the properties required for such cancellations are all imprinted in the solutions for the λ_n and κ_n coefficients. The coefficients "remember" all the information inherited from their EoM, and we see the equivalence principle, mass and momentum conservation respected and manifested in the various limits of the one- and two-loop power spectra that we study below. One can use these properties in evaluating the loop integrals: we do so by first isolating the leading divergences, analytically confirming they are cancelled out, and numerically evaluating the remaining "regularised" parts of the power spectra.

As observables whose calculation (and target of percent-level precision) requires an improvement upon the EdS approximation, we compute the one-loop and two-loop order of the following power spectra

$$(2\pi)^3\delta^D_{\boldsymbol{k}+\boldsymbol{k}'}P_{\delta\delta}(k) = \langle\delta(\boldsymbol{k})\delta(\boldsymbol{k}')\rangle\,, \quad (2\pi)^3\delta^D_{\boldsymbol{k}+\boldsymbol{k}'}P_{\delta\theta}(k) = \langle\delta(\boldsymbol{k})\theta(\boldsymbol{k}')\rangle\,, \quad (2\pi)^3\delta^D_{\boldsymbol{k}+\boldsymbol{k}'}P_{\theta\theta}(k) = \langle\theta(\boldsymbol{k})\theta(\boldsymbol{k}')\rangle\,. \tag{20}$$

A. One-loop results

Using the notation introduced in Eq. (6), the one-loop results are as follows:

$$\begin{aligned}
P^{\text{1-loop}}_{\delta\delta}(k) &= (\boldsymbol{\lambda}_2 \cdot \boldsymbol{I}_{22} \cdot \boldsymbol{\lambda}_2) + 2\,(\boldsymbol{\lambda}_1 \cdot \boldsymbol{I}_{13} \cdot \boldsymbol{\lambda}_3)\,, \\
P^{\text{1-loop}}_{\delta\theta}(k) &= (\boldsymbol{\lambda}_2 \cdot \boldsymbol{I}_{22} \cdot \boldsymbol{\kappa}_2) + (\boldsymbol{\lambda}_1 \cdot \boldsymbol{I}_{13} \cdot \boldsymbol{\kappa}_3 + 1 \leftrightarrow 3)\,, \\
P^{\text{1-loop}}_{\delta\theta}(k) &= (\boldsymbol{\kappa}_2 \cdot \boldsymbol{I}_{22} \cdot \boldsymbol{\kappa}_2) + 2\,(\boldsymbol{\kappa}_1 \cdot \boldsymbol{I}_{13} \cdot \boldsymbol{\kappa}_3)\,,
\end{aligned} \tag{21}$$

where we have defined the scale dependent integrals

$$\boldsymbol{I}_{22} = 2\int_{\boldsymbol{q}} \boldsymbol{H}_2(\boldsymbol{q},\boldsymbol{k}-\boldsymbol{q}) \otimes \boldsymbol{H}_2(\boldsymbol{q},\boldsymbol{k}-\boldsymbol{q})P_{\text{lin}}(\boldsymbol{q})P_{\text{lin}}(\boldsymbol{k}-\boldsymbol{q})\,, \tag{22}$$

$$\boldsymbol{I}_{13} = 3\int_{\boldsymbol{q}} \boldsymbol{H}_1(\boldsymbol{k}) \otimes \boldsymbol{H}_3(\boldsymbol{k},\boldsymbol{q},-\boldsymbol{q})P_{\text{lin}}(\boldsymbol{k})P_{\text{lin}}(\boldsymbol{q})\,.$$

Note that, when seen as matrices, these integrals have the properties: $\boldsymbol{I}^T_{22} = \boldsymbol{I}_{22}$ and $\boldsymbol{I}_{13} = \boldsymbol{I}^T_{31}$.

In this subsection, we describe an efficient method to compute loop power spectra using the one-loop power spectrum as the simplest example before applying it to two-loop calculations. This method is essentially important to avoid artificial residuals of the physical cancellations and achieve high-precision calculations while saving computational resources. Our strategy is simple. We know the integrals $\boldsymbol{I}_{ij}$ in (21) contain the IR and UV contributions, which eventually cancel. Hence we isolate them as in $\boldsymbol{I}_{ij} = \tilde{\boldsymbol{I}}_{ij} + [\boldsymbol{I}_{ij}]_{\text{IR}} + [\boldsymbol{I}_{ij}]_{\text{UV}}$, where $\tilde{\boldsymbol{I}}_{ij}$ is the remaining regular part. The cancellations of $[\boldsymbol{I}_{ij}]_{\text{IR}}$ and $[\boldsymbol{I}_{ij}]_{\text{UV}}$ are analytically confirmed. Then, we focus on the numerical evaluations of the regularised contributions from $\tilde{\boldsymbol{I}}_{ij}$.

We begin with $\boldsymbol{I}_{22}$. One can see that its IR contributions come from two configurations, namely $\boldsymbol{q} \to 0$, and $\boldsymbol{q} \to \boldsymbol{k}$. It is convenient at this point to re-map the second sector to the first one (see [47]) as

$$\boldsymbol{I}_{22} = \int_{|\boldsymbol{q}|<|\boldsymbol{k}-\boldsymbol{q}|} + \int_{|\boldsymbol{q}|\geq|\boldsymbol{k}-\boldsymbol{q}|} = 4\int_{\boldsymbol{q}} \boldsymbol{H}_2(\boldsymbol{q},\boldsymbol{k}-\boldsymbol{q}) \otimes \boldsymbol{H}_2(\boldsymbol{q},\boldsymbol{k}-\boldsymbol{q})\Theta(|\boldsymbol{k}-\boldsymbol{q}|-q)P_{\text{lin}}(\boldsymbol{q})P_{\text{lin}}(\boldsymbol{k}-\boldsymbol{q})\,. \tag{23}$$

We extract the IR and UV contributions in this integrand. Using the asymptotic form of the kernels, one can write

$$\boldsymbol{H}_2(\boldsymbol{q},\boldsymbol{k}-\boldsymbol{q}) \otimes \boldsymbol{H}_2(\boldsymbol{q},\boldsymbol{k}-\boldsymbol{q}) \sim \begin{cases} \boldsymbol{h}^{(2)}_{22,\text{IR}}(\boldsymbol{k},\hat{q})\,\frac{k^2}{q^2} + \boldsymbol{h}^{(1)}_{22,\text{IR}}(\boldsymbol{k},\hat{q})\,\frac{k}{q} + \mathcal{O}(q^0)\,, & \text{as}\;\; q \to 0\,, \\ \boldsymbol{h}^{(4)}_{22,\text{UV}}(\hat{k},\boldsymbol{q})\,\frac{k^4}{q^4} + \mathcal{O}(k^5)\,, & \text{as}\;\; k \to 0\,. \end{cases} \tag{24}$$

For the explicit form of the $\boldsymbol{H}_n$ operators in the various limits, as well as the asymptotics of $\boldsymbol{h}^{(n)}_{22}$, we refer the reader to Appendix E. Having identified both the IR and UV limits of the kernel products, we can introduce the regularised

version of our integral (we label it $\tilde{I}_{22}$) by subtracting these contributions only in the asymptotic regimes. In order to do so, we introduce window functions, $W_{22}^{\mathrm{IR}}(k)$ and $W_{22}^{\mathrm{UV}}(k)$, which ensure that the appropriate asymptotic form is applied only in the IR and UV regimes. The regularised integral is thus given by

$$
\tilde{I}_{22} = \int_q \left[4H_2(q, k-q) \otimes H_2(q, k-q)\Theta(|k-q|-q)P_{\mathrm{lin}}(k-q) \right. \tag{25}
$$
$$
\left. - 4\left(h_{22,\mathrm{IR}}^{(2)}(k,\hat{q})\frac{k^2}{q^2} + h_{22,\mathrm{IR}}^{(1)}(k,\hat{q})\frac{k}{q} \right) W_{22}^{\mathrm{IR}}(k)P_{\mathrm{lin}}(k) - 2h_{22,\mathrm{UV}}^{(4)}(\hat{k},q)\frac{k^4}{q^4}W_{22}^{\mathrm{UV}}(k)P_{\mathrm{lin}}(q) \right] P_{\mathrm{lin}}(q),
$$

where one can write $I_{22} = \tilde{I}_{22} + [I_{22}]_{\mathrm{IR}} + [I_{22}]_{\mathrm{UV}}$, with

$$
[I_{22}]_{\mathrm{IR}} = 4\int_q \left(h_{22,\mathrm{IR}}^{(2)}(k,\hat{q})\frac{k^2}{q^2} + h_{22,\mathrm{IR}}^{(1)}(k,\hat{q})\frac{k}{q} \right) W_{22}^{\mathrm{IR}}P_{\mathrm{lin}}(k)P_{\mathrm{lin}}(q) = \left(h_{22}^{\mathrm{IR}}W_{22}^{\mathrm{IR}} \right) k^2\sigma_2^2 P_{\mathrm{lin}}(k) , \tag{26}
$$
$$
[I_{22}]_{\mathrm{UV}} = 2\int_q h_{22,\mathrm{UV}}^{(4)}(\hat{k},q)\frac{k^4}{q^4}W_{22}^{\mathrm{UV}}P_{\mathrm{lin}}(q)P_{\mathrm{lin}}(q) = \left(h_{22}^{\mathrm{UV}}W_{22}^{\mathrm{UV}} \right) k^4\Sigma_2^2 .
$$

Here we have introduced $\Sigma_2^2 = \frac{1}{3}\int_q P_{\mathrm{lin}}(q)^2/q^2$, $\sigma_2^2 = \frac{1}{3}\int_q P_{\mathrm{lin}}(q)/q^2$, and

$$
h_{22}^{\mathrm{IR}} = \begin{pmatrix} 1 & 1 \\ 1 & 1 \end{pmatrix} \quad \text{and} \quad h_{22}^{\mathrm{UV}} = \frac{1}{2}\begin{pmatrix} \frac{7}{5} & -1 \\ -1 & 3 \end{pmatrix}, \tag{27}
$$

as also shown in Appendix E. Note that the UV contribution does not have an additional factor of two since it does not require a re-map in the low k limit.

Let us specify the window functions W_{22}^{IR} and W_{22}^{UV}. The task we demand of these functions is to effectively restrict the domain of the contribution they are multiplied by into the appropriate momenta configuration, i.e. high and low k regimes respectively. We are free to choose the form of such functions that is best suited for the task at hand. We choose one convenient and simple form

$$
W_{22}^{\mathrm{IR}}(k) = \frac{(k/k_{\mathrm{IR}})^4}{1+(k/k_{\mathrm{IR}})^4}, \quad \text{and} \quad W_{22}^{\mathrm{UV}}(k) = \frac{1}{1+(k/k_{\mathrm{UV}})^6}, \tag{28}
$$

with parameters $k_{\mathrm{IR}} \approx 0.1\mathrm{Mpc}/h$ and $k_{\mathrm{UV}} \approx 0.2\mathrm{Mpc}/h$. It will, of course, be convenient to choose $W_{22}^{\mathrm{IR}} = W_{13}^{\mathrm{IR}}$, in order to quickly arrive at the cancellation of the leading IR contributions in the total one-loop power spectrum.

Let us turn to the I_{13} term, where the asymptotic contributions are

$$
H_1(k) \otimes H_3(k, q, -q) \sim \begin{cases} h_{13,\mathrm{IR}}^{(2)}(k,\hat{q})\frac{k^2}{q^2} + \mathcal{O}(q^0) , & \text{as } q \to 0, \\ h_{13,\mathrm{UV}}^{(0)}(\hat{k},q) + h_{13,\mathrm{UV}}^{(2)}(\hat{k},q)\frac{k^2}{q^2} + \mathcal{O}(k^4) , & \text{as } k \to 0. \end{cases} \tag{29}
$$

In an analogous way to $\tilde{I}_{22}$, we can introduce the regularised integrals as

$$
\tilde{I}_{13} = 3\int_q \left[H_1(k) \otimes H_3(k, q, -q) \right. \tag{30}
$$
$$
\left. - h_{13,\mathrm{IR}}^{(2)}(k,\hat{q})\frac{k^2}{q^2}W_{13}^{\mathrm{IR}} - \left(h_{13,\mathrm{UV}}^{(0)}(\hat{k},q) + h_{13,\mathrm{UV}}^{(2)}(\hat{k},q)\frac{k^2}{q^2} \right) W_{13}^{\mathrm{UV}} \right] P_{\mathrm{lin}}(k)P_{\mathrm{lin}}(q),
$$

i.e. $I_{13} = \tilde{I}_{13} + [I_{13}]_{\mathrm{IR}} + [I_{13}]_{\mathrm{UV}}$ with

$$
[I_{13}]_{\mathrm{IR}} = 3\int_q h_{13,\mathrm{IR}}^{(2)}(k,\hat{q})\frac{k^2}{q^2}W_{13}^{\mathrm{IR}}P_{\mathrm{lin}}(k)P_{\mathrm{lin}}(q) = \left(h_{13}^{\mathrm{IR}}W_{13}^{\mathrm{IR}} \right) k^2\sigma_2^2 P_{\mathrm{lin}}(k) , \tag{31}
$$
$$
[I_{13}]_{\mathrm{UV}} = 3P_{\mathrm{lin}}(k)\int_q h_{13,\mathrm{UV}}^{(2)}(\hat{k},q)\frac{k^2}{q^2}W_{13}^{\mathrm{UV}}P_{\mathrm{lin}}(k)P_{\mathrm{lin}}(q) = \left(h_{13}^{\mathrm{UV}}W_{13}^{\mathrm{UV}} \right) k^2\sigma_2^2 P_{\mathrm{lin}}(k),
$$

where $h_{13}^{\mathrm{IR}} = -\begin{pmatrix} 1 & 1 & 0 & 0 & 1 & 1 \end{pmatrix}$ and $h_{13}^{\mathrm{UV}} = -\left(1, 1, -\frac{12}{5}, 0, 5, 1 \right)$. Here, since $\lambda_3 \cdot h_{13,\mathrm{UV}}^{(0)} = \kappa_3 \cdot h_{13,\mathrm{UV}}^{(0)} = 0$, the term $h_{13,\mathrm{UV}}^{(0)}$ does not contribute to the power spectrum and is not included in $[I_{13}]_{\mathrm{UV}}$. The remaining UV contribution comes only from the next-to-leading order term $h_{13,\mathrm{UV}}^{(2)}$.
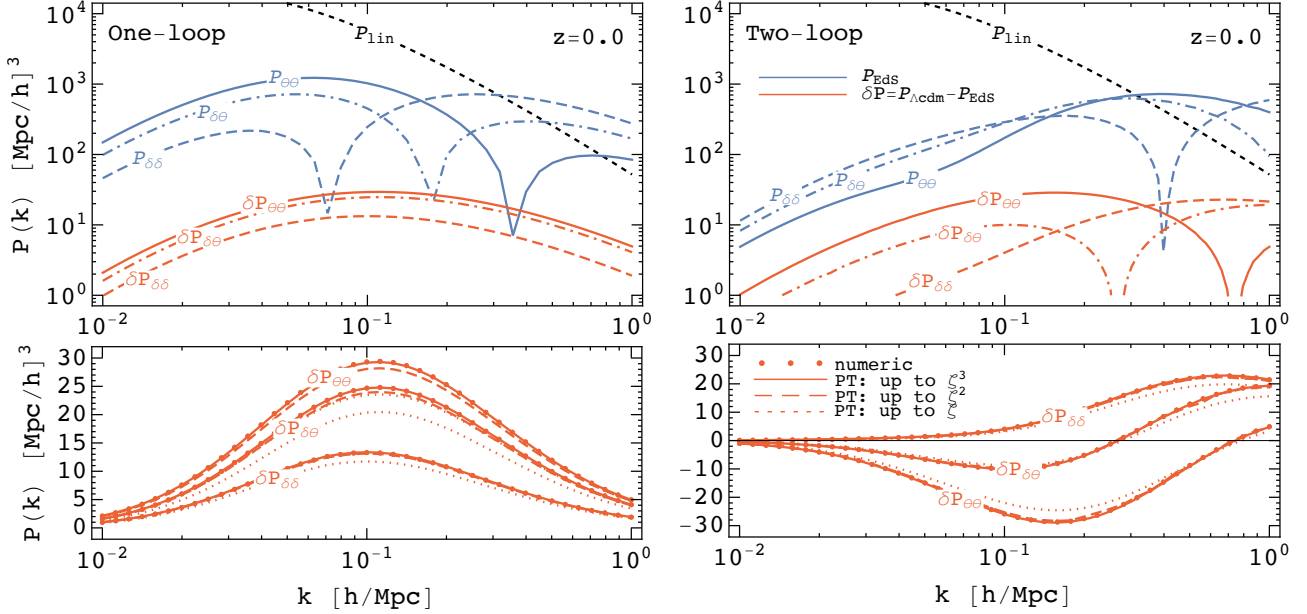
Figure 4: One- (left panel) and two-loop (right panel) contributions to the density-density, density-velocity and velocity-velocity power spectrum. *Upper panels* show the absolute contributions of EdS results (blue lines) compared to the ΛCDM corrections (red lines). We see that the three different spectra $P_{\delta\delta}$ (dashed lines), $P_{\delta\theta}$ (dot-dashed lines) and $P_{\theta\theta}$ (solid lines) receive corrections of different sizes, whose relative importance is also a function of the scale dependence of the EdS terms. *Lower panels* display the ΛCDM corrections $\delta P_{\delta\delta}$, $\delta P_{\delta\theta}$ and $\delta P_{\theta\theta}$ computed using the numerical evaluations of the λ_n and κ_n coefficients (shown in dots). We also show the perturbative time dependence computation as described in Sec. III. The results including the $\mathcal{O}(\zeta^1)$ (dotted lines), $\mathcal{O}(\zeta^2)$ (dashed lines) and $\mathcal{O}(\zeta^3)$ (solid lines) contributions are shown. Results are shown for redshift $z = 0.0$.

This is of course guaranteed by the mass and momentum conservation of the original EoM [8]. We now move to the IR cancellations. As soon as the "22" and "13" terms are combined, we find

$$(\boldsymbol{\lambda}_2 \cdot [\boldsymbol{I}_{22}]_{\mathrm{IR}} \cdot \boldsymbol{\lambda}_2) + 2 (\boldsymbol{\lambda}_1 \cdot [\boldsymbol{I}_{13}]_{\mathrm{IR}} \cdot \boldsymbol{\lambda}_3) = \left[(\boldsymbol{\lambda}_2 \cdot \boldsymbol{h}_{22}^{\mathrm{IR}} \cdot \boldsymbol{\lambda}_2) W_{22}^{\mathrm{IR}} + 2 (\boldsymbol{\lambda}_1 \cdot \boldsymbol{h}_{13}^{\mathrm{IR}} \cdot \boldsymbol{\lambda}_3) W_{13}^{\mathrm{IR}} \right] k^2 \sigma_2^2 P_{\mathrm{lin}}(k) = 0, \qquad (32)$$

where we take $W_{22}^{\mathrm{IR}} = W_{13}^{\mathrm{IR}}$. This is of course the same as the usual IR cancellation between P_{22} and P_{13} in standard perturbation theory (SPT) [8]: it is guaranteed for equal-time correlators by the equivalence principle, as has been discussed in [57, 59, 60, 63–66]. The same cancellations take place for the velocity-velocity spectrum and for the velocity-density cross-spectrum. The final expression for the one-loop density power spectrum is

$$P_{\delta\delta}^{\text{1-loop}}(k) = (\boldsymbol{\lambda}_2 \cdot \boldsymbol{\mathcal{I}}_{22} \cdot \boldsymbol{\lambda}_2) + 2 (\boldsymbol{\lambda}_1 \cdot \boldsymbol{\mathcal{I}}_{13} \cdot \boldsymbol{\lambda}_3), \qquad (33)$$

and analogous expressions hold for the other two observables, $P_{\delta\theta}^{\text{1-loop}}$ and $P_{\theta\theta}^{\text{1-loop}}$, with the appropriate time-dependent coefficients in the same way as Eqs. (21). The momentum dependent matrices $\boldsymbol{\mathcal{I}}_{ij}$ that all the three power spectra share at one-loop order are given by

$$\boldsymbol{\mathcal{I}}_{22} = \tilde{\boldsymbol{I}}_{22} + \left(\boldsymbol{h}_{22}^{\mathrm{UV}} W_{22}^{\mathrm{UV}} \right) k^4 \Sigma_4^2, \qquad \text{and} \qquad \boldsymbol{\mathcal{I}}_{13} = \tilde{\boldsymbol{I}}_{13} + \left(\boldsymbol{h}_{13}^{\mathrm{UV}} W_{13}^{\mathrm{UV}} \right) k^2 \sigma_2^2 P_{\mathrm{lin}}. \qquad (34)$$

We numerically evaluate these regularised expressions, a procedure that circumvents the expensive numerical treatment of the IR and UV cancellations and saves significant computational time.

In the left panels of Figure 4 we show the one-loop contributions for all these power spectra: $P_{\delta\delta}$, $P_{\delta\theta}$ and $P_{\theta\theta}$. In particular, we display the EdS solutions and the corresponding ΛCDM correction to the EdS result, i.e. $\delta P_{\delta\delta} = P_{\delta\delta}^{\Lambda\mathrm{cdm}} - P_{\delta\delta}^{\mathrm{EdS}}$ (and equivalently for the other two spectra). As one can see from the figure, the one-loop ΛCDM corrections are from one to two orders of magnitude smaller than the one-loop EdS contributions. However, the relevant regime lies in the higher k range ($k \gtrsim 0.1h/\mathrm{Mpc}$), given that is where the one-loop contributions start to be comparable in amplitude to the linear result. Moving towards higher redshift the corrections relative to the EdS result decrease further (see Appendix G).

In Figure 5 we show the ratio of the three different total power spectra in ΛCDM relative to the EdS results. The left panels display the one-loop results, where the upper left panel shows the one-loop spectra without adding counterterms to either EdS or ΛCDM solutions. We see that, at $z = 0$, the largest corrections range from a half (for $\delta P_{\delta\delta}$) to a few percent (for $P_{\theta\theta}$) at scales $k \sim 0.4 h/\text{Mpc}$ (scales where higher loop results are also relevant). These results are consistent with the earlier findings shown in [42, 43, 45]). In the bottom panel of the same figure we plot the effects of the EFT counterterms on the total deviations from ΛCDM. First, we note that for the typical values of the counterterms, shown as the central lines within the grey bands, the relative difference in the power spectra is lowered. This is expected since the counterterms contributions to the total power spectrum is of the same size as the loop contributions at the relevant scales and by construction are equivalent in both the ΛCDM and EdS case.

Grey bands around each of the three power spectrum lines show the effects of variations (of order 5%) in the values of the ΛCDM counterterms. As one can see, assuming the $\sim 1\%$ accuracy thresholds, the presence of a counterterm can make up for the deviation between the EdS and the ΛCDM result for the density-density power spectrum. This is not the case for the density-velocity and velocity-velocity power spectra, which exhibit a noticeably steeper scale dependence.

As the last comment on Figure 5, we note that, in addition to the results obtained by numerical evaluation of the λ_n and κ_n coefficients (shown as black lines), we also show in the upper left panel the perturbative results given in Eqs. (19) and (D12). The profiles corresponding to the $\mathcal{O}(\zeta^1)$ perturbative order are shown explicitly (red lines), and we see that they exhibit up to 0.5% agreement with the full numerical solutions. The perturbative solutions accounting up to $\mathcal{O}(\zeta^3)$ order expansion are not shown as they would be indistinguishable from the full numerical solutions already present in these plots.

B. Two-loop results

In the rest of this section we turn our attention to the the two-loop results. Writing the perturbative contributions in the separable form, we have

$$P_{\delta\delta}^{\text{2-loop}}(k) = (\boldsymbol{\lambda}_3 \cdot \boldsymbol{I}_{33} \cdot \boldsymbol{\lambda}_3) + 2\,(\boldsymbol{\lambda}_2 \cdot \boldsymbol{I}_{24} \cdot \boldsymbol{\lambda}_4) + 2\,(\boldsymbol{\lambda}_1 \cdot \boldsymbol{I}_{15} \cdot \boldsymbol{\lambda}_5)\,, \tag{35}$$
$$P_{\delta\theta}^{\text{2-loop}}(k) = (\boldsymbol{\lambda}_3 \cdot \boldsymbol{I}_{33} \cdot \boldsymbol{\kappa}_3) + (\boldsymbol{\lambda}_2 \cdot \boldsymbol{I}_{24} \cdot \boldsymbol{\kappa}_4 + 2 \leftrightarrow 4) + (\boldsymbol{\lambda}_1 \cdot \boldsymbol{I}_{15} \cdot \boldsymbol{\kappa}_5 + 1 \leftrightarrow 5)\,,$$
$$P_{\theta\theta}^{\text{2-loop}}(k) = (\boldsymbol{\kappa}_3 \cdot \boldsymbol{I}_{33} \cdot \boldsymbol{\kappa}_3) + 2\,(\boldsymbol{\kappa}_2 \cdot \boldsymbol{I}_{24} \cdot \boldsymbol{\kappa}_4) + 2\,(\boldsymbol{\kappa}_1 \cdot \boldsymbol{I}_{15} \cdot \boldsymbol{\kappa}_5)\,,$$

where the two-loop integral functions are

$$\boldsymbol{I}_{33} = 3\int_{\boldsymbol{q},\boldsymbol{p}} \bigg(2\boldsymbol{H}_3(\boldsymbol{k}-\boldsymbol{q}-\boldsymbol{p},\boldsymbol{q},\boldsymbol{p}) \otimes \boldsymbol{H}_3(\boldsymbol{k}-\boldsymbol{q}-\boldsymbol{p},\boldsymbol{q},\boldsymbol{p})P_{\text{lin}}(\boldsymbol{k}-\boldsymbol{q}-\boldsymbol{p}) \tag{36}$$

$$+ 3\boldsymbol{H}_3(\boldsymbol{k},-\boldsymbol{q},\boldsymbol{q}) \otimes \boldsymbol{H}_3(\boldsymbol{k},-\boldsymbol{p},\boldsymbol{p})P_{\text{lin}}(\boldsymbol{k}) \bigg) P_{\text{lin}}(\boldsymbol{q})P_{\text{lin}}(\boldsymbol{p})\,,$$

$$\boldsymbol{I}_{24} = 12\int_{\boldsymbol{q},\boldsymbol{p}} \boldsymbol{H}_2(\boldsymbol{k}-\boldsymbol{q},\boldsymbol{q}) \otimes \boldsymbol{H}_4(\boldsymbol{k}-\boldsymbol{q},\boldsymbol{q},\boldsymbol{p},-\boldsymbol{p})P_{\text{lin}}(\boldsymbol{k}-\boldsymbol{q})P_{\text{lin}}(\boldsymbol{q})P_{\text{lin}}(\boldsymbol{p})\,,$$

$$\boldsymbol{I}_{15} = 15\int_{\boldsymbol{q},\boldsymbol{p}} \boldsymbol{H}_1(\boldsymbol{k}) \otimes \boldsymbol{H}_5(\boldsymbol{k},\boldsymbol{q},-\boldsymbol{q},\boldsymbol{p},-\boldsymbol{p})P_{\text{lin}}(\boldsymbol{k})P_{\text{lin}}(\boldsymbol{q})P_{\text{lin}}(\boldsymbol{p})\,.$$

and one may verify that $\boldsymbol{I}_{33}^T = \boldsymbol{I}_{33}$, $\boldsymbol{I}_{24} = \boldsymbol{I}_{42}^T$ and $\boldsymbol{I}_{15}(k) = \boldsymbol{I}_{51}^T(k)$.

In the two-loop calculation, there are two integration variables $\boldsymbol{q}$ and $\boldsymbol{p}$. UV and IR divergences may result from integrating in both these variables. After having identified such divergent contributions, our goal is to subtract them from the integrands and implement the cancellation explicitly, in full analogy with the one-loop case above. The procedure in the two-loop case is somewhat more involved: besides the leading divergencies (when specific limits of both $\boldsymbol{q}$ and $\boldsymbol{p}$ produce a divergent contribution), one can have sub-leading terms associated with a specific limit of only one of the two variables, while the contribution from the other stays finite. We provide more details on the UV and IR properties of the two-loop result in Appendix F, and we briefly summarise some of the key properties below.

Similarly to the one-loop case, the IR contribution extracted from the individual two-loop terms ought to cancel as a consequence of the equivalence principle and consistency relations (see [60] e.g. for a recent explicit treatment).

Hence one may verify the following cancellation

$$\boldsymbol{\lambda}_3 \cdot ([\boldsymbol{I}_{33,\text{I}}]_{\text{IR}} + [\boldsymbol{I}_{33,\text{II}}]_{\text{IR}}) \cdot \boldsymbol{\lambda}_3 + 2\boldsymbol{\lambda}_2 \cdot [\boldsymbol{I}_{24}]_{\text{IR}} \cdot \boldsymbol{\lambda}_4 + 2\boldsymbol{\lambda}_1 \cdot [\boldsymbol{I}_{15}]_{\text{IR}} \cdot \boldsymbol{\lambda}_5 = 0, \tag{37}$$

and similarly for the cross- and auto- correlations including κ_n coefficients. Plugging the expressions derived in Appendix F, we have

$$\left(\boldsymbol{\lambda}_3 \cdot \boldsymbol{h}^{\mathrm{IR}}_{33,\mathrm{I}} \cdot \boldsymbol{\lambda}_3 + 2\boldsymbol{\lambda}_2 \cdot \boldsymbol{h}^{\mathrm{IR}}_{24,\mathrm{II}} \cdot \boldsymbol{\lambda}_4 + 2\boldsymbol{\lambda}_1 \cdot \boldsymbol{h}^{\mathrm{IR}}_{15} \cdot \boldsymbol{\lambda}_5\right) W^{\mathrm{IR}}_{\mathrm{I}} k^2 P_{\mathrm{lin}}(\boldsymbol{k}) = 0 \,, \tag{38}$$
$$\left(\boldsymbol{\lambda}_3 \cdot \boldsymbol{h}^{\mathrm{IR}}_{33,\mathrm{II}} \cdot \boldsymbol{\lambda}_3 + 2\boldsymbol{\lambda}_2 \cdot \boldsymbol{h}^{\mathrm{IR}}_{24,\mathrm{I}} \cdot \boldsymbol{\lambda}_4\right) W^{\mathrm{IR}}_{\mathrm{II}} k^2 = 0 \,,$$

where we used that $W^{\mathrm{IR}}_{33,\mathrm{I}} = W^{\mathrm{IR}}_{24,\mathrm{II}} = W^{\mathrm{IR}}_{15} = W^{\mathrm{IR}}_{\mathrm{I}}$ and $W^{\mathrm{IR}}_{33,\mathrm{II}} = W^{\mathrm{IR}}_{24,\mathrm{I}} = W^{\mathrm{IR}}_{\mathrm{II}}$. The fact that the cancellation occurs independently in two different terms was also pointed out in [47]. More explicitly, we can write

$$\boldsymbol{\lambda}_3 \cdot \hat{\boldsymbol{h}}^{(2)}_{33,\mathrm{I,IR}} \cdot \boldsymbol{\lambda}_3 + 2\boldsymbol{\lambda}_2 \cdot \hat{\boldsymbol{h}}^{(2)}_{24,\mathrm{II,IR}} \cdot \boldsymbol{\lambda}_4 + 2\boldsymbol{\lambda}_1 \cdot \hat{\boldsymbol{h}}^{(2)}_{15,\mathrm{IR}} \cdot \boldsymbol{\lambda}_5 = 0 \,, \tag{39}$$
$$\boldsymbol{\lambda}_3 \cdot \hat{\boldsymbol{h}}^{(2)}_{33,\mathrm{II,IR}} \cdot \boldsymbol{\lambda}_3 + 2\boldsymbol{\lambda}_2 \cdot \hat{\boldsymbol{h}}^{(2)}_{24,\mathrm{I,IR}} \cdot \boldsymbol{\lambda}_4 = 0 \,.$$

In addition, IR and UV cancellations take place as a consequence of the mass and momentum conservation. Thus, in addition to the condition $\boldsymbol{\lambda}_3 \cdot [\boldsymbol{H}_{3,\mathrm{I}}]^{(0)}_{\mathrm{UV}} = \boldsymbol{\kappa}_3 \cdot [\boldsymbol{H}_{3,\mathrm{I}}]^{(0)}_{\mathrm{UV}} = 0$, one may also verify how the contributions from $\boldsymbol{h}^{(0)}_{15}$ vanish after contractions with the $\boldsymbol{\lambda}_5$ and $\boldsymbol{\kappa}_5$ coefficients.

Using such properties in the IR and UV regimes as well as the appropriately defined window functions W^{IR} and W^{UV}, one may introduce the regularised integrals $\tilde{\boldsymbol{I}}_{33,\mathrm{I}}$, $\tilde{\boldsymbol{I}}_{33,\mathrm{II}}$, $\tilde{\boldsymbol{I}}_{24}$ and $\tilde{\boldsymbol{I}}_{15}$, which are shown explicitly in Appendix F. These steps mirror the procedure we employed in the one-loop case and motivate our introducing the regularised two-loop expressions,

$$P^{2\text{-loop}}_{\delta\delta}(k) = (\boldsymbol{\lambda}_3 \cdot \boldsymbol{\mathcal{I}}_{33} \cdot \boldsymbol{\lambda}_3) + 2\left(\boldsymbol{\lambda}_2 \cdot \boldsymbol{\mathcal{I}}_{24} \cdot \boldsymbol{\lambda}_4\right) + 2\left(\boldsymbol{\lambda}_1 \cdot \boldsymbol{\mathcal{I}}_{15} \cdot \boldsymbol{\lambda}_5\right) \,, \tag{40}$$

and similarly for $P^{2\text{-loop}}_{\delta\theta}$ and $P^{2\text{-loop}}_{\theta\theta}$. The regularised integral functions $\boldsymbol{\mathcal{I}}_{ij}$, including the sub-leading UV contributions that are isolated and subsequently computed, read

$$\boldsymbol{\mathcal{I}}_{33} = \tilde{\boldsymbol{I}}_{33,\mathrm{I}} + \tilde{\boldsymbol{I}}_{33,\mathrm{II}} + \left(\boldsymbol{h}^{\mathrm{UV}}_{33,\mathrm{I}} W^{\mathrm{UV}}_{33,\mathrm{I}}\right) k^4 P_{\mathrm{lin}}(k) + \left(\boldsymbol{h}^{\mathrm{UV}}_{33,\mathrm{II}} W^{\mathrm{UV}}_{33,\mathrm{II}}\right) k^4 \,, \tag{41}$$
$$\boldsymbol{\mathcal{I}}_{24} = \tilde{\boldsymbol{I}}_{24} + \left(\boldsymbol{h}^{\mathrm{UV}}_{24} W^{\mathrm{UV}}_{24}\right) k^4 \,,$$
$$\boldsymbol{\mathcal{I}}_{15} = \tilde{\boldsymbol{I}}_{15} + \left(\boldsymbol{h}^{\mathrm{UV}}_{15} W^{\mathrm{UV}}_{15}\right) k^2 P_{\mathrm{lin}} \,,$$

where all the terms are written explicitly in Appendix F.

In the right panels of Figure 4, we show the two-loop contributions for the three power spectra $P_{\delta\delta}$, $P_{\delta\theta}$ and $P_{\theta\theta}$. The two-loop ΛCDM corrections are typically one to two orders of magnitude smaller than the EdS contributions. However, they can in fact dominate in the regimes where EdS contributions have zero crossing.

Figure 5 shows the ratio of the three total power spectra in ΛCDM relative to the EdS results. In the right panels, we plot our two-loop results. The upper right panel displays the two-loop spectra without the effect of counterterms either in the EdS or ΛCDM case. The deviations range from a few percent (for $\delta P_{\delta\delta}$) to a dozen percents (for e.g. $P_{\delta\theta}$) at scales $k \gtrsim 0.4h/\mathrm{Mpc}$.[4] In the bottom panel of the same figure we include the EFT counterterms for both P_{EdS} and $P_{\Lambda\mathrm{cdm}}$. For two-loops, this is done so that the additional counterterms only cancel the $k^2 P_{\mathrm{lin}}$ contributions, and so we effectively only have counterterms that are already present at one-loop order.

These are shown as the central lines within the grey bands, while the bands themselves represent the effects of variations of the ΛCDM counterterms by 5%. One can see how the addition of counterterms can significantly change the relative differences between the ΛCDM and EdS results, reducing it to below ten percent on most of the scales of interest. We stress the high sensitivity of these lines on the values of the counterterms. This is especially so for $P_{\theta\theta}$, in which case the values of the counterterms affect the zero crossing of the total two-loop power spectrum prediction.

As in the case of one-loop results, we also compare our two-loop numerical results (i.e. those obtained using the numerical values for λ_n and κ_n) to their perturbative counterpart. These are shown both in Figure 4 and in Figure 5 as orange lines. We see that adding the linear corrections in the ζ parameter reaches roughly a few percent agreements with the full numerical results, while adding corrections up to ζ^3 renders the results essentially indistinguishable from the numerical findings.

Before closing this section, a few comments on computational methods are in order. Our proposed method for dealing with the cancellation of these divergences differs from the one suggested in [47] in that it explicitly subtracts the contributions that are cancelled at the level of the integrand(s). In the case of EdS, the difference between the two

---

[4]These results also agree with the numerical results obtained in the reference [67].
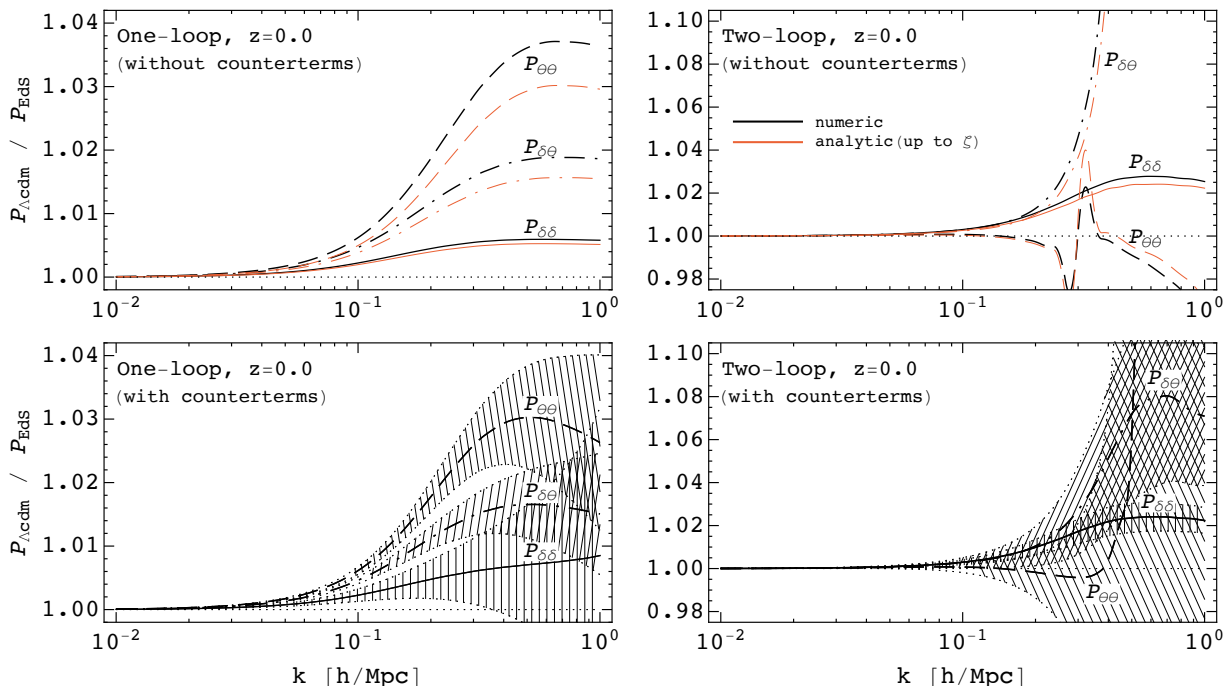
Figure 5: The ratio of the ΛCDM and the EdS density-density (solid lines), density-velocity (dot-dashed lines), velocity-velocity (dashed lines) power spectrum at the redshift $z = 0.0$. *Upper panels* show the ratios of these spectra without any counterterms. Black lines denote spectra computed by numerically evaluating the λ_n and κ_n coefficients, while the orange lines show the perturbatively evaluated coefficients up to the linear corrections in ζ. Adding the corrections up to order ζ^3 would superimpose the perturbative results onto the numerical ones (black lines). *Lower panels* show the ratio of the power spectra when including the leading EFT counterterms ($\sim k^2 P_{\rm lin}$), the latter having been chosen to roughly match the realistic values ($c_{\delta\delta}^2 \approx 3.0$, $c_{\delta\theta}^2 \approx -1.0$, $c_{\theta\theta}^2 \approx -1.5$). Grey hashed bands centred on each of the lines indicate the 5% variation in the values for the counterterms.

recipes is not particularly noteworthy: the cancellations, encoded in the analytic coefficients in the F_n and G_n kernels, can be implemented with machine-level accuracy since they amount to subtractions of simple fractions. In ΛCDM the time coefficients, when obtained numerically, are computed with finite accuracy which can generate some spurious remainders in the cancellations. These can spoil the accuracy when evaluating the various integrals. For this reason, it is quite useful to implement subtraction and cancellation of the key contributions analytically. We also note that in our perturbative treatment of the coefficients λ_n and κ_n given in Eqs. (19) and in Appendix D these cancellations are enforced at each ζ order. Since the corresponding pre-factors of ζ powers are also given as fractions, the implicit method proposed in [47] may also be applied at each ζ order. We are able to confirm that the power spectra with the perturbative coefficients computed in this manner reproduce the same results as our proposed method, thus providing yet another consistency check for our treatment of the regularised integral functions.

V.   DISCUSSION AND CONCLUSIONS

Perturbative approaches to structure formation allow us to develop controlled analytical predictions on the physics of mildly non-linear scales. Although limited in its reach to large scales, the perturbative scheme provides a clean and systematic treatment of LSS dynamics. In particular, it is the ideal framework to highlight the role of symmetries and related properties, such as the equivalence principle, mass and momentum conservation (see [59, 60]), in the construction of cosmological correlations, the key observables in large scale structure.

In this work, we develop exact, separable solutions for PT kernels of density and velocity fields in ΛCDM cosmology. So far, such explicit solutions have been obtained only within the EdS approximation, with the extensions to ΛCDM worked out analytically only to lower orders. In this work, we presented a recursive solution valid up to arbitrary order in perturbation theory, providing in particular an algorithm to obtain separable solutions for the F_n and G_n kernels at each perturbative order n.

The solutions building blocks are elements of the basis of the momentum dependent operators $\boldsymbol{H}_n$. The (upper limit

on the) dimension of the basis depends on the perturbative order n and is given by the number $N(n)$, for which we also provide the explicit recursive expression. To obtain the full kernels F_n and G_n, this momentum operator basis has to be appropriately "contracted" with the time-dependent coefficients for matter and velocity fields, respectively dubbed $\boldsymbol{\lambda}_n$ and $\boldsymbol{\kappa}_n$.

We arrive at the solutions for the time coefficients following two different paths. First, starting from the implicit integral solutions obtained in [45], we obtain the recursive integral solution for $\boldsymbol{\lambda}_n$ and $\boldsymbol{\kappa}_n$. We show that these can be recast as the solutions to a set of coupled differential equations, which we find quite suitable for numerical treatment. We are then able to compute our numerical benchmark solutions, which we use in the remainder of our analysis. The analysis of the differential equations makes it clear that the "clock", i.e. the time evolution, is set by the combination of growth rates f_-/f_+^2, whose time dependence in ΛCDM cosmology is completely determined by the new variable $\zeta = \Omega_{\Lambda,0}/\Omega_{m,0}D_+$. This implies that using ζ as the time variable in solving for the $\boldsymbol{\lambda}_n$ and $\boldsymbol{\kappa}_n$ coefficients one obtains solutions valid universally in ΛCDM, that is irrespective of the choice of cosmological parameters. This significantly simplifies the computational task involved in the cosmological parameter search.

As an alternative path to the solution, equipped with the differential equations we develop an analytic perturbative solution for the $\boldsymbol{\lambda}_n$ and $\boldsymbol{\kappa}_n$ coefficients. The starting point of this perturbative solution lies in the observation that the EdS approximation, a static solution to the set of our differential equations, is an excellent (yet insufficient) approximation to the full set of the $\boldsymbol{\lambda}_n$ and $\boldsymbol{\kappa}_n$ coefficients, especially at lower orders. This suggests that we organise the perturbative treatment around the parameter $\delta f = 3/2 + f_-/f_+^2$. We have obtained the general perturbative solution, laying the basis for an iterative path to the time coefficients. We then applied our algorithm to derive solutions up to the leading correction in δf, and implemented our procedure all the way to the $\boldsymbol{\lambda}_5$ and $\boldsymbol{\kappa}_5$ coefficients needed for the two-loop power spectrum calculations.

The final form of these perturbative solutions is given in terms of the variable ζ so as to fully capture the dependence on cosmological parameters. We investigated the agreement of our perturbative solutions with the full numerical evaluation and found a perfect agreement for all coefficients up to $n = 5$ if terms up to third order in ζ are included. We also note that the perturbative solutions exhibit, at each order in ζ, similar behaviour as the EdS solutions when it comes to IR cancellations and properties that stem from mass and momentum conservation. This makes them particularly well suited for use in the numerical evaluation of higher loop power spectra that rely on accurate cancellations in their integrands. Let us also mention that these findings may be generalised to beyond-ΛCDM scenarios, something we will address in future work.

As an application of our results, we compute one- and two-loop matter and velocity auto- and cross-power spectra. We compare our solutions and explore the differences between the EdS and ΛCDM solutions. The results are summarized in Figures 4 and 5. We find that some care has to be exerted in quantifying these differences since a fraction of the effect in the one- and two-loop contributions can be re-absorbed in the EFT counterterms, which can be treated as free coefficients of the perturbative loop expansion. Specifically, in the one-loop case, the difference in the density-density power spectrum between ΛCDM and EdS can be fully reabsorbed by the counterterms at the scales and accuracy of interest. For the velocity statistics, the deviation is instead more pronounced, at the level of a few percent, even when fully engaging counterterms. At two-loop the ΛCDM deviation from the EdS result increases to a couple of percent, which, to a large extent, can again be covered by counterterms. In terms of the velocity related statistics, the results depend rather heavily on the numerical values of the required counterterms, with the latter requiring calibration against N-body simulations, something that goes beyond the scope of our analysis. Nevertheless, our work clearly shows how the deviation could reach ten percent at the scales of interest, as demonstrated in Figure 5.

Beyond their use in higher loop calculations, our results are also readily applicable in tackling higher n-point functions, such as the bispectrum, the trispectrum, etc. Remarkably, these observables are sensitive to the ΛCDM deviations from the EdS approximation already at tree-level (see [61] and also [44, 68] for the recent investigations).

Lastly, we ought to comment on the fact that the dark matter density and velocity are not directly observable but act as the building components within the more general framework of the biased tracers of large scale structure (see, e.g. [26]). Given the additional dynamics (and degeneracies) associated with the presence of the bias coefficients, one ought to take into account what survives of the discrepancies such as the one between the EdS and ΛCDM solutions at the level of the observables. This has been recently explored in [43] at one loop order. It would be quite interesting to do the corresponding analysis at two loops. This will be possible upon deriving the two-loop results for biased tracers in redshift space. This is yet another line of investigation we plan to pursue in the near future. It is possible that deviations like the ones studied here might well bias our parameter inference and would thus need to be included in the budget of possible theoretical systematic errors. It is important to keep this budget to a minimum given that parameter tensions of several sigmas are nowadays a familiar occurrence in data-driven cosmology.

Appendix A: Linear growth and decay factors and rates

In this appendix, we summarise the linear growth solutions and derive some of the results in a form useful for our subsequent computation. In particular, we derive a specific form in which we can expand the linear growth rate combination f_-/f_+^2 around the EdS value.

We start from the well-known solutions for $D_\pm$, these are

$$D_+ = \frac{5}{2}H_0^2\Omega_{\mathrm{m}0}H(a)\int_0^a \frac{\mathrm{d}\tilde{a}}{\tilde{a}^3 H^3(\tilde{a})}\,, \qquad D_- = \frac{H(a)}{H_0}\,, \tag{A1}$$

where $\Omega_{\mathrm{m}0}$ and $\Omega_{\Lambda 0}$ are the current energy fractions of dark matter and the cosmological constant, respectively. The Hubble parameter is given by $H(a) = H_0\sqrt{\Omega_{m0}a^{-3} + \Omega_{\Lambda 0}}$, where the radiation component can be ignored. Changing the time variable into $q \equiv a^3\Omega_{\Lambda 0}/\Omega_{m0}$ and performing the integral in D_+, we find

$$\hat{D}_+ \equiv \left(\frac{\Omega_{\Lambda 0}}{\Omega_{m0}}\right)^{\frac{1}{3}} D_+ = q^{\frac{1}{3}}\,_2F_1\left(1,\frac{1}{3},\frac{11}{6},-q\right)\,, \tag{A2}$$

where we introduced $\hat{D}_+$, which depends only on q, and $_2F_1(a,b,c,z)$ is the hypergeometric function. Using the above equations, we can compute $\delta f = f_-/f_+^2 + 3/2 = (\mathrm{d}\ln H/\mathrm{d}\ln a)(D_+/a)^2(\mathrm{d}D_+/\mathrm{d}a)^{-2} + 3/2$ obtaining

$$\delta f = \frac{3}{2}\left[1 - 4(1+q)\left(\frac{5}{_2F_1(1,1/3,11/6,-q)} - 3\right)^{-2}\right]\,. \tag{A3}$$

This expression is useful for the purpose of numerical treatments. However, we choose to further reduce $\hat{D}_+$ and δf to obtain simplified expressions. Expanding $\hat{D}_+$ around $q = 0$, one finds

$$\hat{D}_+ \simeq q^{\frac{1}{3}}\left[1 - \epsilon\frac{2}{11}q + \epsilon^2\frac{16}{187}q^2 - \epsilon^3\frac{224}{4301}q^3 + \ldots\right]\,, \tag{A4}$$

where we inserted a bookkeeping parameter ϵ. Inverting the above expression by plugging an ansatz, $q = Q_0 + \epsilon Q_1 + \epsilon^2 Q_2 + \epsilon^3 Q_3 + \cdots$, and solving for Q_n at each order in ϵ, we obtain

$$q \simeq \hat{D}_+^3 + \epsilon\frac{6}{11}\hat{D}_+^6 + \epsilon^2\frac{492}{2057}\hat{D}_+^9 + \epsilon^3\frac{50216}{520421}\hat{D}_+^{12} + \ldots\,. \tag{A5}$$

We can also expand δf around $q = 0$ to obtain

$$\delta f \simeq -\frac{3}{22}q + \epsilon\frac{15}{374}q^2 - \epsilon^2\frac{21585}{1040842}q^3 + \epsilon^3\frac{74212575}{5644486166}q^4 + \cdots\,. \tag{A6}$$

By substituting Eq. (A5) into this equation, one finds an analytic expression for δf in powers of D_+,

$$\delta f \simeq c_1\left(\frac{\Omega_{\Lambda 0}}{\Omega_{m0}}\right)D_+^3 + c_2\left(\frac{\Omega_{\Lambda 0}}{\Omega_{m0}}\right)^2 D_+^6 + c_3\left(\frac{\Omega_{\Lambda 0}}{\Omega_{m0}}\right)^3 D_+^9 + c_4\left(\frac{\Omega_{\Lambda 0}}{\Omega_{m0}}\right)^4 D_+^{12} + \ldots\,, \tag{A7}$$

with c_1, c_2, c_3 given below Eq. (18) and $c_4 = -\frac{15954399}{5644486166}$. Here we omit the higher order correction $\mathcal{O}(D_+^{15})$ and set $\epsilon = 1$. We find that c_4 and the higher order terms obtained in this manner do not significantly improve the fit to δf, as can also be deduced from Figure 1. In this work it will therefore suffice to truncate the expansion so as to include the c_1, c_2 and c_3 coefficients. Nevertheless, we note that the extension to higher orders is straightforward within the formalism developed in this work.

Appendix B: Direct integral solutions of the dark matter kernels

In Section II we have presented the integral solutions for the dark matter kernels. Here we return to these findings providing further details for each component of the solution. We start from the EoMs and briefly review the solutions obtained in [45]. With the symmetrized kernels $F_n(\boldsymbol{q}_1,..,\boldsymbol{q}_n,\eta)$ and $G_n(\boldsymbol{q}_1,..,\boldsymbol{q}_n,\eta)$ in Eq. (4), the EoMs given in Eq. (1) read

$$\dot{F}_n + n\,F_n - G_n = h_\alpha^{(n)}(\boldsymbol{q}_1,..,\boldsymbol{q}_n,\eta)\,, \tag{B1}$$

$$\dot{G}_n + (n-1)\,G_n - \frac{f_-}{f_+^2}\,(G_n - F_n) = h_\beta^{(n)}(\boldsymbol{q}_1,..,\boldsymbol{q}_n,\eta)\,,$$

where we used the shorthand notation $\dot{} = \partial/\partial\eta$ (remember that $\eta \equiv \ln D_+$). The functions $f_{+,-}$ are defined as $f_{+,-} \equiv \mathrm{d}\ln D_{+,-}/\mathrm{d}\ln a$. The source terms are given by:

$$h_\alpha^{(n)}(\boldsymbol{q}_1,..,\boldsymbol{q}_n,\eta) = \sum_{\pi-\text{all}}\sum_{m=1}^{n-1}\alpha(\boldsymbol{p}_m,\boldsymbol{p}_{n-m})G_m(\boldsymbol{q}_1,..,\boldsymbol{q}_m,\eta)F_{n-m}(\boldsymbol{q}_{m+1},..,\boldsymbol{q}_n,\eta) \tag{B2}$$

$$= \sum_{m=1}^{n-1}\frac{m!(n-m)!}{n!}\sum_{\pi-\text{cross}}\alpha(\boldsymbol{p}_m,\boldsymbol{p}_{n-m})G_m F_{n-m}$$

$$= \delta_{\frac{n}{2},\lfloor\frac{n}{2}\rfloor}^K\frac{(n/2!)^2}{n!}\sum_{\pi-\text{cross}}\alpha(\boldsymbol{p}_{n/2},\boldsymbol{p}_{n/2})G_{n/2}F_{n/2}$$

$$+ \sum_{m=1}^{\lfloor(n-1)/2\rfloor}\frac{m!(n-m)!}{n!}\sum_{\pi-\text{cross}}\Big[\alpha(\boldsymbol{p}_m,\boldsymbol{p}_{n-m})G_m F_{n-m} + \alpha(\boldsymbol{p}_{n-m},\boldsymbol{p}_m)G_{n-m}F_m\Big]\,,$$

$$h_\beta^{(n)}(\boldsymbol{q}_1,..,\boldsymbol{q}_n,\eta) = \sum_{\pi-\text{all}}\sum_{m=1}^{n-1}\beta(\boldsymbol{p}_m,\boldsymbol{p}_{m-n})G_m(\boldsymbol{q}_1,..,\boldsymbol{q}_m,\eta)G_{n-m}(\boldsymbol{q}_{m+1},..,\boldsymbol{q}_n,\eta)\,,$$

$$= \delta_{\frac{n}{2},\lfloor\frac{n}{2}\rfloor}^K\frac{(n/2!)^2}{n!}\sum_{\pi-\text{cross}}\beta(\boldsymbol{p}_{n/2},\boldsymbol{p}_{n/2})\,G_{n/2}G_{n/2}$$

$$+ 2\sum_{m=1}^{\lfloor(n-1)/2\rfloor}\frac{m!(n-m)!}{n!}\sum_{\pi-\text{cross}}\beta(\boldsymbol{p}_m,\boldsymbol{p}_{n-m})\,G_m G_{n-m}\,.$$

where the subscript "$\pi-$all" stands for symmetrization over all momenta $\{\mathbf{q}_1\dots\mathbf{q}_n\}$ while $\pi-$cross indicates permutations that exchange the momenta in the $\{1\dots m\}$ set with those in the $\{m+1\dots n\}$ set. In the last line of Eq. (B2) the double counting for the case when n is even has been removed. The following definitions have also been employed: $\boldsymbol{p}_m = \boldsymbol{q}_1 + .. + \boldsymbol{q}_m$; $\boldsymbol{p}_{n-m} = \boldsymbol{q}_{m+1} + .. + \boldsymbol{q}_n$. Combining the two expressions in Eq. (B1) one readily obtains the EoM for the first kernel F_n:

$$\ddot{F}_n + \dot{F}_n\left(2n-1-\frac{f_-}{f_+^2}\right) + (n-1)F_n\left(n-\frac{f_-}{f_+^2}\right) = h_\beta^{(n)} + \left(n-1-\frac{f_-}{f_+^2}\right)h_\alpha^{(n)} + \dot{h}_\alpha^{(n)}\,, \tag{B3}$$

whose solution reads:

$$F_n(\eta) = \int_{-\infty}^\eta \mathrm{d}\tilde{\eta}\,e^{(n-1)(\tilde{\eta}-\eta)}\frac{\tilde{f}_+}{\tilde{f}_+ - \tilde{f}_-}\left[\left(\tilde{h}_\beta^{(n)} - \frac{\tilde{f}_-}{\tilde{f}_+}\tilde{h}_\alpha^{(n)}\right) + e^{\tilde{\eta}-\eta}\frac{D_-(\eta)}{D_-(\tilde{\eta})}\left(\tilde{h}_\alpha^{(n)} - \tilde{h}_\beta^{(n)}\right)\right]\,, \tag{B4}$$

where in deriving the above we have used Eq. (3) for the growing and decaying solutions for the linear growth factor $D_\pm(\eta)$. Using again the first expression in Eq. (B1) one arrives at the solution for the G kernels:

$$G_n(\eta) = \int_{-\infty}^\eta \mathrm{d}\tilde{\eta}\,e^{(n-1)(\tilde{\eta}-\eta)}\frac{\tilde{f}_+}{\tilde{f}_+ - \tilde{f}_-}\left[\left(\tilde{h}_\beta^{(n)} - \frac{\tilde{f}_-}{\tilde{f}_+}\tilde{h}_\alpha^{(n)}\right) + e^{\tilde{\eta}-\eta}\frac{f_-}{f_+}\frac{D_-(\eta)}{D_-(\tilde{\eta})}\left(\tilde{h}_\alpha^{(n)} - \tilde{h}_\beta^{(n)}\right)\right]\,, \tag{B5}$$

where again a function with tilde depends not on the variable a but the variable $\tilde{a}$ (e.g. $\tilde{D}_+ \equiv D_+(\tilde{a})$). Note that the time-dependent coefficients of $\tilde{h}_\alpha^{(n)}$ and $\tilde{h}_\beta^{(n)}$ in the integrands of Eqs. (B4) and (B5), also require integration, thus

implying recursive time integrals, something that is far from ideal for a fast evaluation. Eqs. (B4) and (B5) are the integral solutions, to all orders, as first derived in [45]. Changing the time variable in favour of the scaling factor a, we can express these solutions in the form

$$F_n(\boldsymbol{q}_1, .., \boldsymbol{q}_n, a) = \int_0^a \frac{\mathrm{d}\tilde{a}}{\tilde{a}} \left(w_\alpha^{(n)}(a, \tilde{a}) h_\alpha^{(n)}(\boldsymbol{q}_1, .., \boldsymbol{q}_n, \tilde{a}) + w_\beta^{(n)}(a, \tilde{a}) h_\beta^{(n)}(\boldsymbol{q}_1, .., \boldsymbol{q}_n, \tilde{a}) \right), \tag{B6}$$

$$G_n(\boldsymbol{q}_1, .., \boldsymbol{q}_n, a) = \int_0^a \frac{\mathrm{d}\tilde{a}}{\tilde{a}} \left(u_\alpha^{(n)}(a, \tilde{a}) h_\alpha^{(n)}(\boldsymbol{q}_1, .., \boldsymbol{q}_n, \tilde{a}) + u_\beta^{(n)}(a, \tilde{a}) h_\beta^{(n)}(\boldsymbol{q}_1, .., \boldsymbol{q}_n, \tilde{a}) \right),$$

as was presented in the Eq. (5). The Green's function components are given by

$$w_\alpha^{(n)}(a, \tilde{a}) = w^{(n)}(a, \tilde{a}) \left(1 - \delta(\tilde{a}) d(a, \tilde{a}) \right), \qquad w_\beta^{(n)}(a, \tilde{a}) = -w^{(n)}(a, \tilde{a}) \left(1 - d(a, \tilde{a}) \right), \tag{B7}$$

$$u_\alpha^{(n)}(a, \tilde{a}) = w^{(n)}(a, \tilde{a}) \left(\delta(a) - \delta(\tilde{a}) d(a, \tilde{a}) \right), \qquad u_\beta^{(n)}(a, \tilde{a}) = -w^{(n)}(a, \tilde{a}) \left(\delta(a) - d(a, \tilde{a}) \right),$$

where we introduced the quantities

$$w^{(n)}(a, \tilde{a}) = \left(\frac{\tilde{D}_+}{D_+} \right)^n \frac{\tilde{f}_+^2}{\tilde{f}_+ - \tilde{f}_-} \frac{D_-}{\tilde{D}_-}, \quad d(a, \tilde{a}) = \frac{\tilde{D}_-}{D_-} \frac{D_+}{\tilde{D}_+}, \quad \delta(a) = \frac{f_-}{f_+}. \tag{B8}$$

Moreover, we find that $w_{\alpha,\beta}^{(n)}$ and $u_{\alpha,\beta}^{(n)}$ satisfy a simple relation,

$$w_\alpha^{(n)}(a, \tilde{a}) + w_\beta^{(n)}(a, \tilde{a}) = u_\alpha^{(n)}(a, \tilde{a}) + u_\beta^{(n)}(a, \tilde{a}) = w^{(n)} d(1 - \tilde{\delta}) = \left(\frac{\tilde{D}_+}{D_+} \right)^{n-1} \tilde{f}_+. \tag{B9}$$

Eq. (B9) indicates that not all of the Green's functions are independent: there are relations between them that can be obtained at each order n. We see how these come to play when computing the one- and two- loop power spectra in Section III.

Appendix C: Derivation of the separable kernels

In Appendix B we have shown the explicit integral form of the solutions for the F_n and G_n kernels. In this appendix, we recast such solutions into separable form $F_n = \boldsymbol{\lambda}_n \cdot \boldsymbol{H}_n$ and $G_n = \boldsymbol{\kappa}_n \cdot \boldsymbol{H}_n$, as indicated in Section II. Plugging Eqs. (B2) and (6) into the right hand side of Eq. (5), and separately re-organizing the momentum-dependent and time-dependent terms, one finds

$$F_n(a) = \delta_{\frac{n}{2}, \lfloor \frac{n}{2} \rfloor}^K \sum_{i=1}^{N(n/2)} \sum_{j=1}^{N(n/2)} W_{\alpha;n/2,n/2}^{(ij)} [h_\alpha]_{n/2,n/2}^{(ij)} + \delta_{\frac{n}{2}, \lfloor \frac{n}{2} \rfloor}^K \sum_{i=1}^{N(n/2)} \sum_{j=i}^{N(n/2)} \left[2 - \delta_{ij}^K \right] W_{\beta;n/2,n/2}^{(ij)} [h_\beta]_{n/2,n/2}^{(ij)} \tag{C1}$$

$$+ \sum_{m=1}^{\lfloor (n-1)/2 \rfloor} \sum_{i=1}^{N(m)} \sum_{j=1}^{N(n-m)} \left(W_{\alpha;m,n-m}^{(ij)} [h_\alpha]_{m,n-m}^{(ij)} + W_{\alpha;n-m,m}^{(ji)} [h_\alpha]_{n-m,m}^{(ji)} + 2 W_{\beta;m,n-m}^{(ij)} [h_\beta]_{m,n-m}^{(ij)} \right),$$

$$G_n(a) = \delta_{\frac{n}{2}, \lfloor \frac{n}{2} \rfloor}^K \sum_{i=1}^{N(n/2)} \sum_{j=1}^{N(n/2)} U_{\alpha;n/2,n/2}^{(ij)} [h_\alpha]_{n/2,n/2}^{(ij)} + \delta_{\frac{n}{2}, \lfloor \frac{n}{2} \rfloor}^K \sum_{i=1}^{N(n/2)} \sum_{j=i}^{N(n/2)} \left[2 - \delta_{ij}^K \right] U_{\beta;n/2,n/2}^{(ij)} [h_\beta]_{n/2,n/2}^{(ij)}$$

$$+ \sum_{m=1}^{\lfloor (n-1)/2 \rfloor} \sum_{i=1}^{N(m)} \sum_{j=1}^{N(n-m)} \left(U_{\alpha;m,n-m}^{(ij)} [h_\alpha]_{m,n-m}^{(ij)} + U_{\alpha;n-m,m}^{(ji)} [h_\alpha]_{n-m,m}^{(ji)} + 2 U_{\beta;m,n-m}^{(ij)} [h_\beta]_{m,n-m}^{(ij)} \right),$$

with the momentum basis source terms $[h_\alpha]$ and $[h_\beta]$ defined as

$$[h_\alpha]_{m,n-m}^{(ij)}(\boldsymbol{q}_1, .., \boldsymbol{q}_n) = \frac{m!(n-m)!}{n!} \sum_{\pi-\mathrm{cross}} \alpha(\boldsymbol{q}_m, \boldsymbol{q}_{n-m}) H_m^{(i)}(\boldsymbol{q}_1, .., \boldsymbol{q}_m) H_{n-m}^{(j)}(\boldsymbol{q}_{m+1}, .., \boldsymbol{q}_n), \tag{C2}$$

$$[h_\beta]_{m,n-m}^{(ij)}(\boldsymbol{q}_1, .., \boldsymbol{q}_n) = \frac{m!(n-m)!}{n!} \sum_{\pi-\mathrm{cross}} \beta(\boldsymbol{q}_m, \boldsymbol{q}_{n-m}) H_m^{(i)}(\boldsymbol{q}_1, .., \boldsymbol{q}_m) H_{n-m}^{(j)}(\boldsymbol{q}_{m+1}, .., \boldsymbol{q}_n).$$

We have also introduced the time-dependent coefficients

$$W_{\alpha;m_1,m_2}^{n,(ij)}(a) = \int_0^a \frac{\mathrm{d}\tilde{a}}{\tilde{a}} w_\alpha^{(n)}(a,\tilde{a})\kappa_{m_1}^{(i)}(\tilde{a})\lambda_{m_2}^{(j)}(\tilde{a}), \qquad W_{\beta;m_1,m_2}^{n,(ij)}(a) = \int_0^a \frac{\mathrm{d}\tilde{a}}{\tilde{a}} w_\beta^{(n)}(a,\tilde{a})\kappa_{m_1}^{(i)}(\tilde{a})\kappa_{m_2}^{(j)}(\tilde{a}),$$

$$U_{\alpha;m_1,m_2}^{n,(ij)}(a) = \int_0^a \frac{\mathrm{d}\tilde{a}}{\tilde{a}} u_\alpha^{(n)}(a,\tilde{a})\kappa_{m_1}^{(i)}(\tilde{a})\lambda_{m_2}^{(j)}(\tilde{a}), \qquad U_{\beta;m_1,m_2}^{n,(ij)}(a) = \int_0^a \frac{\mathrm{d}\tilde{a}}{\tilde{a}} u_\beta^{(n)}(a,\tilde{a})\kappa_{m_1}^{(i)}(\tilde{a})\kappa_{m_2}^{(j)}(\tilde{a}), \tag{C3}$$

which are constructed from to the Green's functions introduced in Eq. (B7), as well as from the lower order coefficients λ_n and κ_n.

Note that Eqs. (C1) are already in the form required in Eq. (6). However, there remains to be chosen a counting algorithm that systematically maps (bijectively) the $[h_\alpha]_{m,n-m}^{(ij)}$ and $[h_\beta]_{m,n-m}^{(ij)}$ operators to the $H_n^{(\ell)}$ operators. The running of the various indices in the h operators will correspond to the running of the index ℓ in $H_n^{(\ell)}$ according to $\ell = 1, 2, \ldots, N(n)$ at any given order n. We shall employ the algorithm based on the following five "counting" functions:

$$\phi_1(n,i,j) = N\left(\tfrac{n}{2}\right)(i-1) + j, \qquad \phi_2(n,i,j) = \left(N\left(\tfrac{n}{2}\right)\right)^2 - \frac{1}{2}i(i-1) + \phi_1(n,i,j), \tag{C4}$$

$$\phi_3(n,m,i,j) = \delta_{\frac{n}{2},\lfloor\frac{n}{2}\rfloor}^K \frac{1}{2}N\left(\tfrac{n}{2}\right)\left(3N\left(\tfrac{n}{2}\right)+1\right) + \sum_{k=1}^{m-1} N(k)N(n-k) + (i-1)N(n-m) + j,$$

$$\phi_4(n,m,i,j) = \sum_{k=1}^{\lfloor(n-1)/2\rfloor} N(k)N(n-k) + \phi_3(n,m,i,j), \qquad \phi_5(n,m,i,j) = 2\sum_{k=1}^{\lfloor(n-1)/2\rfloor} N(k)N(n-k) + \phi_3(n,m,i,j).$$

For a given n, the $\phi_{1,\ldots,5}$ counters run through all the relevant values of the indices $\{m,i,j\}$, eventually covering[5] all the $N(n)$ entries and mapping all of the $[h_\alpha]_{m,n-m}^{(ij)}$ and $[h_\beta]_{m,n-m}^{(ij)}$ operators to $H_n^{(\ell)}$ operators. As shown in Eq. (9), using this mapping, we obtain a closed expression

$$H_n^{(\ell)}(\boldsymbol{q}_1,..,\boldsymbol{q}_n) = \delta_{\frac{n}{2},\lfloor\frac{n}{2}\rfloor}^K \sum_{i=1}^{N(n/2)} \left[\sum_{j=1}^{N(n/2)} [h_\alpha]_{\frac{n}{2},\frac{n}{2}}^{(ij)} \delta_{\ell,\phi_1}^K + \sum_{j=i}^{N(n/2)} \left[2 - \delta_{ij}^K\right] [h_\beta]_{\frac{n}{2},\frac{n}{2}}^{(ij)} \delta_{\ell,\phi_2}^K \right] \tag{C5}$$

$$+ \sum_{m=1}^{\lfloor(n-1)/2\rfloor} \sum_{i=1}^{N(m)} \sum_{j=1}^{N(n-m)} \left([h_\alpha]_{m,n-m}^{(ij)} \delta_{\ell,\phi_3}^K + [h_\alpha]_{n-m,m}^{(ji)} \delta_{\ell,\phi_4}^K + 2[h_\beta]_{m,n-m}^{(ij)} \delta_{\ell,\phi_5}^K \right),$$

with the initial terms $H_2^{(1)} = \alpha$ and $H_2^{(2)} = \beta$, and one can systematically compute the higher momentum operators using definition of the sourcing terms $[h_\alpha]$ and $[h_\beta]$ given in Eq. (C2).

Once this mapping is chosen for the $H_n^{(\ell)}$ operators, it immediately fixes the mapping between the $\lambda_n(\kappa_n)$ and W (U) time coefficients. Explicitly we have

$$\lambda_n^{(\ell)}(a) = \delta_{\frac{n}{2},\lfloor\frac{n}{2}\rfloor}^K \sum_{i=1}^{N(n/2)} \left[\sum_{j=1}^{N(n/2)} W_{\alpha;n/2,n/2}^{(ij)} \delta_{\ell,\phi_1}^K + \sum_{j=i}^{N(n/2)} W_{\beta;\frac{n}{2},\frac{n}{2}}^{(ij)} \delta_{\ell,\phi_2}^K \right] \tag{C6}$$

$$+ \sum_{m=1}^{\lfloor(n-1)/2\rfloor} \sum_{i=1}^{N(m)} \sum_{j=1}^{N(n-m)} \left(W_{\alpha;m,n-m}^{(ij)} \delta_{\ell,\phi_3}^K + W_{\alpha;n-m,m}^{(ji)} \delta_{\ell,\phi_4}^K + W_{\beta;m,n-m}^{(ij)} \delta_{\ell,\phi_5}^K \right),$$

$$\kappa_n^{(\ell)}(a) = \delta_{\frac{n}{2},\lfloor\frac{n}{2}\rfloor}^K \sum_{i=1}^{N(n/2)} \left[\sum_{j=1}^{N(n/2)} U_{\alpha;n/2,n/2}^{(ij)} \delta_{\ell,\phi_1}^K + \sum_{j=i}^{N(n/2)} U_{\beta;\frac{n}{2},\frac{n}{2}}^{(ij)} \delta_{\ell,\phi_2}^K \right]$$

$$+ \sum_{m=1}^{\lfloor(n-1)/2\rfloor} \sum_{i=1}^{N(m)} \sum_{j=1}^{N(n-m)} \left(U_{\alpha;m,n-m}^{(ij)} \delta_{\ell,\phi_3}^K + U_{\alpha;n-m,m}^{(ji)} \delta_{\ell,\phi_4}^K + U_{\beta;m,n-m}^{(ij)} \delta_{\ell,\phi_5}^K \right),$$

---

[5]One may choose, for example, to first fix a value for m starting with the lowest possible, $m = 1$, then do the same for the index i, and run through the index j, again running from the lowest to the highest value allowed etc. So long as this is done consistently, no ambiguity arises in the process.

with W and U coefficients given in Eq. (C3). We have thus achieved the separation of the F_n and G_n kernels in the purely momentum dependent operators H_n and time dependent coefficients λ_n and κ_n. However, the time coefficients are still determined by the recursive time integrals given in Eq. (C3). In order to facilitate the evaluation of these coefficients we can recast these integral expressions into differential equations. After some manipulation of our integral solutions, we obtain

$$\dot{W}_{\alpha;m_1,m_2}^{n\,(ij)} + nW_{\alpha;m_1,m_2}^{n\,(ij)} - U_{\alpha;m_1,m_2}^{n\,(ij)} = \kappa_{m_1}^{(i)}\lambda_{m_2}^{(j)}, \quad (C7)$$

$$\dot{W}_{\beta;m_1,m_2}^{n\,(ij)} + nW_{\beta;m_1,m_2}^{n\,(ij)} - U_{\beta;m_1,m_2}^{n\,(ij)} = 0,$$

$$\dot{U}_{\alpha;m_1,m_2}^{n\,(ij)} + (n-1)U_{\alpha;m_1,m_2}^{n\,(ij)} - \frac{f_-}{f_+^2}\left[U_{\alpha;m_1,m_2}^{n\,(ij)} - W_{\alpha;m_1,m_2}^{n\,(ij)}\right] = 0,$$

$$\dot{U}_{\beta;m_1,m_2}^{n\,(ij)} + (n-1)U_{\beta;m_1,m_2}^{n\,(ij)} - \frac{f_-}{f_+^2}\left[U_{\beta;m_1,m_2}^{n\,(ij)} - W_{\beta;m_1,m_2}^{n\,(ij)}\right] = \kappa_{m_1}^{(i)}\kappa_{m_2}^{(j)},$$

which we have also presented in Eq. (13). This form is convenient for the recursive numerical treatment using the $\lambda_1^{(1)} = \kappa_1^{(1)} = 1$ initial conditions. These expressions are used in Section III to compare the results with the analytic perturbative treatment derived in Appendix D.

Before we close this appendix and turn our attention towards obtaining the analytic solutions for these time coefficients, we note that it is useful to count the number of coefficients at each perturbative order n. As we have indicated when postulating the ansatz in Eq. (6), we expect the the number of the basis elements $N(n)$ to be a function of the perturbative order. Thus, counting the terms given either in the Eq. (9), or equivalently in Eq. (11) gives

$$N(n) = \delta_{\frac{n}{2},\lfloor\frac{n}{2}\rfloor}^K \frac{1}{2}N\left(\frac{n}{2}\right)\left(3N\left(\frac{n}{2}\right)+1\right) + 3\sum_{m=1}^{\lfloor(n-1)/2\rfloor} N(m)N(n-m), \quad (C8)$$

which, up to the fifth order, yields the numbers given in Eq. (7). As noted in Section II, not all of these time coefficients are independent, there are indeed several constraints that effectively reduce the dimension of the operators basis down from the upper bound $N(n)$.

Appendix D: Perturbative solution of the time-dependence

In Section III we have summarised the perturbative solution for the time-dependent coefficients $\lambda_n^{(\ell)}$ and $\kappa_n^{(\ell)}$. Here we present the derivation. In this appendix, we show how we can analytically invert the differential equations given in Eqs. (13) (and Eqs. (C7)) and thus represent the solution as a power expansion in δf parameter.

We start by eliminating $U_{\alpha,\beta}^n$ from the equations given in Eqs. (13), to find the EoMs for $W_{\alpha,\beta}^n$. As expected, we end up with the second order differential equations that read

$$\ddot{W}_{\alpha;m_1,m_2}^{n\,(ij)} + \left(2n+\frac{1}{2}-\delta f\right)\dot{W}_{\alpha;m_1,m_2}^{n\,(ij)} + \left(n^2+\frac{n-3}{2}-(n-1)\delta f\right)W_{\alpha;m_1,m_2}^{n\,(ij)} = \left(\partial_\eta+n+\frac{1}{2}-\delta f\right)\kappa_{m_1}^{(i)}\lambda_{m_2}^{(j)}, \quad (D1)$$

$$\ddot{W}_{\beta;m_1,m_2}^{n\,(ij)} + \left(2n+\frac{1}{2}-\delta f\right)\dot{W}_{\beta;m_1,m_2}^{n\,(ij)} + \left(n^2+\frac{n-3}{2}-(n-1)\delta f\right)W_{\beta;m_1,m_2}^{n\,(ij)} = \kappa_{m_1}^{(i)}\kappa_{m_2}^{(j)}.$$

Further on we suppress the indices, n, m_1, m_2 and (ij), that are not relevant for the following calculation, given that they stay the same on the right and the left side of the equations. We can reorganise the above equations perturbatively w.r.t. δf, recasting them as

$$\ddot{W}_\alpha^n + \left(2n+\frac{1}{2}\right)\dot{W}_\alpha^n + \left(n^2+\frac{n}{2}-\frac{3}{2}\right)W_\alpha^n = \left(\partial_\eta+n+\frac{1}{2}\right)\kappa\lambda + \delta f\left(\dot{W}_\alpha^n+(n-1)W_\alpha^n-\kappa\lambda\right), \quad (D2)$$

$$\ddot{W}_\beta^n + \left(2n+\frac{1}{2}\right)\dot{W}_\beta^n + \left(n^2+\frac{n}{2}-\frac{3}{2}\right)W_\beta^n = \kappa\kappa + \delta f\left(\dot{W}_\beta^n+(n-1)W_\beta^n\right).$$

We note that the structure of the left hand side in both these equations is exactly the same. It is straightforward to solve this type of equation,

$$\ddot{W}_\gamma^n(\eta) + \left(2n+\frac{1}{2}\right)\dot{W}_\gamma^n(\eta) + \left(n^2+\frac{n}{2}-\frac{3}{2}\right)W_\gamma^n(\eta) = S_\gamma^n(\eta), \quad (D3)$$

$$\implies W_\gamma^n(\eta) = \mathcal{I}_n[S_\gamma^n] \equiv \frac{2}{5}\int_{-\infty}^\eta d\eta'\left[e^{(n-1)(\eta'-\eta)} - e^{(n+\frac{3}{2})(\eta'-\eta)}\right]S_\gamma^n(\eta'),$$

where $\gamma = \alpha, \beta$ and S_γ^n denotes the source term, including the one proportional to δf. Note that, in the process above, we have also defined the functional integral $\mathcal{I}_n$. Although one initially includes other terms with integration constants $c_1 e^{-(n+3/2)\eta} + c_2 e^{(1-n)\eta}$ in the general solution, these ought to be set to zero in our case in order to reproduce the known EdS results. This is, of course, equivalent to setting the initial conditions to the EdS values. In particular, for a constant source term, the time integration is performed as follows

$$\mathcal{I}_n[\mathcal{C}] = \frac{2}{5}\mathcal{C}\int_{-\infty}^{\eta} d\eta' \left[e^{(n-1)(\eta'-\eta)} - e^{(n+\frac{3}{2})(\eta'-\eta)} \right] = \frac{2\mathcal{C}}{(2n+3)(n-1)}. \tag{D4}$$

We seek to obtain the perturbative solution using this integral representation. As noted in Section III we expand our solutions in δf as

$$W^n = W^{n[0]} + W^{n[1]} + W^{n[2]} + \cdots, \tag{D5}$$

where the superscript $[n]$ denotes the order in powers of δf, with $[0]$ representing the solution in the EdS limit. We obtain the recursive relations

$$W_\alpha^{n[l]} = \mathcal{I}_n \left[\left(\partial_\eta + n + \tfrac{1}{2}\right)(\kappa\lambda)^{[l]} + \delta f \left(\dot{W}_\alpha^{n[l-1]} + (n-1)W_\alpha^{n[l-1]} - (\kappa\lambda)^{[l-1]} \right) \right], \tag{D6}$$

$$W_\beta^{n[l]} = \mathcal{I}_n \left[(\kappa\kappa)^{[l]} + \delta f \left(\dot{W}_\beta^{n[l-1]} + (n-1)W_\beta^{n[l-1]} \right) \right],$$

where $(xy)^{[l]} = x^{[0]}y^{[l]} + x^{[1]}y^{[l-1]} + x^{[2]}y^{[l-2]} + \cdots + x^{[l]}y^{[0]}$ and $(\kappa\lambda)^{[-1]} = 0$. To further reduce the expressions, it is useful to define the second functional expression

$$\tilde{\mathcal{I}}_n[X] \equiv (\partial_\eta + n - 1)\mathcal{I}_n[\delta f\, X] = \frac{2n+1}{5}\int_{-\infty}^{\eta} d\eta' e^{(n+\frac{3}{2})(\eta'-\eta)} \delta f(\eta')X(\eta'). \tag{D7}$$

Repeatedly using the above recursive relation, one finds

$$\dot{W}_\beta^{n[l]} + (n-1)W_\beta^{n[l]} = \tilde{\mathcal{I}}_n \left[\frac{(\kappa\kappa)^{[l]}}{\delta f} + \dot{W}_\beta^{n[l-1]} + (n-1)W_\beta^{n[l-1]} \right] \tag{D8}$$

$$= \tilde{\mathcal{I}}_n \left[\frac{(\kappa\kappa)^{[l]}}{\delta f} + \tilde{\mathcal{I}}_n \left[\frac{(\kappa\kappa)^{[l-1]}}{\delta f} + \dot{W}_\beta^{n[l-2]} + (n-1)W_\beta^{n[l-2]} \right] \right]$$

$$= \sum_{k=1}^{l} \tilde{\mathcal{I}}_n^k \left[\frac{(\kappa\kappa)^{[l-k+1]}}{\delta f} \right] + (n-1)W_\beta^{n[0]}\tilde{\mathcal{I}}_n^l[1],$$

where $\dot{W}_\beta^{n[0]} = 0$ and $\tilde{\mathcal{I}}_n^k[X]$ means the recursive operations of $\tilde{\mathcal{I}}_n$ by k times, for instance, $\tilde{\mathcal{I}}_n^3[X] = \tilde{\mathcal{I}}_n[\tilde{\mathcal{I}}_n[\tilde{\mathcal{I}}_n[X]]]$. In the case of $W_\alpha^{n[l]}$, $(\kappa\kappa)^{[l]}$ in Eq. (D8) is replaced by $\left(\partial_\eta + n + \tfrac{1}{2}\right)(\kappa\lambda)^{[l]} - \delta f(\kappa\lambda)^{[l-1]}$. Plugging these expressions back into Eq. (D6), and restoring the suppressed indices, we obtain the general solutions

$$W_{\alpha;m_1,m_2}^{n\,(ij)} = \left(1 - \frac{2n-2}{2n+1}\sum_{l=1}^{\infty}\mathcal{I}_n\left[\delta f\,\tilde{\mathcal{I}}_n^{l-1}[1]\right]\right)W_{\alpha;m_1,m_2}^{n\,(ij)\,[0]} \tag{D9}$$

$$+ \sum_{l=1}^{\infty}\mathcal{I}_n\left[\left(\partial_\eta + n + \tfrac{1}{2}\right)\left(\kappa_{m_2}^{(i)}\lambda_{m_2}^{(j)}\right)^{[l]}\right] - \sum_{l=2}^{\infty}\mathcal{I}_n\left[\delta f\left(\kappa_{m_2}^{(i)}\lambda_{m_2}^{(j)}\right)^{[l-1]}\right]$$

$$+ \sum_{l=2}^{\infty}\mathcal{I}_n\left[\delta f\sum_{k=1}^{l-1}\tilde{\mathcal{I}}_n^k\left[\delta f^{-1}\left(\partial_\eta + n + \tfrac{1}{2}\right)\left(\kappa_{m_2}^{(i)}\lambda_{m_2}^{(j)}\right)^{[l-k]}\right] - \delta f\sum_{k=1}^{l-2}\tilde{\mathcal{I}}_n^k\left[\left(\kappa_{m_2}^{(i)}\lambda_{m_2}^{(j)}\right)^{[l-k-1]}\right]\right],$$

$$W_{\beta;m_1,m_2}^{n\,(ij)} = \left(1 + (n-1)\sum_{l=1}^{\infty}\mathcal{I}_n\left[\delta f\,\tilde{\mathcal{I}}_n^{l-1}[1]\right]\right)W_{\beta;m_1,m_2}^{n\,(ij)\,[0]}$$

$$+ \sum_{l=1}^{\infty}\mathcal{I}_n\left[\left(\kappa_{m_1}^{(i)}\kappa_{m_2}^{(j)}\right)^{[l]}\right] + \sum_{l=2}^{\infty}\mathcal{I}_n\left[\delta f\sum_{k=1}^{l-1}\tilde{\mathcal{I}}_n^k\left[\delta f^{-1}\left(\kappa_{m_1}^{(i)}\kappa_{m_2}^{(j)}\right)^{[l-k]}\right]\right],$$

where we manipulated the terms with $(\kappa\lambda)^{[0]}$. The results in the EdS limit can be found from (D6) for $l = 0$,

$$W_\alpha^{n[0]} = \mathcal{I}_n\left[\left(n+\tfrac{1}{2}\right)(\kappa\lambda)^{[0]}\right] = \frac{(2n+1)\kappa^{[0]}\lambda^{[0]}}{(2n+3)(n-1)}, \qquad W_\beta^{n[0]} = \mathcal{I}_n\left[(\kappa\kappa)^{[0]}\right] = \frac{2\kappa^{[0]}\kappa^{[0]}}{(2n+3)(n-1)}, \tag{D10}$$

where we used the fact that the zero-th order quantities are constant, $\kappa^{[0]}, \lambda^{[0]} = const.$

In order to utilise these general solutions and employ the explicit form of the $\mathcal{I}_n$ and $\tilde{\mathcal{I}}_n$ integrals we use the expanded form of δf that we put forward in Eq. (18) and derived in Appendix A. Plugging this approximated expression into (D9) and then using (13), at leading order in δf we obtain for $n = 2$

$$\lambda_2^{(1)} = \frac{5}{7} - \frac{c_1}{91}\zeta - \frac{4c_2}{931}\zeta^2 - \frac{2c_3}{875}\zeta^3, \qquad\qquad \lambda_2^{(2)} = \frac{2}{7} + \frac{c_1}{91}\zeta + \frac{4c_2}{931}\zeta^2 + \frac{2c_3}{875}\zeta^3, \qquad (D11)$$

$$\kappa_2^{(1)} = \frac{3}{7} - \frac{5c_1}{91}\zeta - \frac{32c_2}{931}\zeta^2 - \frac{22c_3}{875}\zeta^3, \qquad\qquad \kappa_2^{(2)} = \frac{4}{7} + \frac{5c_1}{91}\zeta + \frac{32c_2}{931}\zeta^2 + \frac{22c_3}{875}\zeta^3,$$

shown also in Eq. (19). In the same way, we compute the $n = 3$ time-dependent coefficients

$$\lambda_3^{(1)} = \frac{5}{18} - \frac{29c_1}{4725}\zeta - \frac{22c_2}{9261}\zeta^2 - \frac{118c_3}{93555}\zeta^3, \qquad \lambda_3^{(2)} = \frac{1}{9} + \frac{c_1}{4725}\zeta - \frac{5c_2}{18522}\zeta^2 - \frac{2c_3}{8505}\zeta^3, \qquad (D12)$$

$$\lambda_3^{(3)} = \frac{1}{6} - \frac{19c_1}{1575}\zeta - \frac{31c_2}{6174}\zeta^2 - \frac{86c_3}{31185}\zeta^3, \qquad \lambda_3^{(4)} = \frac{2}{9} + \frac{29c_1}{4725}\zeta + \frac{22c_2}{9261}\zeta^2 + \frac{118c_3}{93555}\zeta^3,$$

$$\lambda_3^{(5)} = \frac{1}{21} + \frac{22c_1}{20475}\zeta + \frac{85c_2}{117306}\zeta^2 + \frac{368c_3}{779625}\zeta^3, \qquad \lambda_3^{(6)} = \frac{4}{63} + \frac{298c_1}{61425}\zeta + \frac{338c_2}{175959}\zeta^2 + \frac{2396c_3}{2338875}\zeta^3,$$

$$\kappa_3^{(1)} = \frac{5}{42} - \frac{529c_1}{20475}\zeta - \frac{334c_2}{19551}\zeta^2 - \frac{10018c_3}{779625}\zeta^3, \qquad \kappa_3^{(2)} = \frac{1}{21} - \frac{199c_1}{20475}\zeta - \frac{263c_2}{39102}\zeta^2 - \frac{362c_3}{70875}\zeta^3,$$

$$\kappa_3^{(3)} = \frac{1}{14} - \frac{17c_1}{975}\zeta - \frac{141c_2}{13034}\zeta^2 - \frac{2066c_3}{259875}\zeta^3, \qquad \kappa_3^{(4)} = \frac{2}{21} - \frac{53c_1}{2925}\zeta - \frac{254c_2}{19551}\zeta^2 - \frac{7802c_3}{779625}\zeta^3,$$

$$\kappa_3^{(5)} = \frac{1}{7} + \frac{44c_1}{6825}\zeta + \frac{85c_2}{13034}\zeta^2 + \frac{1472c_3}{259875}\zeta^3, \qquad \kappa_3^{(6)} = \frac{4}{21} + \frac{596c_1}{20475}\zeta + \frac{338c_2}{19551}\zeta^2 + \frac{9584c_3}{779625}\zeta^3.$$

and the result for $n = 4$

$$\lambda_4^{(1)} = \frac{45}{539} - \frac{900c_1\zeta}{119119} - \frac{2272c_2\zeta^2}{706629} - \frac{3496c_3\zeta^3}{1953875}, \qquad \lambda_4^{(2)} = \frac{18}{539} - \frac{489c_1\zeta}{238238} - \frac{724c_2\zeta^2}{706629} - \frac{2381c_3\zeta^3}{3907750}, \qquad (D13)$$

$$\lambda_4^{(3)} = \frac{60}{539} + \frac{2425c_1\zeta}{714714} + \frac{3232c_2\zeta^2}{2119887} + \frac{10147c_3\zeta^3}{11723250}, \qquad \lambda_4^{(4)} = \frac{24}{539} + \frac{947c_1\zeta}{357357} + \frac{2032c_2\zeta^2}{2119887} + \frac{2861c_3\zeta^3}{5861625},$$

$$\lambda_4^{(5)} = \frac{6}{539} - \frac{32c_1\zeta}{119119} + \frac{188c_2\zeta^2}{4946403} + \frac{19c_3\zeta^3}{279125}, \qquad \lambda_4^{(6)} = \frac{8}{539} + \frac{257c_1\zeta}{357357} + \frac{5680c_2\zeta^2}{14839209} + \frac{197c_3\zeta^3}{837375},$$

$$\lambda_4^{(7)} = \frac{32}{1617} + \frac{856c_1\zeta}{357357} + \frac{14144c_2\zeta^2}{14839209} + \frac{424c_3\zeta^3}{837375}, \qquad \lambda_4^{(8)} = \frac{5}{66} - \frac{223c_1\zeta}{117810} - \frac{244c_2\zeta^2}{334719} - \frac{13c_3\zeta^3}{33495},$$

$$\lambda_4^{(9)} = \frac{1}{33} - \frac{43c_1\zeta}{117810} - \frac{149c_2\zeta^2}{669438} - \frac{3c_3\zeta^3}{22330}, \qquad \lambda_4^{(10)} = \frac{1}{22} - \frac{31c_1\zeta}{13090} - \frac{179c_2\zeta^2}{223146} - \frac{13c_3\zeta^3}{33495},$$

$$\lambda_4^{(11)} = \frac{2}{33} + \frac{13c_1\zeta}{117810} - \frac{50c_2\zeta^2}{334719} - \frac{3c_3\zeta^3}{22330}, \qquad \lambda_4^{(12)} = \frac{1}{77} - \frac{c_1\zeta}{85085} - \frac{43c_2\zeta^2}{4239774} - \frac{c_3\zeta^3}{76125},$$

$$\lambda_4^{(13)} = \frac{4}{231} + \frac{373c_1\zeta}{765765} + \frac{530c_2\zeta^2}{6359661} + \frac{c_3\zeta^3}{76125}, \qquad \lambda_4^{(14)} = \frac{5}{154} - \frac{6469c_1\zeta}{1531530} - \frac{12352c_2\zeta^2}{6359661} - \frac{313c_3\zeta^3}{279125},$$

$$\lambda_4^{(15)} = \frac{1}{77} - \frac{2449c_1\zeta}{1531530} - \frac{9743c_2\zeta^2}{12719322} - \frac{249c_3\zeta^3}{558250}, \qquad \lambda_4^{(16)} = \frac{3}{154} - \frac{1439c_1\zeta}{510510} - \frac{5185c_2\zeta^2}{4239774} - \frac{193c_3\zeta^3}{279125},$$

$$\lambda_4^{(17)} = \frac{2}{77} - \frac{4601c_1\zeta}{1531530} - \frac{9446c_2\zeta^2}{6359661} - \frac{489c_3\zeta^3}{558250}, \qquad \lambda_4^{(18)} = \frac{3}{77} + \frac{16c_1\zeta}{36465} + \frac{1741c_2\zeta^2}{4239774} + \frac{81c_3\zeta^3}{279125},$$

$$\lambda_4^{(19)} = \frac{4}{77} + \frac{394c_1\zeta}{109395} + \frac{9026c_2\zeta^2}{6359661} + \frac{632c_3\zeta^3}{837375}, \qquad \lambda_4^{(20)} = \frac{5}{693} - \frac{944c_1\zeta}{11486475} + \frac{218c_2\zeta^2}{4946403} + \frac{6857c_3\zeta^3}{135654750},$$

$$\lambda_4^{(21)} = \frac{2}{693} - \frac{239c_1\zeta}{11486475} + \frac{277c_2\zeta^2}{14839209} + \frac{1384c_3\zeta^3}{67827375}, \qquad \lambda_4^{(22)} = \frac{1}{231} - \frac{334c_1\zeta}{3828825} + \frac{311c_2\zeta^2}{14839209} + \frac{17c_3\zeta^3}{587250},$$

$$\lambda_4^{(23)} = \frac{4}{693} - \frac{181c_1\zeta}{11486475} + \frac{620c_2\zeta^2}{14839209} + \frac{37c_3\zeta^3}{880875}, \qquad \lambda_4^{(24)} = \frac{2}{231} + \frac{2434c_1\zeta}{3828825} + \frac{1553c_2\zeta^2}{4946403} + \frac{4111c_3\zeta^3}{22609125},$$

$$\lambda_4^{(25)} = \frac{8}{693} + \frac{14356c_1\zeta}{11486475} + \frac{7444c_2\zeta^2}{14839209} + \frac{18292c_3\zeta^3}{67827375}, \qquad \kappa_4^{(1)} = \frac{15}{539} - \frac{152c_1\zeta}{17017} - \frac{28492c_2\zeta^2}{4946403} - \frac{8444c_3\zeta^3}{1953875},$$

$$\kappa_4^{(2)} = \frac{6}{539} - \frac{115c_1\zeta}{34034} - \frac{11212c_2\zeta^2}{4946403} - \frac{6709c_3\zeta^3}{3907750}, \qquad \kappa_4^{(3)} = \frac{20}{539} - \frac{941c_1\zeta}{102102} - \frac{101648c_2\zeta^2}{14839209} - \frac{63317c_3\zeta^3}{11723250},$$

$$\kappa_4^{(4)} = \frac{8}{539} - \frac{25c_1\zeta}{7293} - \frac{39920c_2\zeta^2}{14839209} - \frac{12571c_3\zeta^3}{5861625}, \qquad \kappa_4^{(5)} = \frac{24}{539} - \frac{32c_1\zeta}{17017} + \frac{1880c_2\zeta^2}{4946403} + \frac{247c_3\zeta^3}{279125},$$

$$\kappa_4^{(6)} = \frac{32}{539} + \frac{257c_1\zeta}{51051} + \frac{56800c_2\zeta^2}{14839209} + \frac{2561c_3\zeta^3}{837375}, \qquad \kappa_4^{(7)} = \frac{128}{1617} + \frac{856c_1\zeta}{51051} + \frac{141440c_2\zeta^2}{14839209} + \frac{5512c_3\zeta^3}{837375},$$

$$\kappa_4^{(8)} = \frac{5}{198} - \frac{12569c_1\zeta}{1767150} - \frac{3838c_2\zeta^2}{781011} - \frac{10267c_3\zeta^3}{2713095}, \qquad \kappa_4^{(9)} = \frac{1}{99} - \frac{4889c_1\zeta}{1767150} - \frac{3055c_2\zeta^2}{1562022} - \frac{8201c_3\zeta^3}{5426190},$$

$$\kappa_4^{(10)} = \frac{1}{66} - \frac{2659c_1\zeta}{589050} - \frac{4687c_2\zeta^2}{1562022} - \frac{2069c_3\zeta^3}{904365}, \qquad \kappa_4^{(11)} = \frac{2}{99} - \frac{9481c_1\zeta}{1767150} - \frac{3022c_2\zeta^2}{781011} - \frac{16321c_3\zeta^3}{5426190},$$

$$\kappa_4^{(12)} = \frac{1}{231} - \frac{4429c_1\zeta}{3828825} - \frac{24515c_2\zeta^2}{29678418} - \frac{14533c_3\zeta^3}{22609125}, \qquad \kappa_4^{(13)} = \frac{4}{693} - \frac{16561c_1\zeta}{11486475} - \frac{16138c_2\zeta^2}{14839209} - \frac{57901c_3\zeta^3}{67827375},$$

$$\kappa_4^{(14)} = \frac{5}{462} - \frac{9523c_1\zeta}{2552550} - \frac{104122c_2\zeta^2}{44517627} - \frac{5581c_3\zeta^3}{3229875}, \qquad \kappa_4^{(15)} = \frac{1}{231} - \frac{3763c_1\zeta}{2552550} - \frac{83159c_2\zeta^2}{89035254} - \frac{4463c_3\zeta^3}{6459750},$$

$$\kappa_4^{(16)} = \frac{1}{154} - \frac{279c_1\zeta}{121550} - \frac{41893c_2\zeta^2}{29678418} - \frac{7829c_3\zeta^3}{7536375}, \qquad \kappa_4^{(17)} = \frac{2}{231} - \frac{1061c_1\zeta}{364650} - \frac{82862c_2\zeta^2}{44517627} - \frac{62401c_3\zeta^3}{45218250},$$

$$\kappa_4^{(18)} = \frac{1}{77} - \frac{1436c_1\zeta}{425425} - \frac{71675c_2\zeta^2}{29678418} - \frac{14257c_3\zeta^3}{7536375}, \qquad \kappa_4^{(19)} = \frac{4}{231} - \frac{1658c_1\zeta}{425425} - \frac{137806c_2\zeta^2}{44517627} - \frac{56104c_3\zeta^3}{22609125},$$

$$\kappa_4^{(20)} = \frac{20}{693} - \frac{944c_1\zeta}{1640925} + \frac{2180c_2\zeta^2}{4946403} + \frac{89141c_3\zeta^3}{135654750}, \qquad \kappa_4^{(21)} = \frac{8}{693} - \frac{239c_1\zeta}{1640925} + \frac{2770c_2\zeta^2}{14839209} + \frac{17992c_3\zeta^3}{67827375},$$

$$\kappa_4^{(22)} = \frac{4}{231} - \frac{334c_1\zeta}{546975} + \frac{3110c_2\zeta^2}{14839209} + \frac{221c_3\zeta^3}{587250}, \qquad \kappa_4^{(23)} = \frac{16}{693} - \frac{181c_1\zeta}{1640925} + \frac{6200c_2\zeta^2}{14839209} + \frac{481c_3\zeta^3}{880875},$$

$$\kappa_4^{(24)} = \frac{8}{231} + \frac{2434c_1\zeta}{546975} + \frac{15530c_2\zeta^2}{4946403} + \frac{53443c_3\zeta^3}{22609125}, \qquad \kappa_4^{(25)} = \frac{32}{693} + \frac{14356c_1\zeta}{1640925} + \frac{74440c_2\zeta^2}{14839209} + \frac{237796c_3\zeta^3}{67827375}.$$

One can continue this exercise up to an arbitrary n. For the purposes of this work, it suffices to run this procedure up to $n = 5$: F_5 and G_5 are the highest order kernels necessary for the calculation of the two-loop power spectra, and therefore we may stop at the $\lambda_5^{(i)}, \kappa_5^{(i)}$ set of time coefficients (all coefficients and corresponding kernels are given in the *Mathematica* notebook, provided in the *arXiv* source file of this paper).

Appendix E: IR and UV limits of kernels

In this appendix, we consider the IR and UV limits of the $\boldsymbol{H}_n$ kernels in the momenta configurations contributing to the one- and two-loop calculations. For IR limits, we have the following expansions

$$\boldsymbol{H}_2(\boldsymbol{p}, \boldsymbol{k} - \boldsymbol{p}) \sim [\boldsymbol{H}_2]_{\mathrm{IR}}^{(1)}(\hat{p}) \frac{k}{p} + [\boldsymbol{H}_2]_{\mathrm{IR}}^{(0)}(\hat{p}) + \mathcal{O}(p^1), \tag{E1}$$

$$\boldsymbol{H}_3(\boldsymbol{k}, \boldsymbol{p}, -\boldsymbol{p}) \sim [\boldsymbol{H}_{3,\mathrm{I}}]_{\mathrm{IR}}^{(2)}(\hat{p}) \frac{k^2}{p^2} + [\boldsymbol{H}_{3,\mathrm{I}}]_{\mathrm{IR}}^{(0)}(\hat{p}) + \mathcal{O}(p^1),$$

$$\boldsymbol{H}_3(\boldsymbol{k} - \boldsymbol{q} - \boldsymbol{p}, \boldsymbol{q}, \boldsymbol{p}) \sim [\boldsymbol{H}_{3,\mathrm{II}}]_{\mathrm{IR}}^{(1)}(\hat{p}) \frac{k}{p} + [\boldsymbol{H}_{3,\mathrm{II}}]_{\mathrm{IR}}^{(0)}(\hat{p}) + \mathcal{O}(p^1),$$

$$\boldsymbol{H}_4(\boldsymbol{k} - \boldsymbol{q}, \boldsymbol{q}, \boldsymbol{p}, -\boldsymbol{p}) \sim [\boldsymbol{H}_{4,\mathrm{I}}]_{\mathrm{IR}}^{(2)}(\hat{p}) \frac{k^2}{p^2} + [\boldsymbol{H}_{4,\mathrm{I}}]_{\mathrm{IR}}^{(0)}(\hat{p}) + \mathcal{O}(p^1),$$

$$\boldsymbol{H}_4(\boldsymbol{k} - \boldsymbol{p}, \boldsymbol{p}, \boldsymbol{q}, -\boldsymbol{q}) \sim [\boldsymbol{H}_{4,\mathrm{II}}]_{\mathrm{IR}}^{(1)}(\hat{p}) \frac{k}{p} + [\boldsymbol{H}_{4,\mathrm{II}}]_{\mathrm{IR}}^{(0)}(\hat{p}) + \mathcal{O}(p^1),$$

$$\boldsymbol{H}_5(\boldsymbol{k}, \boldsymbol{q}, -\boldsymbol{q}, \boldsymbol{p}, -\boldsymbol{p}) \sim [\boldsymbol{H}_5]_{\mathrm{IR}}^{(2)}(\hat{p}) \frac{k^2}{p^2} + [\boldsymbol{H}_5]_{\mathrm{IR}}^{(0)}(\hat{p}) + \mathcal{O}(p^1),$$

as $p \to 0$. We can write explicitly the first few coefficients as $[\boldsymbol{H}_2]_{\mathrm{IR}}^{(1)} = \frac{\mu}{2}(1,1)$ and $[\boldsymbol{H}_2]_{\mathrm{IR}}^{(0)} = \frac{1}{2}(1, 2\mu^2 - 1)$, and $[\boldsymbol{H}_{3,\mathrm{I}}]_{\mathrm{IR}}^{(2)} = -\frac{\mu^2}{3}(1,1,0,0,1,1)$, $[\boldsymbol{H}_{3,\mathrm{I}}]_{\mathrm{IR}}^{(0)} = -\frac{1}{3}(\mu^2, \mu^2, \mu^2 - 2, -\mu^2, 2 - 6\mu^2 + 4\mu^4, 0)$, where $\mu = \hat{k} \cdot \hat{p}$. We shall not give the explicit form here for the remaining coefficients. These are obtained in a similar manner and can be arrived at by expanding the full kernels.

In computing the loop contribution, it is crucial to isolate the leading product divergencies of the kernel products.

Focusing on the IR limit at one-loop we have

$$
\boldsymbol{h}_{22,\mathrm{IR}}^{(2)} = [\boldsymbol{H}_2]_{\mathrm{IR}}^{(1)} \otimes [\boldsymbol{H}_2]_{\mathrm{IR}}^{(1)} = \frac{\mu^2}{4} \begin{pmatrix} 1 & 1 \\ 1 & 1 \end{pmatrix}, \tag{E2}
$$

$$
\boldsymbol{h}_{22,\mathrm{IR}}^{(1)} = [\boldsymbol{H}_2]_{\mathrm{IR}}^{(1)} \otimes [\boldsymbol{H}_2]_{\mathrm{IR}}^{(0)} + [\boldsymbol{H}_2]_{\mathrm{IR}}^{(0)} \otimes [\boldsymbol{H}_2]_{\mathrm{IR}}^{(1)} = \frac{\mu}{2} \begin{pmatrix} 1 & \mu^2 \\ \mu^2 & 2\mu^2 - 1 \end{pmatrix},
$$

$$
\boldsymbol{h}_{13,\mathrm{IR}}^{(2)} = \boldsymbol{H}_1(\boldsymbol{k}) \otimes [\boldsymbol{H}_{3,\mathrm{I}}]_{\mathrm{IR}}^{(2)} = -\frac{\mu^2}{3} \begin{pmatrix} 1 & 1 & 0 & 0 & 1 & 1 \end{pmatrix},
$$

while at two-loops one finds

$$
\boldsymbol{h}_{33,\mathrm{I},\mathrm{IR}}^{(2)} = \boldsymbol{H}_3(\boldsymbol{k}, \boldsymbol{q}, -\boldsymbol{q}) \otimes [\boldsymbol{H}_{3,\mathrm{I}}]_{\mathrm{IR}}^{(2)}, \tag{E3}
$$

$$
\boldsymbol{h}_{33,\mathrm{II},\mathrm{IR}}^{(2)} = [\boldsymbol{H}_{3,\mathrm{II}}]_{\mathrm{IR}}^{(1)} \otimes [\boldsymbol{H}_{3,\mathrm{II}}]_{\mathrm{IR}}^{(1)},
$$

$$
\boldsymbol{h}_{33,\mathrm{II},\mathrm{IR}}^{(1)} = [\boldsymbol{H}_{3,\mathrm{II}}]_{\mathrm{IR}}^{(1)} \otimes [\boldsymbol{H}_{3,\mathrm{II}}]_{\mathrm{IR}}^{(0)} + [\boldsymbol{H}_{3,\mathrm{II}}]_{\mathrm{IR}}^{(0)} \otimes [\boldsymbol{H}_{3,\mathrm{II}}]_{\mathrm{IR}}^{(1)},
$$

$$
\boldsymbol{h}_{24,\mathrm{I},\mathrm{IR}}^{(2)} = \boldsymbol{H}_2(\boldsymbol{k} - \boldsymbol{q}, \boldsymbol{q}) \otimes [\boldsymbol{H}_{4,\mathrm{I}}]_{\mathrm{IR}}^{(2)},
$$

$$
\boldsymbol{h}_{24,\mathrm{II},\mathrm{IR}}^{(2)} = [\boldsymbol{H}_2]_{\mathrm{IR}}^{(1)} \otimes [\boldsymbol{H}_{4,\mathrm{II}}]_{\mathrm{IR}}^{(1)},
$$

$$
\boldsymbol{h}_{24,\mathrm{II},\mathrm{IR}}^{(1)} = [\boldsymbol{H}_2]_{\mathrm{IR}}^{(1)} \otimes [\boldsymbol{H}_{4,\mathrm{II}}]_{\mathrm{IR}}^{(0)} + [\boldsymbol{H}_2]_{\mathrm{IR}}^{(0)} \otimes [\boldsymbol{H}_{4,\mathrm{II}}]_{\mathrm{IR}}^{(1)},
$$

$$
\boldsymbol{h}_{15,\mathrm{IR}}^{(2)} = \boldsymbol{H}_1(\boldsymbol{k}) \otimes [\boldsymbol{H}_5]_{\mathrm{IR}}^{(2)}.
$$

Similarly, one can derive the UV limit of the various terms, which are given by

$$
\boldsymbol{H}_2(\boldsymbol{p}, \boldsymbol{k} - \boldsymbol{p}) \sim [\boldsymbol{H}_2]_{\mathrm{UV}}^{(2)}(\hat{k})\frac{k^2}{p^2} + [\boldsymbol{H}_2]_{\mathrm{UV}}^{(3)}(\hat{k})\frac{k^3}{p^3} + \mathcal{O}(k^4), \tag{E4}
$$

$$
\boldsymbol{H}_3(\boldsymbol{k}, \boldsymbol{p}, -\boldsymbol{p}) \sim [\boldsymbol{H}_{3,\mathrm{I}}]_{\mathrm{UV}}^{(0)}(\hat{k}) + [\boldsymbol{H}_{3,\mathrm{I}}]_{\mathrm{UV}}^{(2)}(\hat{k})\frac{k^2}{p^2} + \mathcal{O}(k^4),
$$

$$
\boldsymbol{H}_3(\boldsymbol{k} - \boldsymbol{q} - \boldsymbol{p}, \boldsymbol{q}, \boldsymbol{p}) \sim [\boldsymbol{H}_{3,\mathrm{II}}]_{\mathrm{UV}}^{(1)}(\hat{k})\frac{k}{p} + [\boldsymbol{H}_{3,\mathrm{II}}]_{\mathrm{UV}}^{(2)}(\hat{k})\frac{k^2}{p^2} + [\boldsymbol{H}_{3,\mathrm{II}}]_{\mathrm{UV}}^{(3)}(\hat{k})\frac{k^3}{p^3} + \mathcal{O}(k^4),
$$

$$
\boldsymbol{H}_4(\boldsymbol{k} - \boldsymbol{q}, \boldsymbol{q}, \boldsymbol{p}, -\boldsymbol{p}) \sim [\boldsymbol{H}_4]_{\mathrm{UV}}^{(2)}(\hat{k})\frac{k^2}{p^2} + [\boldsymbol{H}_4]_{\mathrm{UV}}^{(3)}(\hat{k})\frac{k^3}{p^3} + \mathcal{O}(k^4),
$$

$$
\boldsymbol{H}_5(\boldsymbol{k}, \boldsymbol{q}, -\boldsymbol{q}, \boldsymbol{p}, -\boldsymbol{p}) \sim [\boldsymbol{H}_5]_{\mathrm{UV}}^{(0)}(\hat{k}) + [\boldsymbol{H}_5]_{\mathrm{UV}}^{(2)}(\hat{k})\frac{k^2}{p^2} + \mathcal{O}(k^4),
$$

as $k \to 0$. Again, the first few coefficients can be written as $[\boldsymbol{H}_2]_{\mathrm{UV}}^{(2)} = \frac{1}{2}\left(1 - 2\mu^2, -1\right)$, $[\boldsymbol{H}_2]_{\mathrm{UV}}^{(3)} = \frac{\mu}{2}\left(3 - 4\mu^2, -1\right)$, $[\boldsymbol{H}_{3,\mathrm{I}}]_{\mathrm{UV}}^{(0)} = \frac{\mu^2}{3}(-1, -1, 1, 1, 0, 0)$ and $[\boldsymbol{H}_{3,\mathrm{I}}]_{\mathrm{UV}}^{(2)} = -\frac{1}{3}\left(\mu^2, \mu^2, 2(1 - \mu^2)(2\mu^2 - 1), 0, 2 - \mu^2, \mu^2\right)$. The kernel products relevant for the UV divergencies in the power spectra are, at one-loop power,

$$
\boldsymbol{h}_{22,\mathrm{UV}}^{(4)} = [\boldsymbol{H}_2]_{\mathrm{UV}}^{(2)} \otimes [\boldsymbol{H}_2]_{\mathrm{UV}}^{(2)} = \frac{1}{4} \begin{pmatrix} \left(2\mu^2 - 1\right)^2 & 2\mu^2 - 1 \\ 2\mu^2 - 1 & 1 \end{pmatrix}, \tag{E5}
$$

$$
\boldsymbol{h}_{13,\mathrm{UV}}^{(0)} = \boldsymbol{H}_1 \otimes [\boldsymbol{H}_{3,\mathrm{I}}]_{\mathrm{UV}}^{(0)} = -\frac{\mu^2}{3} \begin{pmatrix} -1 & -1 & 1 & 1 & 0 & 0 \end{pmatrix},
$$

$$
\boldsymbol{h}_{13,\mathrm{UV}}^{(2)} = \boldsymbol{H}_1 \otimes [\boldsymbol{H}_{3,\mathrm{I}}]_{\mathrm{UV}}^{(2)} = -\frac{1}{3} \begin{pmatrix} \mu^2 & \mu^2 & 2(1 - \mu^2)(2\mu^2 - 1) & 0 & 2 - \mu^2 & \mu^2 \end{pmatrix},
$$

and, at two-loop,

$$\boldsymbol{h}_{33,\mathrm{I,UV}}^{(0)} = [\boldsymbol{H}_{3,\mathrm{I}}]_{\mathrm{UV}}^{(0)} \otimes [\boldsymbol{H}_{3,\mathrm{I}}]_{\mathrm{UV}}^{(0)} , \tag{E6}$$

$$\boldsymbol{h}_{33,\mathrm{I,UV}}^{(2)} = [\boldsymbol{H}_{3,\mathrm{I}}]_{\mathrm{UV}}^{(0)} \otimes [\boldsymbol{H}_{3,\mathrm{I}}]_{\mathrm{UV}}^{(2)} , \quad \text{not symmetric in } \hat{q} \text{ and } \hat{p},$$

$$\boldsymbol{h}_{33,\mathrm{I,UV}}^{(4)} = [\boldsymbol{H}_{3,\mathrm{I}}]_{\mathrm{UV}}^{(2)} \otimes [\boldsymbol{H}_{3,\mathrm{I}}]_{\mathrm{UV}}^{(2)} ,$$

$$\boldsymbol{h}_{33,\mathrm{II,UV}}^{(2)} = [\boldsymbol{H}_{3,\mathrm{II}}]_{\mathrm{UV}}^{(1)} \otimes [\boldsymbol{H}_{3,\mathrm{II}}]_{\mathrm{UV}}^{(1)} ,$$

$$\boldsymbol{h}_{33,\mathrm{II,UV}}^{(3)} = [\boldsymbol{H}_{3,\mathrm{II}}]_{\mathrm{UV}}^{(1)} \otimes [\boldsymbol{H}_{3,\mathrm{II}}]_{\mathrm{UV}}^{(2)} + [\boldsymbol{H}_{3,\mathrm{II}}]_{\mathrm{UV}}^{(2)} \otimes [\boldsymbol{H}_{3,\mathrm{II}}]_{\mathrm{UV}}^{(1)} ,$$

$$\boldsymbol{h}_{33,\mathrm{II,UV}}^{(4)} = [\boldsymbol{H}_{3,\mathrm{II}}]_{\mathrm{UV}}^{(2)} \otimes [\boldsymbol{H}_{3,\mathrm{II}}]_{\mathrm{UV}}^{(2)} + [\boldsymbol{H}_{3,\mathrm{II}}]_{\mathrm{UV}}^{(1)} \otimes [\boldsymbol{H}_{3,\mathrm{II}}]_{\mathrm{UV}}^{(3)} + [\boldsymbol{H}_{3,\mathrm{II}}]_{\mathrm{UV}}^{(3)} \otimes [\boldsymbol{H}_{3,\mathrm{II}}]_{\mathrm{UV}}^{(1)} ,$$

$$\boldsymbol{h}_{24,\mathrm{UV}}^{(4)} = [\boldsymbol{H}_2]_{\mathrm{UV}}^{(2)} \otimes [\boldsymbol{H}_4]_{\mathrm{UV}}^{(2)} ,$$

$$\boldsymbol{h}_{15,\mathrm{UV}}^{(0)} = \boldsymbol{H}_1(\boldsymbol{k}) \otimes [\boldsymbol{H}_5]_{\mathrm{UV}}^{(0)} ,$$

$$\boldsymbol{h}_{15,\mathrm{UV}}^{(2)} = \boldsymbol{H}_1(\boldsymbol{k}) \otimes [\boldsymbol{H}_5]_{\mathrm{UV}}^{(2)} .$$

Appendix F: Two-loop basis power spectra, IR and UV properties

In this appendix, we look into the IR and UV properties of the integrands given in Eq. (36). We first look at the $\boldsymbol{I}_{33}$ term, which has two distinct contributions. It is convenient to remap the contributions (see [47]) as

$$\boldsymbol{I}_{33,\mathrm{I}} = 9 P_{\mathrm{lin}}(\boldsymbol{k}) \int_{\boldsymbol{q},\boldsymbol{p}} \boldsymbol{H}_3(\boldsymbol{k}, -\boldsymbol{q}, \boldsymbol{q}) \otimes \boldsymbol{H}_3(\boldsymbol{k}, -\boldsymbol{p}, \boldsymbol{p}) P_{\mathrm{lin}}(\boldsymbol{q}) P_{\mathrm{lin}}(\boldsymbol{p}) \tag{F1}$$

$$= 9 P_{\mathrm{lin}}(\boldsymbol{k}) \int_{\boldsymbol{q},\boldsymbol{p}} \Big[\boldsymbol{H}_3(\boldsymbol{k}, -\boldsymbol{q}, \boldsymbol{q}) \otimes \boldsymbol{H}_3(\boldsymbol{k}, -\boldsymbol{p}, \boldsymbol{p}) \Theta(q - p) + \boldsymbol{q} \leftrightarrow \boldsymbol{p} \Big] P_{\mathrm{lin}}(\boldsymbol{q}) P_{\mathrm{lin}}(\boldsymbol{p}).$$

The IR and UV limits can be expressed as

$$\boldsymbol{H}_3(\boldsymbol{k}, -\boldsymbol{q}, \boldsymbol{q}) \otimes \boldsymbol{H}_3(\boldsymbol{k}, -\boldsymbol{p}, \boldsymbol{p}) \sim \begin{cases} \boldsymbol{h}_{33,\mathrm{I,IR}}^{(2)}(\boldsymbol{k}, \boldsymbol{q}, \hat{p}) \frac{k^2}{p^2} + \mathcal{O}(p^0) , & \text{as } p \to 0, \\ \boldsymbol{h}_{33,\mathrm{I,UV}}^{(0)}(\hat{k}, \boldsymbol{q}, \boldsymbol{p}) + \Big(\boldsymbol{h}_{33,\mathrm{I,UV}}^{(2)}(\hat{k}, \boldsymbol{q}, \boldsymbol{p}) \frac{k^2}{q^2} + \boldsymbol{q} \leftrightarrow \boldsymbol{p} \Big) \\ \qquad\qquad + \boldsymbol{h}_{33,\mathrm{I,UV}}^{(4)}(\hat{k}, \boldsymbol{q}, \boldsymbol{p}) \frac{k^4}{p^2 q^2} + \mathcal{O}(k^5) , & \text{as } k \to 0, \end{cases} \tag{F2}$$

and we can thus write the regularized integral as

$$\tilde{\boldsymbol{I}}_{33,\mathrm{I}} = 18 P_{\mathrm{lin}}(\boldsymbol{k}) \int_{\boldsymbol{q},\boldsymbol{p}} \Bigg[\boldsymbol{H}_3(\boldsymbol{k}, -\boldsymbol{q}, \boldsymbol{q}) \otimes \boldsymbol{H}_3(\boldsymbol{k}, -\boldsymbol{p}, \boldsymbol{p}) - \boldsymbol{h}_{33,\mathrm{I,IR}}^{(2)}(\boldsymbol{k}, \boldsymbol{q}, \hat{p}) \frac{k^2}{p^2} W_{33,\mathrm{I}}^{\mathrm{IR}} \tag{F3}$$

$$- \Bigg(\boldsymbol{h}_{33,\mathrm{I,UV}}^{(0)}(\hat{k}, \boldsymbol{q}, \boldsymbol{p}) + \Big(\boldsymbol{h}_{33,\mathrm{I,UV}}^{(2)}(\hat{k}, \boldsymbol{q}, \boldsymbol{p}) \frac{k^2}{q^2} + \boldsymbol{q} \leftrightarrow \boldsymbol{p} \Big) + \boldsymbol{h}_{33,\mathrm{I,UV}}^{(4)}(\hat{k}, \boldsymbol{q}, \boldsymbol{p}) \frac{k^4}{p^2 q^2} \Bigg) W_{33,\mathrm{I}}^{\mathrm{UV}} \Bigg] \Theta(q - p) P_{\mathrm{lin}}(\boldsymbol{q}) P_{\mathrm{lin}}(\boldsymbol{p}).$$

Given that $\boldsymbol{\lambda}_3 \cdot [\boldsymbol{H}_{3,\mathrm{I}}]_{\mathrm{UV}}^{(0)} = \boldsymbol{\kappa}_3 \cdot [\boldsymbol{H}_{3,\mathrm{I}}]_{\mathrm{UV}}^{(0)} = 0$, both in EdS and ΛCDM case, the terms $\boldsymbol{h}_{33,\mathrm{I,UV}}^{(0)}$ and $\boldsymbol{h}_{33,\mathrm{I,UV}}^{(2)}$ are zero. We thus have $\boldsymbol{I}_{33,\mathrm{I}}(k) = \tilde{\boldsymbol{I}}_{33,\mathrm{I}}(k) + [\boldsymbol{I}_{33,\mathrm{I}}]_{\mathrm{IR}} + [\boldsymbol{I}_{33,\mathrm{I}}]_{\mathrm{UV}}$, where

$$[\boldsymbol{I}_{33,\mathrm{I}}]_{\mathrm{IR}} = 18 P_{\mathrm{lin}}(\boldsymbol{k}) \int_{\boldsymbol{q},\boldsymbol{p}} \boldsymbol{h}_{33,\mathrm{I,IR}}^{(2)}(\boldsymbol{k}, \boldsymbol{q}, \hat{p}) \frac{k^2}{p^2} W_{33,\mathrm{I}}^{\mathrm{IR}} \Theta(q - p) P_{\mathrm{lin}}(\boldsymbol{q}) P_{\mathrm{lin}}(\boldsymbol{p}) = \big(\boldsymbol{h}_{33,\mathrm{I}}^{\mathrm{IR}} W_{33,\mathrm{I}}^{\mathrm{IR}} \big) k^2 P_{\mathrm{lin}}(k) , \tag{F4}$$

$$[\boldsymbol{I}_{33,\mathrm{I}}]_{\mathrm{UV}} = 9 P_{\mathrm{lin}}(\boldsymbol{k}) \int_{\boldsymbol{q},\boldsymbol{p}} \boldsymbol{h}_{33,\mathrm{I,UV}}^{(4)}(\hat{k}, \boldsymbol{q}, \boldsymbol{p}) \frac{k^4}{p^2 q^2} W_{33,\mathrm{I}}^{\mathrm{UV}} P_{\mathrm{lin}}(\boldsymbol{q}) P_{\mathrm{lin}}(\boldsymbol{p}) = \big(\boldsymbol{h}_{33,\mathrm{I}}^{\mathrm{UV}} W_{33,\mathrm{I}}^{\mathrm{UV}} \big) k^4 P_{\mathrm{lin}}(k).$$

In the last integral we have reverted back to the symmetric form of the integrand. We used the fact that

$$\boldsymbol{h}_{33,\mathrm{I}}^{\mathrm{IR}} = \int_{\boldsymbol{q}} \hat{\boldsymbol{h}}_{33,\mathrm{I,IR}}^{(2)}(\boldsymbol{k}, \boldsymbol{q}) \sigma_2^2(q) P_{\mathrm{lin}}(\boldsymbol{q}) , \quad \text{and} \quad \boldsymbol{h}_{33,\mathrm{I}}^{\mathrm{UV}} = 2 \big(\boldsymbol{h}_{13}^{\mathrm{UV}} \otimes \boldsymbol{h}_{13}^{\mathrm{UV}} \big) \big(\sigma_2^2 \big)^2 , \tag{F5}$$

where we have introduced the coefficients $\hat{\boldsymbol{h}}_{33,\mathrm{I,IR}}^{(2)}(\boldsymbol{k},\boldsymbol{q}) = 54 \int \frac{d\Omega_{\hat{p}}}{4\pi} \, \boldsymbol{h}_{33,\mathrm{I,IR}}^{(2)}(\boldsymbol{k},\boldsymbol{q},\hat{p})$, integrating the $\boldsymbol{h}_{33,\mathrm{I,IR}}^{(2)}$ over $\hat{p}$. We have also introduced the variance due to the p modes smaller than q as

$$\sigma_2^2(q) = \frac{1}{3}\int_{\boldsymbol{p}} \Theta(q-p)P_{\mathrm{lin}}(\boldsymbol{p})/p^2 = \frac{1}{3}\int_0^q \frac{dp}{2\pi^2}\, P_{\mathrm{lin}}(p)\,. \tag{F6}$$

Note that the final IR term $\boldsymbol{h}_{33,\mathrm{I}}^{\mathrm{IR}}(k)$ is k dependent.

Next we consider the $\boldsymbol{I}_{33,\mathrm{II}}$ integral

$$\boldsymbol{I}_{33,\mathrm{II}} = 6\int_{\boldsymbol{q},\boldsymbol{p}} \boldsymbol{H}_3(\boldsymbol{k}-\boldsymbol{q}-\boldsymbol{p},\boldsymbol{q},\boldsymbol{p}) \otimes \boldsymbol{H}_3(\boldsymbol{k}-\boldsymbol{q}-\boldsymbol{p},\boldsymbol{q},\boldsymbol{p})P_{\mathrm{lin}}(\boldsymbol{k}-\boldsymbol{q}-\boldsymbol{p})P_{\mathrm{lin}}(\boldsymbol{q})P_{\mathrm{lin}}(\boldsymbol{p})\,, \tag{F7}$$

which has leading divergencies when $\boldsymbol{q}$ and $\boldsymbol{p}$ go to zero, and when one of these momenta goes to zero while the other approaches $\boldsymbol{k}$. The sub-leading divergencies arise when $\boldsymbol{q}$ or $\boldsymbol{p}$ go to zero, while the other is finite, and when $\boldsymbol{q}+\boldsymbol{p}\to\boldsymbol{k}$. Since the integral can be symmetrized by introducing the delta function (see e.g. [47]), we can remap some of these divergencies into others by writing

$$\boldsymbol{I}_{33,\mathrm{II}} = 36\int_{\boldsymbol{q},\boldsymbol{p}} \boldsymbol{H}_3(\boldsymbol{k}-\boldsymbol{q}-\boldsymbol{p},\boldsymbol{q},\boldsymbol{p}) \otimes \boldsymbol{H}_3(\boldsymbol{k}-\boldsymbol{q}-\boldsymbol{p},\boldsymbol{q},\boldsymbol{p})\Theta(q-p)\Theta(|\boldsymbol{k}-\boldsymbol{q}-\boldsymbol{p}|-q)P_{\mathrm{lin}}(\boldsymbol{k}-\boldsymbol{q}-\boldsymbol{p})P_{\mathrm{lin}}(\boldsymbol{q})P_{\mathrm{lin}}(\boldsymbol{p}), \tag{F8}$$

where the leading divergencies appear only when $\boldsymbol{q}$ and $\boldsymbol{p}$ go to zero and the subleading ones appear when $\boldsymbol{q}$ goes to zero for finite $\boldsymbol{p}$. The product of the kernels can be written as

$$\boldsymbol{H}_3(\boldsymbol{k}-\boldsymbol{q}-\boldsymbol{p},\boldsymbol{q},\boldsymbol{p}) \otimes \boldsymbol{H}_3(\boldsymbol{k}-\boldsymbol{q}-\boldsymbol{p},\boldsymbol{q},\boldsymbol{p}) \sim \begin{cases} \boldsymbol{h}_{33,\mathrm{II,IR}}^{(2)}(\boldsymbol{k},\boldsymbol{q},\hat{p})\frac{k^2}{p^2} + \boldsymbol{h}_{33,\mathrm{II,IR}}^{(1)}(\boldsymbol{k},\boldsymbol{q},\hat{p})\frac{k}{p} + \mathcal{O}(p^0)\,, & \text{as } \; p\to 0\,, \\ \boldsymbol{h}_{33,\mathrm{II,UV}}^{(2)}(\hat{k},\boldsymbol{p},\boldsymbol{q})\frac{k^2}{p^2} + \boldsymbol{h}_{33,\mathrm{II,UV}}^{(3)}(\hat{k},\boldsymbol{p},\boldsymbol{q})\frac{k^3}{p^3} \\ \qquad + \boldsymbol{h}_{33,\mathrm{II,UV}}^{(4)}(\hat{k},\boldsymbol{p},\boldsymbol{q})\frac{k^4}{p^4} + \mathcal{O}(k^5) \end{cases}\,, \quad \text{as } \; k\to 0\,. \tag{F9}$$

We can thus write the regularized integral as

$$\begin{aligned}
\tilde{\boldsymbol{I}}_{33,\mathrm{II}} = 36\int_{\boldsymbol{q},\boldsymbol{p}} \Bigg[& \boldsymbol{H}_3(\boldsymbol{k}-\boldsymbol{q}-\boldsymbol{p},\boldsymbol{q},\boldsymbol{p}) \otimes \boldsymbol{H}_3(\boldsymbol{k}-\boldsymbol{q}-\boldsymbol{p},\boldsymbol{q},\boldsymbol{p})\Theta(|\boldsymbol{k}-\boldsymbol{q}-\boldsymbol{p}|-q)P_{\mathrm{lin}}(\boldsymbol{k}-\boldsymbol{q}-\boldsymbol{p}) && \text{(F10)} \\
& - \left(\boldsymbol{h}_{33,\mathrm{II,IR}}^{(2)}(\boldsymbol{k},\boldsymbol{q},\hat{p})\frac{k^2}{p^2} + \boldsymbol{h}_{33,\mathrm{II,IR}}^{(1)}(\boldsymbol{k},\boldsymbol{q},\hat{p})\frac{k}{p} \right) W_{33,\mathrm{II}}^{\mathrm{IR}}\Theta(|\boldsymbol{k}-\boldsymbol{q}|-q)P_{\mathrm{lin}}(\boldsymbol{k}-\boldsymbol{q}) \\
& - \left(\boldsymbol{h}_{33,\mathrm{II,UV}}^{(2)}(\hat{k},\boldsymbol{p},\boldsymbol{q})\frac{k^2}{p^2} + \boldsymbol{h}_{33,\mathrm{II,UV}}^{(3)}(\hat{k},\boldsymbol{p},\boldsymbol{q})\frac{k^3}{p^3} + \boldsymbol{h}_{33,\mathrm{II,UV}}^{(4)}(\hat{k},\boldsymbol{p},\boldsymbol{q})\frac{k^4}{p^4} \right) W_{33,\mathrm{II}}^{\mathrm{UV}}\Theta(|\boldsymbol{q}+\boldsymbol{p}|-q)P_{\mathrm{lin}}(\boldsymbol{q}+\boldsymbol{p}) \Bigg] \\
& \times \Theta(q-p)P_{\mathrm{lin}}(\boldsymbol{q})P_{\mathrm{lin}}(\boldsymbol{p})\,.
\end{aligned}$$

After integrating over the $\hat{p}$ we see that the $\boldsymbol{h}_{33,\mathrm{II,IR}}^{(1)}$ term does not contribute. Similarly, the contribution of $\boldsymbol{h}_{33,\mathrm{II,UV}}^{(2)}$ and $\boldsymbol{h}_{33,\mathrm{II,UV}}^{(3)}$ vanish once contracted with $\boldsymbol{\lambda}_3$ and $\boldsymbol{\kappa}_3$. This is so since $\boldsymbol{\lambda}_3 \cdot [\boldsymbol{H}_{3,\mathrm{II}}]_{\mathrm{UV}}^{(1)} = \boldsymbol{\kappa}_3 \cdot [\boldsymbol{H}_{3,\mathrm{II}}]_{\mathrm{UV}}^{(1)} = 0$. Note also that only the first term in $\boldsymbol{h}_{33,\mathrm{II,UV}}^{(4)}$ actually contributes. To compute the full $\boldsymbol{I}_{33,\mathrm{II}}$ we have $\boldsymbol{I}_{33,\mathrm{II}}(k) = \tilde{\boldsymbol{I}}_{33,\mathrm{II}} + [\boldsymbol{I}_{33,\mathrm{II}}]_{\mathrm{IR}} + [\boldsymbol{I}_{33,\mathrm{II}}]_{\mathrm{UV}}$ where

$$[\boldsymbol{I}_{33,\mathrm{II}}]_{\mathrm{IR}} = 36\int_{\boldsymbol{q},\boldsymbol{p}} \boldsymbol{h}_{33,\mathrm{II,IR}}^{(2)}(\boldsymbol{k},\boldsymbol{q},\hat{p})\frac{k^2}{p^2} W_{33,\mathrm{II}}^{\mathrm{IR}}\Theta(|\boldsymbol{k}-\boldsymbol{q}|-q)\Theta(q-p)P_{\mathrm{lin}}(\boldsymbol{k}-\boldsymbol{q})P_{\mathrm{lin}}(\boldsymbol{q})P_{\mathrm{lin}}(\boldsymbol{p}) = \left(\boldsymbol{h}_{33,\mathrm{II}}^{\mathrm{IR}} W_{33,\mathrm{II}}^{\mathrm{IR}} \right) k^2\,, \tag{F11}$$

$$[\boldsymbol{I}_{33,\mathrm{II}}]_{\mathrm{UV}} = 6\int_{\boldsymbol{q},\boldsymbol{p}} \boldsymbol{h}_{33,\mathrm{II,UV}}^{(4)}(\hat{k},\boldsymbol{p},\boldsymbol{q})\frac{k^4}{p^4} W_{33,\mathrm{II}}^{\mathrm{UV}}P_{\mathrm{lin}}(\boldsymbol{q}+\boldsymbol{p})P_{\mathrm{lin}}(\boldsymbol{q})P_{\mathrm{lin}}(\boldsymbol{p}) = \left(\boldsymbol{h}_{33,\mathrm{II}}^{\mathrm{UV}} W_{33,\mathrm{II}}^{\mathrm{UV}} \right) k^4\,.$$

The leading IR contribution gives

$$\boldsymbol{h}_{33,\mathrm{II}}^{\mathrm{IR}} = \int_{\boldsymbol{q}} \hat{\boldsymbol{h}}_{33,\mathrm{II,IR}}^{(2)}(\boldsymbol{k},\boldsymbol{q})\sigma_2^2(q)\Theta(|\boldsymbol{k}-\boldsymbol{q}|-q)P_{\mathrm{lin}}(\boldsymbol{k}-\boldsymbol{q})P_{\mathrm{lin}}(\boldsymbol{q})\,, \tag{F12}$$

$$\boldsymbol{h}_{33,\mathrm{II}}^{\mathrm{UV}} = \int_{\boldsymbol{q},\boldsymbol{p}} \hat{\boldsymbol{h}}_{33,\mathrm{II,UV}}^{(4)}(\boldsymbol{p},\boldsymbol{q})P_{\mathrm{lin}}(\boldsymbol{q}+\boldsymbol{p})P_{\mathrm{lin}}(\boldsymbol{q})P_{\mathrm{lin}}(\boldsymbol{p})\,, \tag{F13}$$

where we have introduced the coefficients $\hat{\boldsymbol{h}}_{33,\text{II},\text{IR}}^{(2)}(\boldsymbol{k},\boldsymbol{q}) = 108 \int \frac{d\Omega_{\hat{p}}}{4\pi} \, \boldsymbol{h}_{33,\text{II},\text{IR}}^{(2)}(\boldsymbol{k},\boldsymbol{q},\hat{p})$. We also have the variance due to the p modes smaller than q, defined in Eq. (F6). We have defined the short scale noise $\boldsymbol{h}_{33,\text{II}}^{\text{UV}}$ contribution, which is scale independent given that $\hat{\boldsymbol{h}}_{33,\text{II},\text{UV}}^{(4)}(\boldsymbol{p},\boldsymbol{q}) = 6 \int \frac{d\Omega_{\hat{k}}}{4\pi} h_{33,\text{II},\text{UV}}^{(4)}/p^4$.

Next we look first at the $\boldsymbol{I}_{24}$ terms. The integrals are of the form

$$\boldsymbol{I}_{24} = 12 \int_{\boldsymbol{q},\boldsymbol{p}} \boldsymbol{H}_2(\boldsymbol{k}-\boldsymbol{q},\boldsymbol{q}) \otimes \boldsymbol{H}_4(\boldsymbol{k}-\boldsymbol{q},\boldsymbol{q},\boldsymbol{p},-\boldsymbol{p})P_{\text{lin}}(\boldsymbol{k}-\boldsymbol{q})P_{\text{lin}}(\boldsymbol{q})P_{\text{lin}}(\boldsymbol{p}), \tag{F14}$$

and the leading divergencies arise when $p \to 0$ & $q \to 0$, and $p \to 0$ and $\boldsymbol{q} \to \boldsymbol{k}$. The latter divergence can be re-mapped again into $p \to 0$ & $q \to 0$ in the same way as was done for the $\boldsymbol{I}_{22}$ term. We have

$$\boldsymbol{I}_{24} = \int_{\boldsymbol{p},q<|\boldsymbol{k}-\boldsymbol{q}|} + \int_{\boldsymbol{p},q>|\boldsymbol{k}-\boldsymbol{q}|} = 24 \int_{\boldsymbol{p},\boldsymbol{q}} \boldsymbol{H}_2(\boldsymbol{k}-\boldsymbol{q},\boldsymbol{q}) \otimes \boldsymbol{H}_4(\boldsymbol{k}-\boldsymbol{q},\boldsymbol{q},\boldsymbol{p},-\boldsymbol{p})\Theta(|\boldsymbol{k}-\boldsymbol{q}|-q)P_{\text{lin}}(\boldsymbol{k}-\boldsymbol{q})P_{\text{lin}}(\boldsymbol{q})P_{\text{lin}}(\boldsymbol{p}).$$

The remaining divergencies are now in $p \to 0$ and $q \to 0$. Since the integral is not symmetric in these variables the two divergencies are distinct. However, we can symmetrise the integral first to get

$$\boldsymbol{I}_{24} = 12 \int_{\boldsymbol{p},\boldsymbol{q}} \left[\boldsymbol{H}_2(\boldsymbol{k}-\boldsymbol{q},\boldsymbol{q}) \otimes \boldsymbol{H}_4(\boldsymbol{k}-\boldsymbol{q},\boldsymbol{q},\boldsymbol{p},-\boldsymbol{p})P_{\text{lin}}(\boldsymbol{k}-\boldsymbol{q})\Theta(|\boldsymbol{k}-\boldsymbol{q}|-q) + \boldsymbol{q} \leftrightarrow \boldsymbol{p} \right] P_{\text{lin}}(\boldsymbol{q})P_{\text{lin}}(\boldsymbol{p}). \tag{F15}$$

We can remap the integral as

$$\boldsymbol{I}_{24} = 24 \int_{\boldsymbol{p},\boldsymbol{q}} \left[\boldsymbol{H}_2(\boldsymbol{k}-\boldsymbol{q},\boldsymbol{q}) \otimes \boldsymbol{H}_4(\boldsymbol{k}-\boldsymbol{q},\boldsymbol{q},\boldsymbol{p},-\boldsymbol{p})P_{\text{lin}}(\boldsymbol{k}-\boldsymbol{q})\Theta(|\boldsymbol{k}-\boldsymbol{q}|-q) + \boldsymbol{q} \leftrightarrow \boldsymbol{p} \right] \Theta(q-p)P_{\text{lin}}(\boldsymbol{q})P_{\text{lin}}(\boldsymbol{p}), \tag{F16}$$

where the $q \to 0$ divergencies have been remapped into $p \to 0$ ones. The two terms obviously give equal contributions to the leading divergence while in the sub-leading case they are different. In the IR limit, we thus have

$$\boldsymbol{H}_2(\boldsymbol{k}-\boldsymbol{q},\boldsymbol{q}) \otimes \boldsymbol{H}_4(\boldsymbol{k}-\boldsymbol{q},\boldsymbol{q},\boldsymbol{p},-\boldsymbol{p}) \sim \begin{cases} \boldsymbol{h}_{24,\text{I},\text{IR}}^{(2)}(\boldsymbol{k},\boldsymbol{q},\hat{p})\frac{k^2}{p^2} + \mathcal{O}(p^0), & \text{as } p \to 0, \\ \boldsymbol{h}_{24,\text{UV}}^{(4)}(\hat{k},\boldsymbol{q},\boldsymbol{p})\frac{k^4}{p^4} + \mathcal{O}(k^5), & \text{as } k \to 0, \end{cases} \tag{F17}$$

$$\boldsymbol{H}_2(\boldsymbol{k}-\boldsymbol{p},\boldsymbol{p}) \otimes \boldsymbol{H}_4(\boldsymbol{k}-\boldsymbol{p},\boldsymbol{p},\boldsymbol{q},-\boldsymbol{q}) \sim \begin{cases} \boldsymbol{h}_{24,\text{II},\text{IR}}^{(2)}(\boldsymbol{k},\boldsymbol{q},\hat{p})\frac{k^2}{p^2} + \boldsymbol{h}_{24,\text{II},\text{IR}}^{(1)}(\boldsymbol{k},\boldsymbol{q},\hat{p})\frac{k}{p} + \mathcal{O}(p^0), & \text{as } p \to 0, \\ \boldsymbol{h}_{24,\text{UV}}^{(4)}(\hat{k},\boldsymbol{p},\boldsymbol{q})\frac{k^4}{q^4} + \mathcal{O}(k^5), & \text{as } k \to 0. \end{cases}$$

We thus have

$$\tilde{\boldsymbol{I}}_{24} = 24 \int_{\boldsymbol{p},\boldsymbol{q}} \left[\left(\boldsymbol{H}_2(\boldsymbol{k}-\boldsymbol{q},\boldsymbol{q}) \otimes \boldsymbol{H}_4(\boldsymbol{k}-\boldsymbol{q},\boldsymbol{q},\boldsymbol{p},-\boldsymbol{p}) - \boldsymbol{h}_{24,\text{I},\text{IR}}^{(2)}(\boldsymbol{k},\boldsymbol{q},\hat{p})\frac{k^2}{p^2} W_{24,\text{I}}^{\text{IR}} \right) P_{\text{lin}}(\boldsymbol{k}-\boldsymbol{q})\Theta(|\boldsymbol{k}-\boldsymbol{q}|-q) \right. \tag{F18}$$
$$+ \boldsymbol{H}_2(\boldsymbol{k}-\boldsymbol{p},\boldsymbol{p}) \otimes \boldsymbol{H}_4(\boldsymbol{k}-\boldsymbol{p},\boldsymbol{p},\boldsymbol{q},-\boldsymbol{q})P_{\text{lin}}(\boldsymbol{k}-\boldsymbol{p})\Theta(|\boldsymbol{k}-\boldsymbol{p}|-p)$$
$$- \left(\boldsymbol{h}_{24,\text{II},\text{IR}}^{(2)}(\boldsymbol{k},\boldsymbol{q},\hat{p})\frac{k^2}{p^2} + \boldsymbol{h}_{24,\text{II},\text{IR}}^{(1)}(\boldsymbol{k},\boldsymbol{q},\hat{p})\frac{k}{p} \right) W_{24,\text{II}}^{\text{IR}} P_{\text{lin}}(\boldsymbol{k})$$
$$\left. - \left(\boldsymbol{h}_{24,\text{UV}}^{(4)}(\hat{k},\boldsymbol{q},\boldsymbol{p})\frac{k^4}{p^4} P_{\text{lin}}(\boldsymbol{q}) + \boldsymbol{q} \leftrightarrow \boldsymbol{p} \right) W_{24}^{\text{UV}} \right] P_{\text{lin}}(\boldsymbol{q})P_{\text{lin}}(\boldsymbol{p})\Theta(q-p).$$

To compute the full $\boldsymbol{I}$, we have $\boldsymbol{I}_{24} = \tilde{\boldsymbol{I}}_{24}(k) + [\boldsymbol{I}_{24,\text{I}}]_{\text{IR}} + [\boldsymbol{I}_{24,\text{II}}]_{\text{IR}} + [\boldsymbol{I}_{24}]_{\text{UV}}$, where

$$[\boldsymbol{I}_{24,\text{I}}]_{\text{IR}} = 24 \int_{\boldsymbol{p},\boldsymbol{q}} \boldsymbol{h}_{24,\text{I},\text{IR}}^{(2)}(\boldsymbol{k},\boldsymbol{q},\hat{p})\frac{k^2}{p^2} W_{24,\text{I}}^{\text{IR}}\Theta(|\boldsymbol{k}-\boldsymbol{q}|-q)\Theta(q-p)P_{\text{lin}}(\boldsymbol{k}-\boldsymbol{q})P_{\text{lin}}(\boldsymbol{q})P_{\text{lin}}(\boldsymbol{p}) = \left(\boldsymbol{h}_{24,\text{I}}^{\text{IR}} W_{24,\text{I}}^{\text{IR}} \right) k^2, \tag{F19}$$

$$[\boldsymbol{I}_{24,\text{II}}]_{\text{IR}} = 24 P_{\text{lin}}(\boldsymbol{k}) \int_{\boldsymbol{p},\boldsymbol{q}} \boldsymbol{h}_{24,\text{II},\text{IR}}^{(2)}(\boldsymbol{k},\boldsymbol{q},\hat{p})\frac{k^2}{p^2} W_{24,\text{II}}^{\text{IR}}\Theta(q-p)P_{\text{lin}}(\boldsymbol{q})P_{\text{lin}}(\boldsymbol{p}) = \left(\boldsymbol{h}_{24,\text{II}}^{\text{IR}} W_{24,\text{II}}^{\text{IR}} \right) k^2 P_{\text{lin}}(k),$$

where

$$\boldsymbol{h}_{24,\text{I}}^{\text{IR}} = \int_{\boldsymbol{q}} \hat{\boldsymbol{h}}_{24,\text{I},\text{IR}}^{(2)}(\boldsymbol{k},\boldsymbol{q})\sigma_2^2(q)\Theta(|\boldsymbol{k}-\boldsymbol{q}|-q)P_{\text{lin}}(\boldsymbol{k}-\boldsymbol{q})P_{\text{lin}}(\boldsymbol{q}), \quad \text{where} \quad \hat{\boldsymbol{h}}_{24,\text{I},\text{IR}}^{(2)} = 72 \int \frac{d\Omega_{\hat{p}}}{4\pi} \, \boldsymbol{h}_{24,\text{I},\text{IR}}^{(2)}(\boldsymbol{k},\boldsymbol{q},\hat{p}), \tag{F20}$$

$$\boldsymbol{h}_{24,\text{II}}^{\text{IR}} = \int_{\boldsymbol{q}} \hat{\boldsymbol{h}}_{24,\text{II},\text{IR}}^{(2)}(\boldsymbol{k},\boldsymbol{q})\sigma_2^2(q)P_{\text{lin}}(\boldsymbol{q}), \quad \text{where} \quad \hat{\boldsymbol{h}}_{24,\text{II},\text{IR}}^{(2)} = 72 \int \frac{d\Omega_{\hat{p}}}{4\pi} \, \boldsymbol{h}_{24,\text{II},\text{IR}}^{(2)}(\boldsymbol{k},\boldsymbol{q},\hat{p}).$$

The UV components give

$$[\boldsymbol{I}_{24}]_{\text{UV}} = 12 \int_{\boldsymbol{p},\boldsymbol{q}} \boldsymbol{h}^{(4)}_{24,\text{UV}}(\hat{k},\boldsymbol{q},\boldsymbol{p}) \frac{k^4}{p^4} W^{\text{UV}}_{24} P_{\text{lin}}(\boldsymbol{q})^2 P_{\text{lin}}(\boldsymbol{p}) = \left(\boldsymbol{h}^{\text{UV}}_{24} W^{\text{UV}}_{24}\right) k^4 \,, \tag{F21}$$

where

$$\boldsymbol{h}^{\text{UV}}_{24} = \int_{\boldsymbol{p},\boldsymbol{q}} \hat{\boldsymbol{h}}^{(4)}_{24,\text{UV}}(\boldsymbol{q},\boldsymbol{p}) P_{\text{lin}}(\boldsymbol{q})^2 P_{\text{lin}}(\boldsymbol{p}), \quad \text{where} \quad \hat{\boldsymbol{h}}^{(4)}_{24,\text{UV}}(\boldsymbol{q},\boldsymbol{p}) = 12 \int \frac{d\Omega_{\hat{k}}}{4\pi} \, \hat{\boldsymbol{h}}^{(4)}_{24,\text{UV}}(\hat{k},\boldsymbol{q},\boldsymbol{p}). \tag{F22}$$

At last, let us look at the $\boldsymbol{I}_{15}$ term. The integrals are of the form

$$\boldsymbol{I}_{15} = 15 P_{\text{lin}}(\boldsymbol{k}) \int_{\boldsymbol{q},\boldsymbol{p}} \boldsymbol{H}_1(\boldsymbol{k}) \otimes \boldsymbol{H}_5(\boldsymbol{k},\boldsymbol{q},-\boldsymbol{q},\boldsymbol{p},-\boldsymbol{p}) P_{\text{lin}}(\boldsymbol{q}) P_{\text{lin}}(\boldsymbol{p}). \tag{F23}$$

The leading divergencies arise when $p \to 0$ & $q \to 0$. We can re-map this so that we have

$$\boldsymbol{I}_{15} = 30 P_{\text{lin}}(\boldsymbol{k}) \int_{\boldsymbol{q},\boldsymbol{p}} \boldsymbol{H}_1(\boldsymbol{k}) \otimes \boldsymbol{H}_5(\boldsymbol{k},\boldsymbol{q},-\boldsymbol{q},\boldsymbol{p},-\boldsymbol{p}) \theta(q-p) P_{\text{lin}}(\boldsymbol{q}) P_{\text{lin}}(\boldsymbol{p}). \tag{F24}$$

The IR and UV limits are

$$\boldsymbol{H}_1(\boldsymbol{k}) \otimes \boldsymbol{H}_5(\boldsymbol{k},\boldsymbol{q},-\boldsymbol{q},\boldsymbol{p},-\boldsymbol{p}) \sim \begin{cases} \boldsymbol{h}^{(2)}_{15,\text{IR}}(\boldsymbol{k},\boldsymbol{q},\hat{p}) \frac{k^2}{p^2} + \mathcal{O}(p^0), & \text{as } p \to 0, \\ \boldsymbol{h}^{(0)}_{15,\text{UV}}(\hat{k},\boldsymbol{q},\boldsymbol{p}) + \boldsymbol{h}^{(2)}_{15,\text{UV}}(\hat{k},\boldsymbol{q},\boldsymbol{p}) \frac{k^2}{p^2} + \mathcal{O}(p^0) & \text{as } k \to 0. \end{cases}$$

The regularised integrals are thus

$$\tilde{\boldsymbol{I}}_{15}(k) = 30 P_{\text{lin}}(\boldsymbol{k}) \int_{\boldsymbol{q},\boldsymbol{p}} \Bigg[\boldsymbol{H}_1(\boldsymbol{k}) \otimes \boldsymbol{H}_5(\boldsymbol{k},\boldsymbol{q},-\boldsymbol{q},\boldsymbol{p},-\boldsymbol{p}) - \frac{k^2}{p^2} \boldsymbol{h}^{(2)}_{15,\text{IR}}(\boldsymbol{k},\boldsymbol{q},\hat{p}) W^{\text{IR}}_{15} \tag{F25}$$

$$- \left(\boldsymbol{h}^{(0)}_{15,\text{UV}}(\hat{k},\boldsymbol{q},\boldsymbol{p}) + \boldsymbol{h}^{(2)}_{15,\text{UV}}(\hat{k},\boldsymbol{q},\boldsymbol{p}) \frac{k^2}{p^2} \right) W^{\text{UV}}_{15} \Bigg] \theta(q-p) P_{\text{lin}}(\boldsymbol{q}) P_{\text{lin}}(\boldsymbol{p}) \,.$$

The contributions from $\boldsymbol{h}^{(0)}_{15}$ vanish after contractions with the $\boldsymbol{\lambda}_5$ and $\boldsymbol{\kappa}_5$ coefficients. To compute the full integral we have $\boldsymbol{I}_{15}(k) = \tilde{\boldsymbol{I}}_{15}(k) + [\boldsymbol{I}_{15}]_{\text{IR}} + [\boldsymbol{I}_{15}]_{\text{UV}}$, with

$$[\boldsymbol{I}_{15}]_{\text{IR}} = 30 P_{\text{lin}}(\boldsymbol{k}) \int_{\boldsymbol{q},\boldsymbol{p}} \boldsymbol{h}^{(2)}_{15,\text{IR}}(\boldsymbol{k},\boldsymbol{q},\hat{p}) \frac{k^2}{p^2} W^{\text{IR}}_{15} \theta(q-p) P_{\text{lin}}(\boldsymbol{q}) P_{\text{lin}}(\boldsymbol{p}) = \left(\boldsymbol{h}^{\text{IR}}_{15} W^{\text{IR}}_{15} \right) k^2 P_{\text{lin}}(\boldsymbol{k}) \,, \tag{F26}$$

$$[\boldsymbol{I}_{15}]_{\text{UV}} = 15 P_{\text{lin}}(\boldsymbol{k}) \int_{\boldsymbol{q},\boldsymbol{p}} \boldsymbol{h}^{(2)}_{15,\text{UV}}(\hat{k},\boldsymbol{q},\boldsymbol{p}) \frac{k^2}{p^2} W^{\text{UV}}_{15} P_{\text{lin}}(\boldsymbol{q}) P_{\text{lin}}(\boldsymbol{p}) = \left(\boldsymbol{h}^{\text{UV}}_{15} W^{\text{UV}}_{15} \right) k^2 P_{\text{lin}}(\boldsymbol{k}) \,.$$

We have also introduced

$$\boldsymbol{h}^{\text{IR}}_{15} = \int_{\boldsymbol{q}} \hat{\boldsymbol{h}}^{(2)}_{15,\text{IR}}(\boldsymbol{k},\boldsymbol{q}) \sigma_2^2(q) P_{\text{lin}}(\boldsymbol{q}) \quad \text{and} \quad \boldsymbol{h}^{\text{UV}}_{15} = \int_{\boldsymbol{q}} \hat{\boldsymbol{h}}^{(2)}_{15,\text{UV}}(\boldsymbol{q},\boldsymbol{p}) \frac{1}{p^2} P_{\text{lin}}(\boldsymbol{q}) P_{\text{lin}}(\boldsymbol{p}) \,, \tag{F27}$$

where $\hat{\boldsymbol{h}}^{(2)}_{15,\text{IR}}(\boldsymbol{k},\boldsymbol{q}) = 90 \int \frac{d\Omega_{\hat{p}}}{4\pi} \, \boldsymbol{h}^{(2)}_{15,\text{IR}}(\boldsymbol{k},\boldsymbol{q},\hat{p})$, and $\hat{\boldsymbol{h}}^{(2)}_{15,\text{UV}}(\boldsymbol{q},\boldsymbol{p}) = 15 \int \frac{d\Omega_{\hat{k}}}{4\pi} \, \boldsymbol{h}^{(2)}_{15,\text{IR}}(\hat{k},\boldsymbol{q},\boldsymbol{p})/p^2$.

Appendix G: One- and two-loop results at redshift $z = 1.0$.

In this appendix, we present the results of one- and two-loop contributions to the density-density, density-velocity and velocity-velocity power spectrum at redshift $z = 1.0$, similar to what was presented in Sec.IV for the $z = 0.0$ case. In analogy to the Figure 4, the left panels of Figure 6 show the one-loop contributions for power spectra of density and velocity fields at $z = 1.0$: $P_{\delta\delta}$, $P_{\delta\theta}$ and $P_{\theta\theta}$. We again show the EdS results and the corresponding ΛCDM correction. We see that the one-loop ΛCDM corrections at $z = 1.0$ are approximately two orders of magnitude smaller than the one-loop EdS contributions. Note that in the wavelength range where the EdS results exhibit the zero crossing the relative importance of ΛCDM correction is larger and similar in magnitude to the two-loop EdS results.

Analogous results hold for the two-loop order, shown on the right-hand side of Figure 6. One can observe that the corresponding ΛCDM corrections are approximately two orders of magnitude smaller than the EdS results (except in the $P_{\theta\theta}$ case for $k < 0.1h/\text{Mpc}$, where the corrections can reach up to 5%). Here too, the exception is the wavenumber interval in the proximity of the k-value corresponding to the zero crossing of the EdS result. The correction due to such contributions can be partially mitigated once the UV counterterms are added, as was shown for the $z = 0.0$ case in Figure 5. In general, we see that these beyond-EdS corrections are overall smaller and less relevant at higher redshifts than is the case at $z = 0.0$, as one would expect.
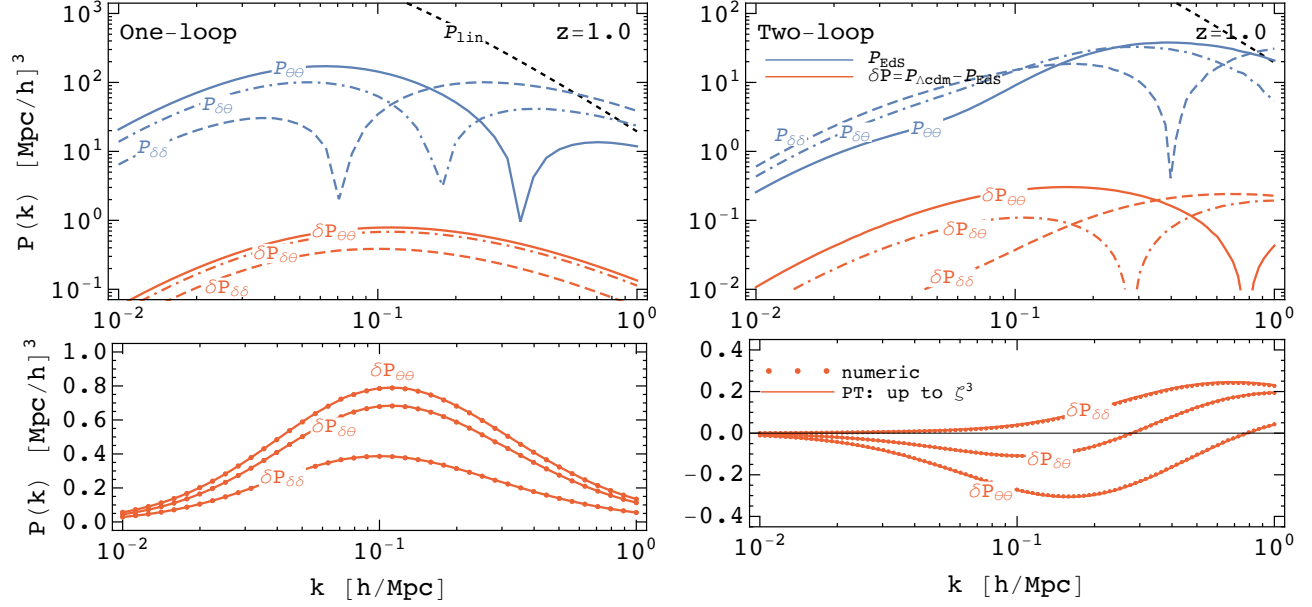
Figure 6: Plotted above are the same quantities shown in Figure 4, but this time at $z = 1.0$. *Upper panels* show the absolute contributions of EdS results (blue lines) compared to the ΛCDM corrections (red lines). We again see that the three different spectra $P_{\delta\delta}$ (dashed lines), $P_{\delta\theta}$ (dot-dashed lines) and $P_{\theta\theta}$ (solid lines) receive corrections of different size, whose relative importance is also a function of the scale dependence of the EdS terms. *Lower panels* display the ΛCDM corrections $\delta P_{\delta\delta}$, $\delta P_{\delta\theta}$ and $\delta P_{\theta\theta}$ computed using the numerical evaluations of the λ_n and κ_n coefficients (show in dots). We also show the perturbative time dependence computation as described in Sec. III up to the third order (solid lines).

References

[1] L. Amendola et al., Living Rev. Rel. **21**, 2 (2018), 1606.00180.
[2] P. A. Abell et al. (LSST Science, LSST Project) (2009), 0912.0201.
[3] D. J. Bacon et al. (SKA), Publ. Astron. Soc. Austral. **37**, e007 (2020), 1811.02743.
[4] M. H. Goroff, B. Grinstein, S. J. Rey, and M. B. Wise, Astrophys. J. **311**, 6 (1986).
[5] T. Buchert and J. Ehlers, Mon. Not. Roy. Astron. Soc. **264**, 375 (1993).
[6] B. Jain and E. Bertschinger, Astrophys. J. **431**, 495 (1994), astro-ph/9311070.
[7] P. Valageas, Astron. Astrophys. **379**, 8 (2001), astro-ph/0107015.
[8] F. Bernardeau, S. Colombi, E. Gaztanaga, and R. Scoccimarro, Phys. Rept. **367**, 1 (2002), astro-ph/0112551.
[9] A. Taruya and T. Hiramatsu, Astrophys. J. **674**, 617 (2008), 0708.1367.
[10] P. McDonald, JCAP **04**, 032 (2011), 0910.1002.
[11] J. Carlson, M. White, and N. Padmanabhan, Phys. Rev. D **80**, 043531 (2009), 0905.0479.
[12] D. Baumann, A. Nicolis, L. Senatore, and M. Zaldarriaga, JCAP **07**, 051 (2012), 1004.2488.
[13] J. J. M. Carrasco, M. P. Hertzberg, and L. Senatore, JHEP **09**, 082 (2012), 1206.2926.
[14] D. Bertolini, K. Schutz, M. P. Solon, and K. M. Zurek, JCAP **06**, 052 (2016), 1604.01770.
[15] T. Fujita, V. Mauerhofer, L. Senatore, Z. Vlah, and R. Angulo, JCAP **01**, 009 (2020), 1609.00717.
[16] E. Pajer and M. Zaldarriaga, JCAP **08**, 037 (2013), 1301.7182.
[17] P. McDonald and Z. Vlah, Phys. Rev. D **97**, 023508 (2018), 1709.02834.
[18] T. Matsubara, Phys. Rev. D **78**, 083519 (2008), [Erratum: Phys.Rev.D 78, 109901 (2008)], 0807.1733.
[19] T. Matsubara, Phys. Rev. D **77**, 063530 (2008), 0711.2521.
[20] J. Carlson, B. Reid, and M. White, Mon. Not. Roy. Astron. Soc. **429**, 1674 (2013), 1209.0780.
[21] R. A. Porto, L. Senatore, and M. Zaldarriaga, JCAP **05**, 022 (2014), 1311.2168.
[22] M. Bartelmann, F. Fabis, D. Berg, E. Kozlikin, R. Lilow, and C. Viermann, New J. Phys. **18**, 043020 (2016), 1411.0806.
[23] Z. Vlah, U. Seljak, and T. Baldauf, Phys. Rev. D **91**, 023508 (2015), 1410.1617.
[24] Z. Vlah, M. White, and A. Aviles, JCAP **09**, 014 (2015), 1506.05264.
[25] Z. Vlah and M. White, JCAP **03**, 007 (2019), 1812.02775.

[26] V. Desjacques, D. Jeong, and F. Schmidt, Phys. Rept. **733**, 1 (2018), 1611.09787.

[27] G. Cabass, M. M. Ivanov, M. Lewandowski, M. Mirbabayi, and M. Simonović, in *2022 Snowmass Summer Study* (2022), 2203.08232.

[28] M. M. Ivanov, M. Simonović, and M. Zaldarriaga, JCAP **05**, 042 (2020), 1909.05277.

[29] G. D'Amico, J. Gleyzes, N. Kokron, K. Markovic, L. Senatore, P. Zhang, F. Beutler, and H. Gil-Marín, JCAP **05**, 005 (2020), 1909.05271.

[30] M. M. Ivanov, Phys. Rev. D **104**, 103514 (2021), 2106.12580.

[31] S.-F. Chen, Z. Vlah, and M. White, JCAP **02**, 008 (2022), 2110.05530.

[32] P. Zhang, G. D'Amico, L. Senatore, C. Zhao, and Y. Cai, JCAP **02**, 036 (2022), 2110.07539.

[33] O. H. E. Philcox and M. M. Ivanov, Phys. Rev. D **105**, 043517 (2022), 2112.04515.

[34] G. S. Farren, O. H. E. Philcox, and B. D. Sherwin, Phys. Rev. D **105**, 063503 (2022), 2112.10749.

[35] S.-F. Chen, M. White, J. DeRose, and N. Kokron (2022), 2204.10392.

[36] F. Bernardeau, Astrophys. J. **433**, 1 (1994), astro-ph/9312026.

[37] R. Takahashi, Prog. Theor. Phys. **120**, 549 (2008), 0806.1437.

[38] T. Matsubara, Phys. Rev. D **92**, 023534 (2015), 1505.01481.

[39] C. Rampf, B. Villone, and U. Frisch, Mon. Not. Roy. Astron. Soc. **452**, 1421 (2015), 1504.00032.

[40] M. Lewandowski, A. Maleknejad, and L. Senatore, JCAP **05**, 038 (2017), 1611.07966.

[41] F. Schmidt, JCAP **04**, 033 (2021), 2012.09837.

[42] M. Garny and P. Taule, JCAP **01**, 020 (2021), 2008.00013.

[43] Y. Donath and L. Senatore, JCAP **10**, 039 (2020), 2005.04805.

[44] T. Steele and T. Baldauf, Phys. Rev. D **103**, 023520 (2021), 2009.01200.

[45] M. Fasiello and Z. Vlah, Phys. Rev. D **94**, 063516 (2016), 1604.04612.

[46] D. Blas, M. Garny, and T. Konstandin, JCAP **09**, 024 (2013), 1304.1546.

[47] J. J. M. Carrasco, S. Foreman, D. Green, and L. Senatore, JCAP **07**, 056 (2014), 1304.4946.

[48] D. Blas, M. Garny, and T. Konstandin, JCAP **01**, 010 (2014), 1309.3308.

[49] J. J. M. Carrasco, S. Foreman, D. Green, and L. Senatore, JCAP **07**, 057 (2014), 1310.0464.

[50] T. Baldauf, L. Mercolli, and M. Zaldarriaga, Phys. Rev. D **92**, 123007 (2015), 1507.02256.

[51] S. Foreman, H. Perrier, and L. Senatore, JCAP **05**, 027 (2016), 1507.05326.

[52] T. Konstandin, R. A. Porto, and H. Rubira, JCAP **11**, 027 (2019), 1906.00997.

[53] T. Baldauf, M. Garny, P. Taule, and T. Steele, Phys. Rev. D **104**, 123551 (2021), 2110.13930.

[54] A. Taruya, T. Nishimichi, and D. Jeong, Phys. Rev. D **105**, 103507 (2022), 2109.06734.

[55] D. Alkhanishvili, C. Porciani, E. Sefusatti, M. Biagetti, A. Lazanu, A. Oddo, and V. Yankelevich, Mon. Not. Roy. Astron. Soc. **512**, 4961 (2022), 2107.08054.

[56] R. Scoccimarro and J. Frieman, Astrophys. J. Suppl. **105**, 37 (1996), astro-ph/9509047.

[57] M. Peloso and M. Pietroni, JCAP **1305**, 031 (2013), 1302.0223.

[58] P. J. E. Peebles, *The large-scale structure of the universe* (1980).

[59] G. D'Amico, M. Marinucci, M. Pietroni, and F. Vernizzi, JCAP **10**, 069 (2021), 2109.09573.

[60] T. Fujita and Z. Vlah, JCAP **10**, 059 (2020), 2003.10114.

[61] E. Sefusatti and F. Vernizzi, JCAP **1103**, 047 (2011), 1101.1026.

[62] C. Rampf, S. O. Schobesberger, and O. Hahn, Mon. Not. Roy. Astron. Soc. **516**, 2840 (2022), 2205.11347.

[63] A. Kehagias and A. Riotto, Nucl. Phys. **B873**, 514 (2013), 1302.0130.

[64] P. Creminelli, J. Noreña, M. Simonović, and F. Vernizzi, JCAP **1312**, 025 (2013), 1309.3557.

[65] M. Peloso and M. Pietroni, JCAP **1404**, 011 (2014), 1310.7915.

[66] P. Creminelli, J. Gleyzes, M. Simonović, and F. Vernizzi, JCAP **1402**, 051 (2014), 1311.0290.

[67] M. Garny and P. Taule, JCAP **09**, 054 (2022), 2205.11533.

[68] T. Steele and T. Baldauf, Phys. Rev. D **103**, 103518 (2021), 2101.10289.